



**INTERNAL DOCUMENT No. 314**

**A high resolution study of climatic variability  
in the Benguela Current system of the  
southeastern Atlantic off the Namib Desert,  
southwestern Africa**

**R Hearn**

**1992**

**INSTITUTE OF OCEANOGRAPHIC SCIENCES  
DEACON LABORATORY**

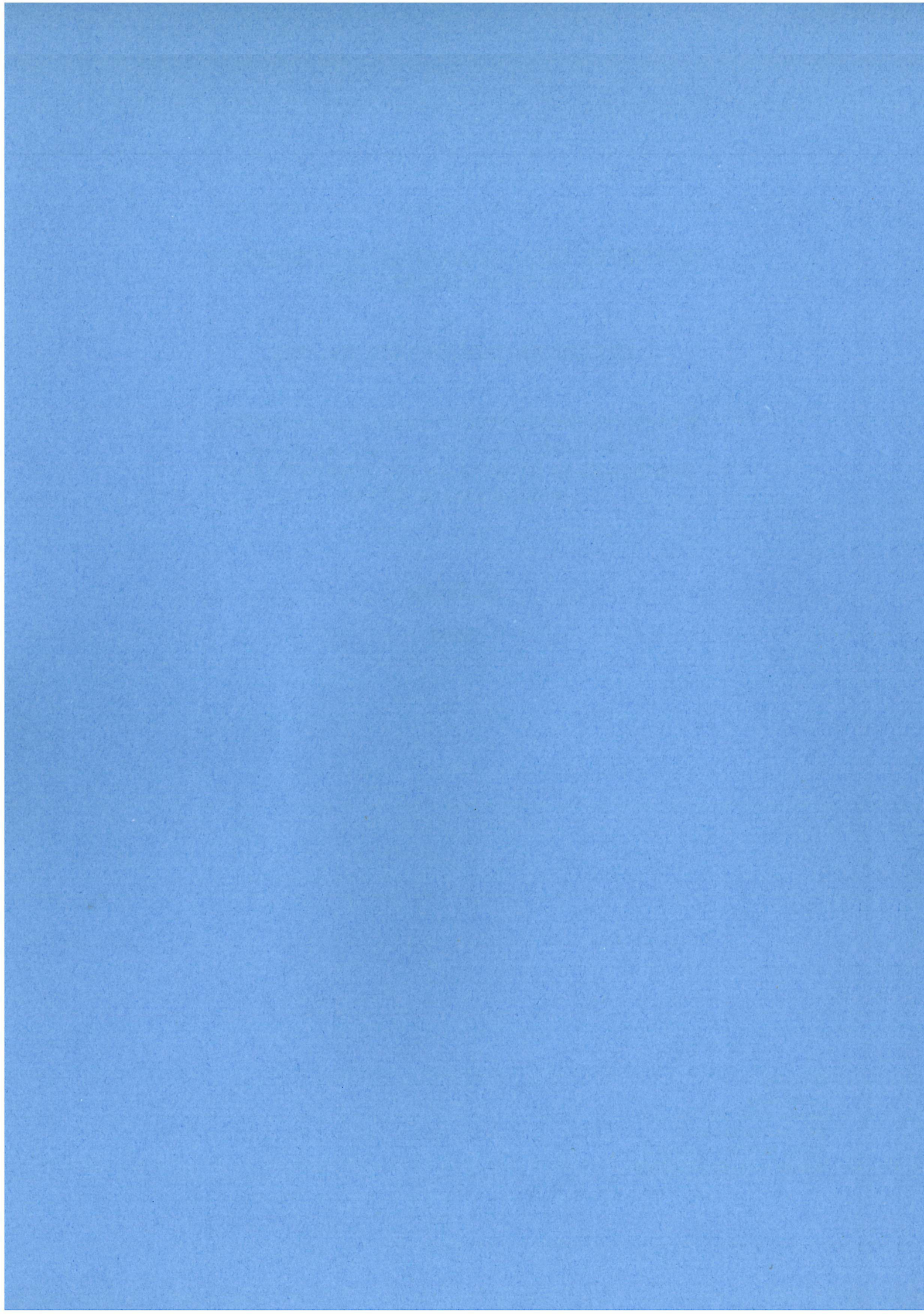
**INTERNAL DOCUMENT No. 314**

**A high resolution study of climatic variability  
in the Benguela Current system of the  
southeastern Atlantic off the Namib Desert,  
southwestern Africa**

**R Hearn**

**1992**

Wormley  
Godalming  
Surrey GU8 5UB UK  
Tel +44-(0)428 684141  
Telex 858833 OCEANS G  
Telefax +44-(0)428 683066



# DOCUMENT DATA SHEET

AUTHOR HEARN, R	PUBLICATION DATE 1992
TITLE  A high resolution study of climatic variability in the Benguela Current system of the southeastern Atlantic off the Namib Desert, southwestern Africa.	
REFERENCE  Institute of Oceanographic Sciences Deacon Laboratory, Internal Document, No. 314, 148pp. (Unpublished manuscript)	
ABSTRACT	
KEYWORDS  OBS OCEAN BOTTOM INSTRUMENT PDAS SEISMIC RECORDER	
ISSUING ORGANISATION  Institute of Oceanographic Sciences Deacon Laboratory Wormley, Godalming Surrey GU8 5UB. UK. Director: Colin Summerhayes DSc	
Copies of this report are available from: <b>The Library</b> , PRICE £0.00	

## CONTENTS

	Page
1. Introduction	9
2. Project Outline	10
2.1 The Area	10
2.2 Collection of the core	10
2.3 Previous data	11
2.4 Other data from the South East Atlantic	12
2.5 Co-investigators	13
3. Analytical work at IOSDL	21
3.1 Sample distribution and preparation	21
3.2 Coulometrics	22
3.2.1 The apparatus and technique	
3.2.2 The carbonate-free organic carbon plot	
3.2.3 Results and discussion	
3.2.4 Problems encountered	
3.3 ICP-AES	34
3.3.1 Apparatus and techniques	
3.3.2 Sample preparatus	
3.3.3 The results and discussion	
3.3.4 Problems and limitations	
3.4 Statistics	41
3.4.1 Accuracy and Precision	
3.4.2 Fast fourier transform	
3.4.3 Factor analysis	
3.5 Use of Computers	47
4. Related analytical work	119
4.1 Biostratigraphic data	119
4.1.1 Introduction	
4.1.2 Method	
4.1.3 Results and discussion	
4.2 Organic Geochemical data	121
4.2.1 Introduction	
4.2.2 Sample preparation and analysis	
4.2.3 Results	
4.2.4 Discussion and interpretation of results	
4.3 Inorganic Geochemistry and oxygen isotope stratigraphy	124
5. Interpretation and conclusions	135
5.1 Comparison and interpretation of all available data sets	135
5.2 Further possible studies	136

## LIST OF FIGURES

<b>Figure</b>		
		Page
1	Bathymetric map of the south east Atlantic off Walvis Bay showing the location of PC12, PC13 and PC16.	15
2	Chain cruise 115 report previously obtained from PG/PC12.	16
3	Various files previously obtained from PG/PC12.	17
4	Eight of the inorganic geochemistry profiles obtained from PC12.	18
5	Operation of a piston corer that is tripped with a gravity (or pilot) corer.	19
6	The coulometer cell.	49
7	Acidification apparatus for carbonate analysis.	50
8	Combustion apparatus for total carbon analysis.	51
9	Diagram to show the possible position of PC12 on the boundary of a current carrying plant populations.	52
10	The coulometric data.	53
11	An example of how $\text{CaCO}_3\%$ might vary with influx of terrestrial material.	55
12	Map of the Walvis Bay area showing the locations of PC12 and three of the 4000 series cores.	56
13	Comparison of the $\text{CaCO}_3\%$ and $\text{C}_{\text{org}}\%$ profiles for PG/PC12 and three of the 4000 series cores.	57
14	Comparison of $\text{C}_{\text{org}}\%$ at IOSDL and at the University of Cape Town.	58
15	The ICP torch.	59
16	The concentric nebuliser.	60
17	The ICP-AES system.	61
18	The coulometric data for core section 260-360cm.	62
19	The first group of ICP results.	65
20	The second group of ICP results.	77
21	The calculated silica plots.	100
22	Limitations of the ICP-AEC system.	102
23	The FFT of $\text{CaCO}_3\%$ .	107
24	The FFT of $\text{C}_{\text{org}}\%$ .	108
25	The FFT of CF $\text{C}_{\text{org}}\%$ .	109

	Page
26 The FFT of CaCO <sub>3</sub> % after removing the first 2 components.	110
27 The FFT of C <sub>org</sub> % after removing the first 2 components.	111
28 The FFT of CF C <sub>org</sub> % after removing the first 2 components.	112
29 The FFT of CF C <sub>org</sub> % after removing the first 5 components.	113
30 The FFT of CaCO <sub>3</sub> % after removal of the first 14 components.	114
31 The FFT of C <sub>org</sub> % after removing of first 14 components.	115
32 The FFT of CF C <sub>org</sub> % after removing the first 14 components.	116
33 The FFT of CF C <sub>org</sub> % after removal of N = 28.	117
34 Two examples of coccolith types.	127
35 Generalised coccolith stratigraphy for temperate waters.	128
36 The relative abundances of two coccolith species in PG/PC12.	129
37 The relative abundances of 6 coccolith species in PC12.	130
38 An example of a gas chromatogram from a PC12 sample.	131
39 The organic geochemistry results.	132
40 The oxygen isotope record.	133
41 The oxygen isotope curve for PG/PC12.	134
42 Comparison of the organic geochemistry and the coulometric data sets.	139

## LIST OF APPENDICES

	<b>Page</b>
Appendix 1 Comparison of CaCO <sub>3</sub> % and total carbon % before and after re-drying.	141
Appendix 2 Total carbon analysis of PC12 104-105cm.	142
Appendix 3 Comparison of original PG12 samples.	143
Appendix 4 The results obtained whilst investigating the suspicion of high organic carbon values.	144
Appendix 5 Shale composition from three literature sources.	146

## LIST OF TABLES

Table 1 Rotated factor pattern	46
--------------------------------	----

## 1. INTRODUCTION

Seafloor sediments contain a historical record of the production of planktonic organisms like foraminifera, coccoliths and diatoms. Analysing this record can tell us about past ocean circulation patterns which, in turn, can tell us about past climatic conditions. The sedimentary record, then, can be a record of past climate change.

In this project we set out to see if sediments from a piston core collected off Southwest Africa could tell us about past circulation and past climate change in the southeastern Atlantic and, by inference, in southwestern Africa, over the past 100-200,000 years. We hoped to determine the highest resolution environmental signal possible by analysing variability at 1cm intervals and also to improve the basis for climate prediction by examining the cyclicity of the data obtained. The work reported here focussed on the analysis of calcium carbonate (representing the skeletal remains of planktonic organisms like foraminifera and coccoliths that secrete a carbonate skeleton) and organic carbon (representing the soft parts of these and many other planktonic organisms).

The work was carried out as part of an industrial training studentship, in the Chemistry Department of the Institute of Oceanographic Sciences Deacon Laboratory, the UK's centre for research on the biology, physics, geology and chemistry of the deep oceans and the ocean bed.

## 2. PROJECT OUTLINE

### 2.1 The Area

The core was collected at latitude  $22^{\circ}16.00^{\prime}\text{S}$  and longitude  $12^{\circ}32.28^{\prime}\text{E}$  in a water depth of 1017 metres. This is just seawards of the Benguela current system of the south-eastern Atlantic, off-shore from Walvis Bay (Fig. 1). The area is of particular interest as it is one of the world's few major upwelling zones. In these zones the trade winds blow the surface waters out to sea, forcing cold, nutrient-rich subsurface waters upwards to replace them. In response to this increased influx of nutrients, the surface waters are biologically highly productive. Marine plants (phytoplankton) become abundant, providing abundant food for organisms higher in the food chain. These areas make rich fishing grounds. Because the surface waters are so productive, lots of planktonic remains build up on the seafloor, sometimes making piles of organic rich mud stinking of hydrogen sulphide. The reducing conditions in the muds help to preserve the organic matter beneath the Benguela Current. These muds carry the record of environmental change.

### 2.2 Collection of the core

The core was collected on 29th December 1973 during Chain cruise 115, using a piston corer triggered by a pilot corer. Fig. 5 shows how the process of piston coring takes place. Inside its barrel, the piston corer has a piston that reduces friction and utilises hydrostatic pressure during the coring operation, the corer can therefore take up to 20 metres of sediment.

One of the difficulties in obtaining a complete record of the sediment is that the falling piston corer pushes water ahead of it, blasting away the top layer of the sediment. Fortunately, this layer is commonly sampled in the pilot corer. Because the pilot corer has no piston it may compress the layers of sediment penetrated. It is also possible that the pilot core will bounce two or three times into the sediment or perhaps even fall over and take a horizontal core just of the sediment surface. This has to be taken into consideration before coming to any conclusions about the pilot core data.

In this project, the piston core is labelled PC12. The usable part of the core is 537cm long above a section that flowed in (Fig. 5). The pilot core, labelled PG12, is 82cm long. Together PC12 and PG12 make up a sedimentary record 619cm long. As discussed in text, there may be some section missing between the two.

## 2.3 Previous Data

Three main sets of data were available for our study:

- 1) the cruise report
- 2) previous analyses of the core (PC12)
- 3) data from other cores in the area

### 1) The Cruise Report

After collection, the core was returned to the laboratory and stored for a while before being split into two (a working half and an archive half) and described. Fig. 2 shows a copy of the descriptions of PC12, which include sedimentary structures, colour, texture, and mineralogy. Examination of smear slides showed that the core consisted of calcareous ooze dominated by clay and coccoliths (calcareous plankton composed of  $\text{CaCO}_3$ ). Very few siliceous organisms (diatoms, sponges, radiolaria) were seen.

### 2) Previous Analysis of PC12

Core PC12 had been previously analysed for various components, as explained below.

#### Calcium Carbonate (Fig. 3)

Summerhayes, Bornhold and Embley (1979) used the LECO system to analyse PC12 for carbonate at 20cm intervals down the core, beginning at 0cm.

Bremner (unpublished) also analysed for carbonate at every 20cm, beginning at 4cm. He used the Karbonate-Bombe method. Both sets of data show large fluctuations in carbonate down core, suggesting that there had been substantial environmental change over time at this site.

#### Organic carbon (Fig. 3)

Bremner (unpublished) measured organic carbon content on the same samples as he had analysed for carbonate, using Morgan's Wet Chemical Technique. Summerhayes (1983) analysed an additional five samples down the core for total organic carbon, using the LECO method.

### Inorganic Geochemistry (Fig. 4)

Bremner (unpublished) analysed PC12 for 25 inorganic elements and minerals. However, because of flaws in the analytical procedure Bremner felt that only the data from eight of the elements were safe to use. These elements are listed in Fig. 4, together with their profiles of abundance against depth in the core.

### Others (Fig. 3)

Information was also available on the sand content (Summerhayes et al, 1979) and nitrogen content (Summerhayes, 1983), and on the abundances of three clay minerals - montmorillonite, illite and kaolinite (Summerhayes unpublished). The estimated age of this core is also shown in Fig. 3 (Summerhayes et al, 1979).

The sand data broadly follow the carbonate data, and represent mainly skeletal carbonate in the shape of foraminifera, suggesting a climatic control. The nitrogen data follow the carbon data and seem crudely inverse to carbonate. The clay data suggest a single source for the fine non-carbonate fraction, probably the nearby Namib Desert.

### Summary

Both the cruise report and the previous analytical data gave an idea of what results might be expected from our analyses. Although our study was at a much higher resolution than previous analyses, we still expected our new data sets to follow the same basic patterns. However, we anticipated that the higher resolution study would give us a more detailed picture of environmental change with time. The previous data were also useful for cross-references and provided us with the basis for comparisons between analytical techniques once the new data sets had been obtained.

### 2.4 Other data from the South East Atlantic

Of the seven piston cores collected during Chain cruise 115, three came from the slope off Walvis Bay - PC12 (our core), PC13 and PC16. PC13 was taken within a major submarine landslide scar, and so was unsuitable for our purposes. PC16 came from lower down the slope at a depth of 2199m, near PC12. Diester-Haass et al (1988) analysed PC16 and indicated high sedimentation rate of 12cm/1000 years. Given this high rate of sedimentation, and the location of PC16 in an area of major slides it seemed possible that the high rate was the result of a

physical process (eg. slumping of large masses of sediment down the slope) rather than a true, steady, sedimentation rate. That was why PC13 and PC16 were not used in our study.

Other studies were made on other sets of cores from this area. Bornhold (1973), Diester-Haass (1985), and Diester-Haass et al (1986) analysed cores from the Walvis Ridge area and north of Walvis Ridge. They found that there was more opal\* and less organic carbon in interglacial periods than in glacial periods. Diester-Haass (1985) interpreted this to signify that the Benguela Current, which flows northwards off the coast of SW Africa between 15° and 30°S, had turned westwards during interglacials, carrying opal out over the coring sites. She suggested that during glacials organic matter was moved seawards onto the Walvis Ridge by bottom currents.

Surprisingly, Diester-Haass's analysis of PC16 from the slide on the slope near Walvis Bay, some 250 n.miles south of the Walvis Ridge cores, indicated the same pattern of organic carbon and opal fluxes between glacial and interglacial periods as seen in the Walvis Ridge cores. It seems unreasonable to expect that the Benguela Current can have turned west in two such widely separated areas, so we believe that some alternative explanation is called for to explain these flux patterns.

One of our objectives, therefore, was to analyse PC12 to determine the rates of accumulation of various components, to help us to decide whether the observed enrichment in organic matter during glacials was a result of increased productivity, or of erosion and redeposition.

## 2.5 Co-investigations

To meet our objectives it was necessary to analyse the core using a battery of methods not all of them available at IOSDL. For this reason, the project was a multidisciplinary one involving a team of different experts from around the country.

One of the difficulties faced by the investigating team was the limited amount of sediment available. PC12 and PG12 were sampled at one centimetre intervals. In some places there was very little original material available because the core had been sampled previously at 20cm intervals. This meant that the samples were sometimes very small. With most of the analytical techniques being non-conservative (ie. once treated, sub-samples could not be used for a

---

\* opal - a hydrous cryptocrystalline form of silica which is incorporated in the cell wall of microscopic marine plants called diatoms. After death, the cell walls are well preserved in the sediment and retain their opaline composition. Thus, opal in sediments is good indication of diatoms in the ocean.

different analysis), we had to choose only the most important analyses to do, farming out the samples very carefully to the different investigators.

Three establishments were chosen to make up the team, and their participation is summarised below:

#### **The Institute of Oceanographic Sciences Deacon Laboratory**

The project coordinator was Dr Colin Summerhayes, the Director at IOSDL. Under his supervision, I measured calcium carbonate and organic carbon percentages using a coulometer. I also investigated the mineralogy of the core through major and trace element analyses made by using the Inductively Coupled Plasma-Atomic Emission Spectrometer (ICP-AES).

Dr R Jordan at IOSDL determined the nannoplankton biostratigraphy and the abundances of siliceous planktonic organisms - radiolaria and diatoms.

#### **University of Bristol**

Prof. Geoff Eglington and Antoni Rosell at the School of Chemistry, University of Bristol, agreed to use their organic geochemical methods (especially gas chromatography - mass spectrometry) to determine the proportions of pigment, alkenones and alkenoates in the samples. They were able to estimate past sea surface temperatures from the alkenone data.

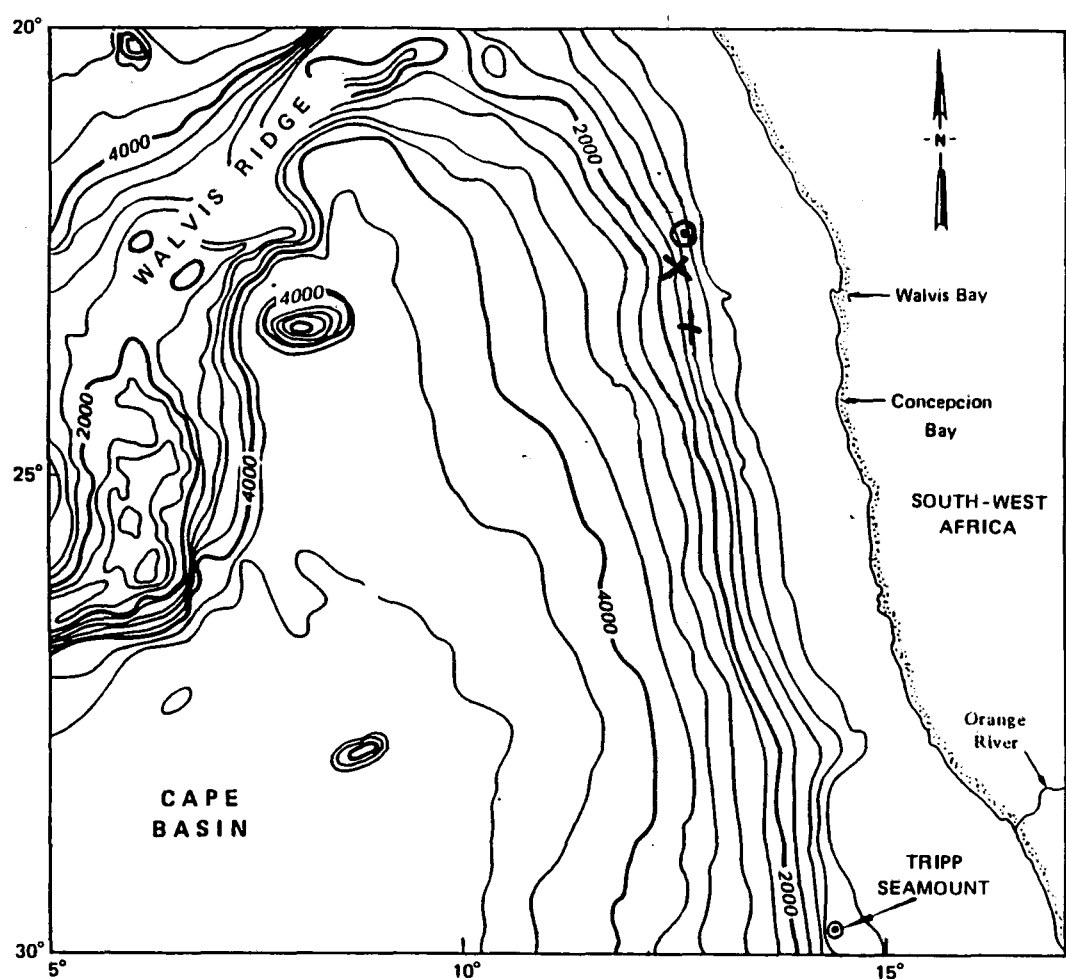
#### **University of Edinburgh**

Dr R Kroon was to use mass spectrometry to measure the oxygen isotopes in the foraminifera in the sediment so as to estimate past temperatures and to provide age constraints. He also planned to study the various foram species present to determine environmental changes with time.

Dr B Price agreed to use x-ray fluorescence to analyse the core for opal and for inorganic geochemical constituents, to assist in assessing environmental change with time (eg. changes in input of desert dust by Trade Winds).

Detailed accounts of all of these analytical techniques are given later in this report.

Fig 1. Bathymetric map of the south east Atlantic off Walvis Bay showing the location of PC12, PC13 and PC16.



① PC12

X PC13

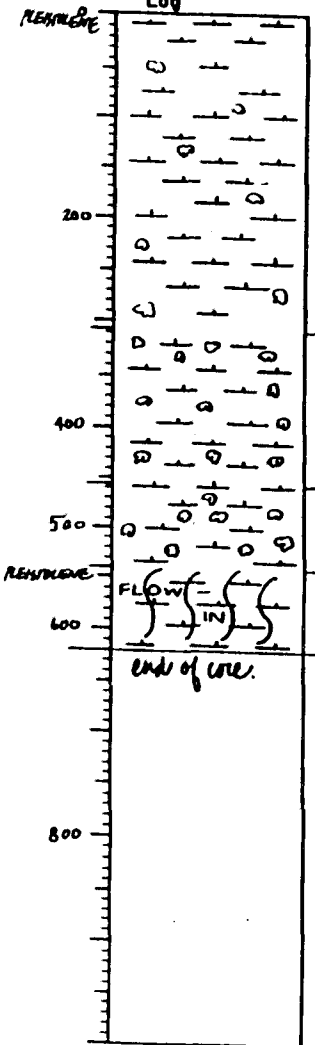
† PC16

Fig 2. Chain cruise 115 report previously obtained from PG/PC12.

### VISUAL CORE DESCRIPTION

Ship CHAIN Cruise 115 Leg 2 Sta. 20 Core No. 124PC  
 Total Length 620 cm. Lat. 22° 16.0'S Long. 12° 32.28'E Depth 1017 m. farr.  
 Core condition EXCELLENT Date Described 11MAY52 by J. H. D.  
 Physiographic location SOUTHWEST AFRICAN SLOPE: WALVIS BAY

### Lithologic



#### Detailed Description

3-308  
**CALC 002E**  
 SY 3/2 dk olive gray  
 faint laminations, bands, and mottles of olive gray SY 4/2 and  
 olive 4/4 found commonly throughout  
 moist slick, rubbery lutite with abund. tiny white flecks  
 (shell frags?) found throughout  
 79-81 cm band of extremely abund. white flecks, distinct but  
 irregular olive band 69-74 cm.  
 S, I 10°

308-456  
**CALC 002E**  
 SY 4/2 olive gray  
 extensive olive and dark olive gray mottling 310-340 cm, common  
 dk olive gray burrows and bands, 340-356 cm  
 moist slick, rubbery lutite with white flecks common throughout

C  
 456-560  
**CALC 002E**  
 SY 3/2 dk olive gray  
 extensive olive gray and olive mottling 456-476 cm, common  
 476-560 cm  
 moist rubbery lutite with common white flecks

C  
 - 540-620  
**FLOW LN**  
 end of core

SMEAR SLIDE DESCRIPTIONS - W.H.O.I. SEDIMENT CORES

Ship: Chain  
Expedition 113  
Leg No. 2

Fig 3. Various data files previously obtained from PG/PC12.

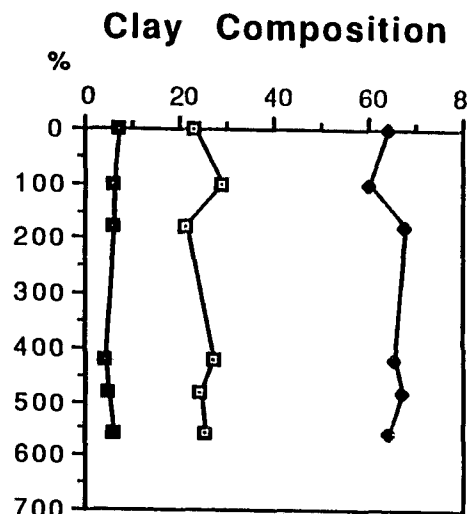
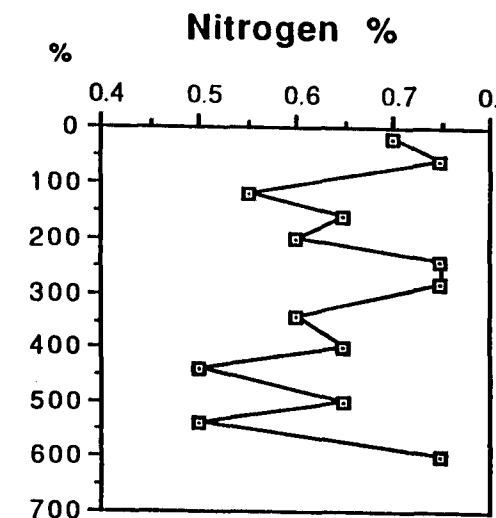
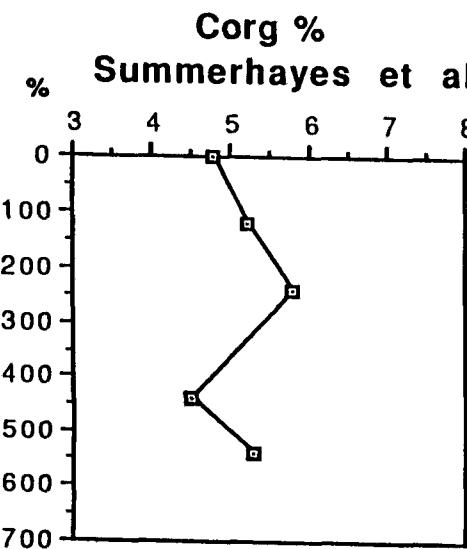
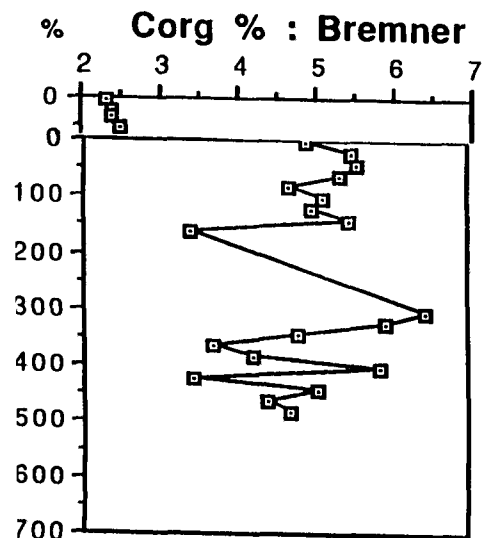
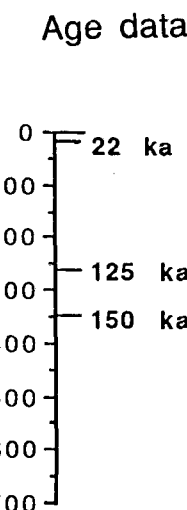
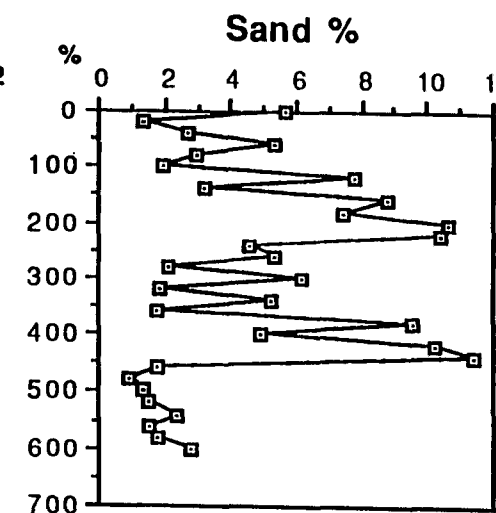
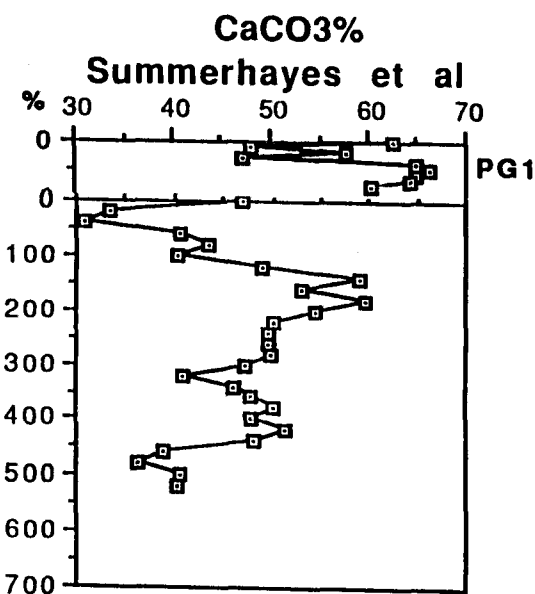
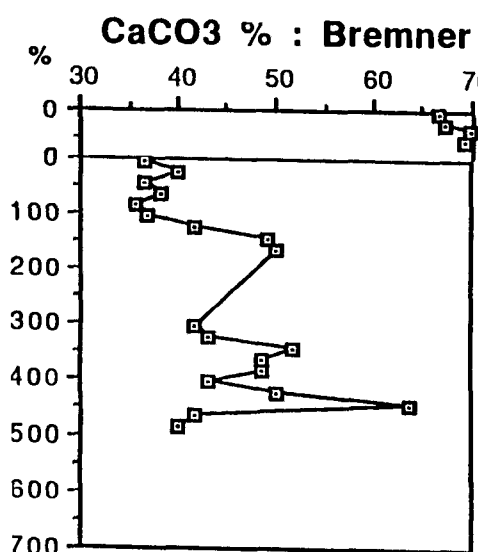


Fig 4. Eight of the inorganic geochemistry profiles obtained from PC12.

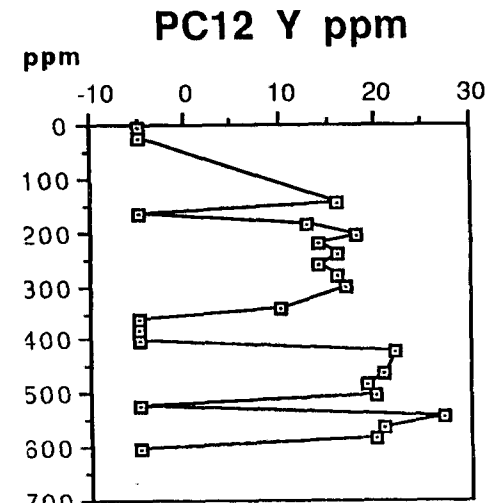
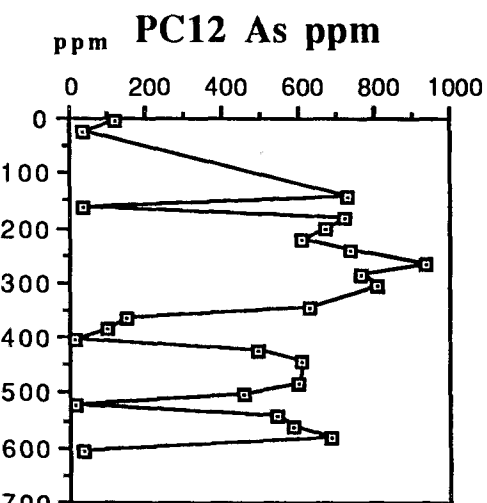
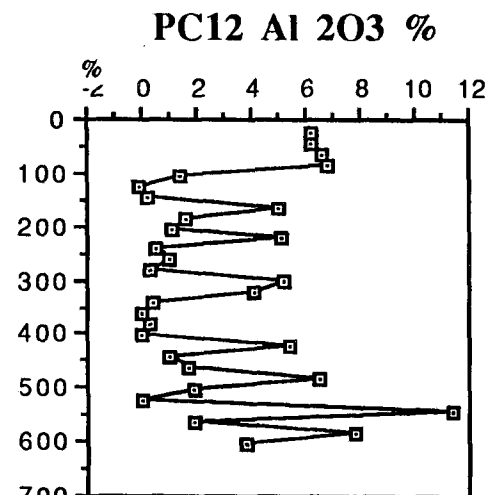
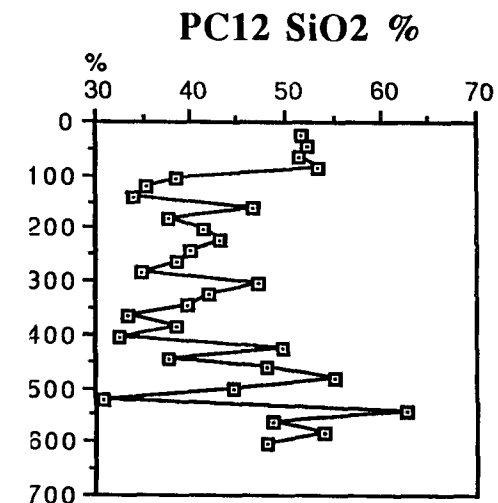
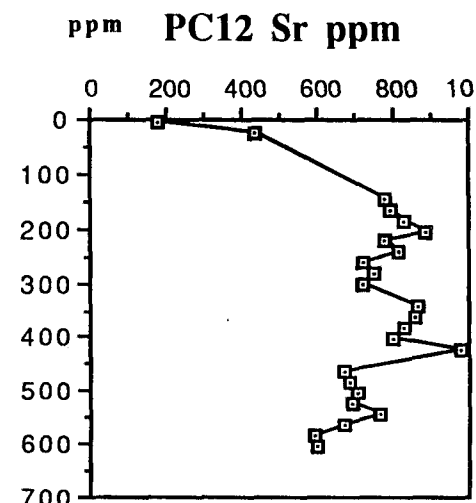
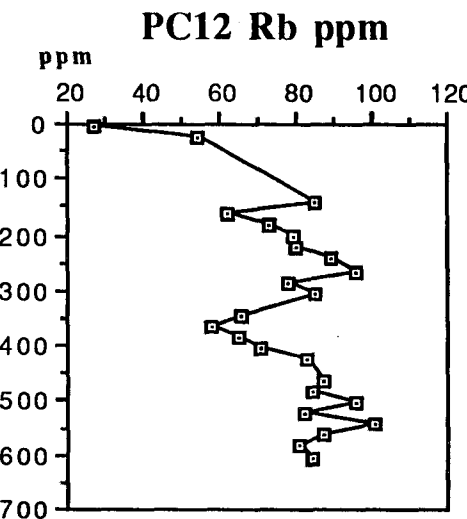
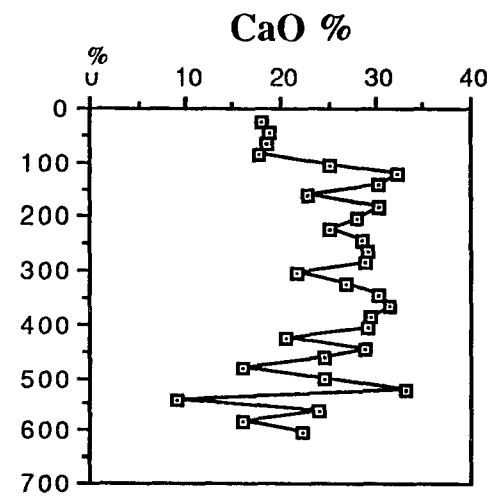
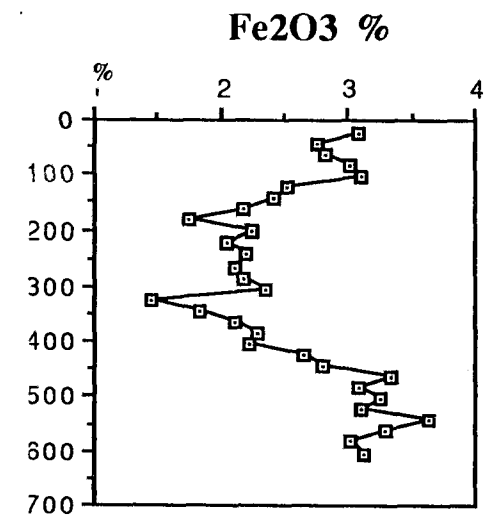
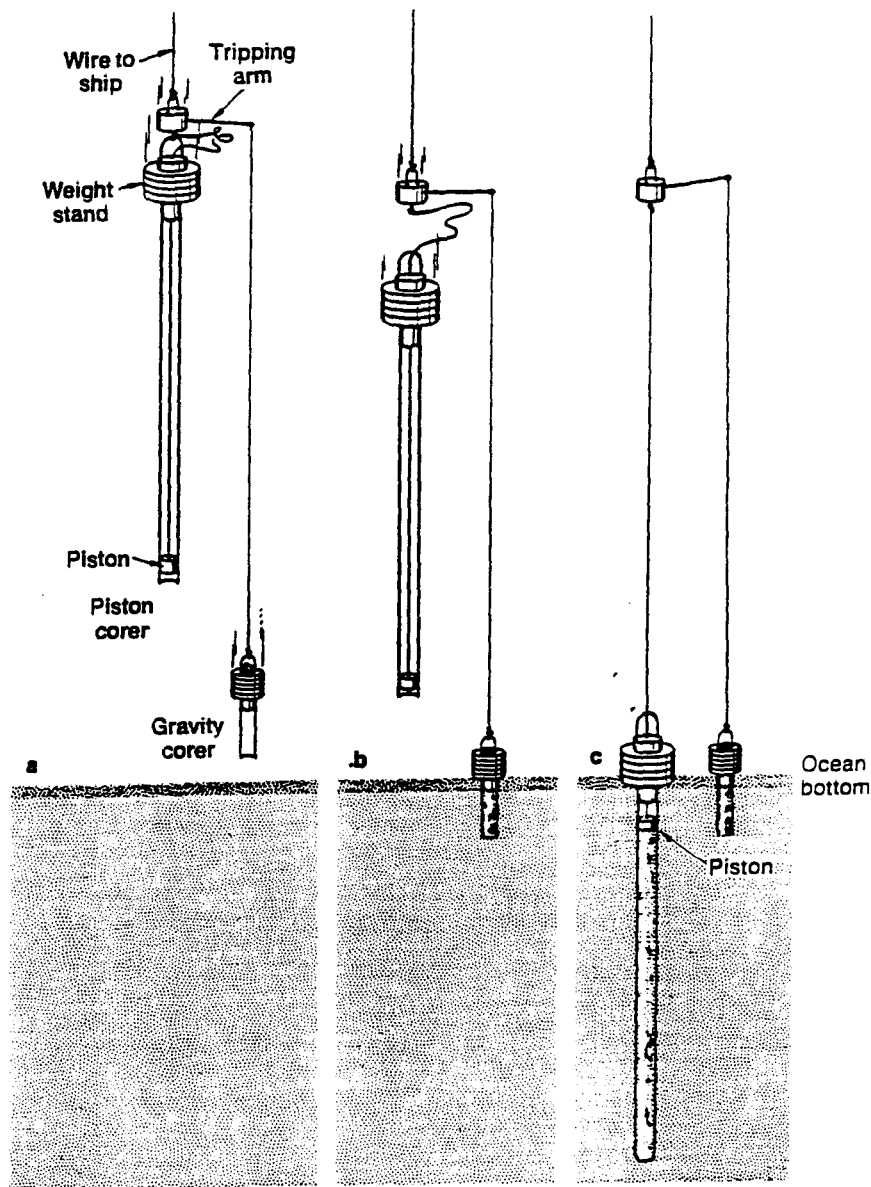


Fig 5. Operation of a piston corer that is tripped with a gravity (or pilot) corer.



- a) Lowering position.
- b) When the gravity corer hits the bottom, the piston corer is released and free-falls to the bottom. At the moment of impact the line to the piston tightens and the core barrel moves past it; this reduces friction within the core barrel.
- c) Completion of the coring operation prior to retrieval.



### 3 ANALYTICAL WORK AT IOSDL

#### 3.1 Sample distribution and preparation

The core had been stored since its collection in December 1973 in the core store of the Woods Hole Oceanographic Institution, Massachusetts. It had first been cut in half length-ways to create (a) the working half, which is where samples for analysis are taken from, and (b) the archive half, which is kept in the store as a record. In some places down the core all of the working half had been used, so the archive half had to be sub-sampled. When this happened the archive half was divided in two, so that only half of it was sampled so as to leave an archive record in the store.

The samples were taken from the core at 1cm intervals and put into clean, labelled, sealable, plastic bags. To prevent contamination, the samples were not touched. Both in sampling and in sample preparation a spatula was used to transfer the sediment, and this was cleaned between each sample to prevent cross-sample contamination.

When the piston core barrel moves into the sediment a smear zone develops between the plastic core liner and the sediment. The smeared sediment zone had to be cut off the outside of each 1cm sub-sample.

From each sample, firstly, very small amounts of sediment (about 0.05 gms) were put into clean, glass vials for Dr Jordan's biostratigraphic analysis. The samples were not ground, as this would break up the coccoliths he would be counting. Then, some sediment (about 0.5 gms) was transferred into glass vials for organic geochemical analysis at Bristol University. I sent them raw (untreated) samples, as oven drying would probably destroy some of the organic compounds they wanted to look at. I then transferred samples (1 gm) into glass vials for my own analyses. All the remaining sediment in each sample was sent to Edinburgh University. They needed 1 gm for foraminifera and oxygen isotope analysis; 0.5 gm for opal (diatom) analysis; and 3.5 gm for inorganic geochemical analysis. They were asked to store any unused material.

Eleven of the samples contained solid crystalline pieces, believed to be crystals formed from the pore water whilst the core was in storage. The crystals were separated from the rest of the sediment and sent to Edinburgh University for analysis.

Having distributed all the necessary amount of sample to all the analysts, I began the preparation of my own samples.

The samples were dried in an oven at 100°C for about 24 hours and then ground using a pestle and mortar which was washed and dried between each sample. An automatic grinder was available, but the small amount of sediment made it quicker and more economic (in terms of sediment) to grind them manually. The ground sediment was transferred into clean, labelled, glass vials.

### 3.2 Coulometrics

#### 3.2.1 The Apparatus and Techniques

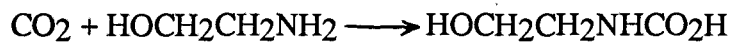
Most of the analytical work that I did at the Institute involved the use of coulometrics to determine the percentages of carbonate and organic carbon in each of the 520 sediment samples.

The coulometer can be used to analyse an acid gas in any gas stream. At the Institute, it is mainly used to analyse carbon dioxide. In sediment analysis, the sample is combusted or purged with acid to produce the carbon dioxide that is measured in the coulometric cell.

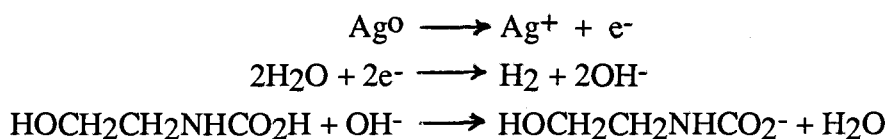
#### The Coulometer Cell (Fig. 6)

Two different solutions are used in the cell. The cathode solution consists of dimethylsulphoxide (DMSO), a non-aqueous solvent; tetraethylammonium bromide, which acts as the electrolyte; a thymolphthein indicator; water as the reducible species; and ethanolamine, which reacts with the carbon dioxide. The anode solution is essentially a saturated solution of potassium iodide in DMSO.

The incoming carbon dioxide reacts with the ethanolamine to produce hydroxycarbonic acid:



This is a strong titratable acid which causes the blue indicator colour to fade. The photometer recognises the colour fade and initiates electrochemical generation of a base

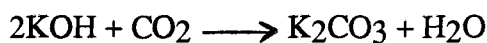


The current needed to bring the indicator back to its original colour is integrated and displayed as  $\mu\text{g C}$ .

In the following pages I discuss how the carbonate and organic carbon in the sediment are converted to carbon dioxide gas in order to be measured.

### Carbonate Analysis by Acidification (Fig. 7)

Small sample boats were made from aluminium foil. A sediment sample (about 15-30mg) was weighed into a boat which was then placed in a small pear-shaped flask. This was connected to the bottom of the condenser. Phosphoric acid (10%, 5ml) was added to the sample and the timer on the coulometer was started. Air was pumped through a potassium hydroxide solution (45% wt/wt) to remove all carbon dioxide before reaching the sample:



The gas given off from the sample was taken up in the gas stream and passed through a potassium iodide scrubber to remove all other acidic product gases such as  $\text{SO}_2$ ,  $\text{H}_2\text{S}$ ,  $\text{HCl}$  and  $\text{NO}_x$ . The carbon dioxide produced from the reaction of acid with the carbonate in the sediment passed into the coulometric cell where it was analysed. The analysis ran for six minutes.



### Organic Carbon Analysis

Organic carbon percentage was not measured directly by the coulometric method. Instead it was derived by combusting the sample. Combustion converts both the carbonate and the organic carbon to carbon dioxide, thus giving a total carbon value. Since this value is the sum of the inorganic carbon (from the acidification method described above) and the organic carbon, the organic carbon can be easily calculated from the two data sets:-  $\text{C}_{\text{org}} = \text{TC} - \text{IC}$ .

[NB. It is possible to measure organic carbon directly by combustion by first removing the carbonate from the sediment by acidification, but this method is more susceptible to errors.]

### Total Carbon Analysis by Combustion (See Fig. 8)

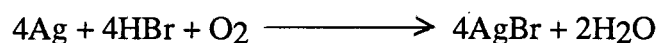
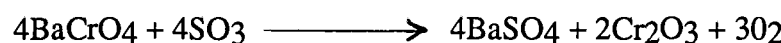
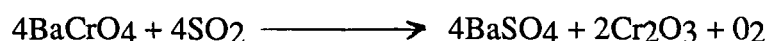
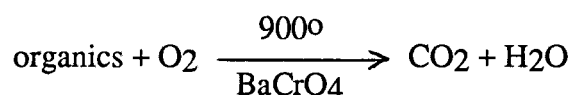
Small sheets of nickel were cut and folded to make sample boats. These were put in a high temperature furnace at  $1200^\circ\text{C}$  for about ten minutes to burn off any carbon. After this, the boats were only handled with metal tweezers. Samples were weighed into the boats (15-30mg) and a small amount of tungsten trioxide was added to help protect the glassware in the coulometric furnace.

The coulometer furnace was set at 900°C. The sample was placed in a quartz glass ladle which was pushed into the centre of the furnace with a magnet.

The carrier gas was oxygen from a cylinder and had been passed through scrubbers prior to being introduced to the sample. The first of the precombustion scrubbers was barium chromate which was heated in the furnace. This reacted with any sulphur compounds or hydrocarbons and removed them from the gas stream. This is perhaps of more importance where an external air stream is used rather than an oxygen cylinder. The second precombustion scrubber was potassium hydroxide solution, as used for the carbonate analysis.

The gases produced from the burning of the sample passed through several scrubbers, the reactions of which are summarised below. Product gases may include hydrogen chloride and oxides of sulphur depending on the nature of the sediment.

Reactions in the combustion tube:



Reaction in the magnesium perchlorate scrubber:



The gas stream then passed into the coulometer cell and the carbon dioxide was analysed as before. The analysis ran for six minutes.

## Day to Day Running of Coulometer

Blank readings (with no sample present) were taken frequently throughout a day's analysis and used in the calculations (see below). This reading was a measure of the residual carbon dioxide in the system.

Performance of the equipment was checked by regularly running bulk samples (samples of known total carbon and carbonate percentage) and comparing the actual result with the theoretical ones. If these did not match well, then one had to assume there was a fault in the equipment which must be dealt with before proceeding with sample analysis (see "3.2.4 Problems encountered").

The anode and cathode solutions were thrown away at the end of each day's analysis and the cell cleaned thoroughly with distilled water. The glass frit was cleaned by drawing distilled water through it with a vacuum pump. The electrodes were cleaned before use. The silver electrode wears away in the electrochemical reaction in the cell and must be replaced when it becomes thin. The potassium hydroxide and iodide scrubbers should be changed every four to five days or when determinations on bulk samples become too high or erratic.

The aluminium boats for carbonate analysis were used only once. The nickel boats for total carbon analysis were used several times in one day. The boats were 'cleaned' between each sample run by heating in the high temperature furnace for five minutes. They were thrown away at the end of each day's analysis.

## Calculations from the Coulometer Readings

For both the carbonate and the total carbon analyses, the reading on the coulometer was given in  $\mu\text{g}$  carbon.

Suppose,      Reading =  $A \mu\text{g C}$   
                   Blank =  $B \mu\text{g C}$   
                   Mass of sediment =  $M \text{ mg of sediment}$

Then,      True reading,  $X, = (A-B) \mu\text{g C}$

$X \mu\text{g C}$  contained in  $M \text{ mg sediment}$

$\frac{X}{1000} \text{ mg C contained in } M \text{ mg sediment}$

$\%C = \frac{X/1000}{M} \times 100\%$

This is the total carbon percentage (TC%) for total carbon analysis or the inorganic carbon percentage (IC%) for carbonate analysis. To obtain the percentage calcium carbonate from this, we use the relative molecular mass:

$$\begin{aligned}\% \text{ CaCO}_3 &= \% \text{C} \times \frac{\text{RMM}(\text{CaCO}_3)}{\text{RMM}(\text{C})} \\ &= \% \text{C} \times \frac{100}{12}\end{aligned}$$

In order to obtain an organic carbon percentage (C<sub>org</sub>%) for a particular sample:

$$\text{TC\%} - \text{IC\%} = \text{C}_{\text{org}}\%$$

I also calculated organic carbon on a calcium carbonate-free basis for each sample. This expresses the organic carbon as a percentage of the non-carbonate part of the sediment, thus removing the carbonate dilutant from the organic carbon signal.

$$\text{CaCO}_3 = \chi\%$$

$$\text{non-CaCO}_3 = 100 - \chi\%$$

$$\text{Carbonate-free organic carbon} = \text{OC\%} \times \frac{100\%}{(100 - \chi)}$$

### 3.2.2 The Carbonate-Free Organic Carbon Plot.

Many marine sediment analysts would not calculate carbonate-free organic carbon because they feel that carbonate and organic carbon are too closely related to each other in the water column. This is because, for their samples, the main source of these two constituents is from one animal population - the grazers (forams and pteropods). As a result the two constituents tend to co-vary down core. This rule might not apply at site PC12, which is thought to be near the boundary between two planktonic populations - the plants and the grazers.

The Grazers:

	skeleton	soft
	constituent	parts
- forams	CaCO <sub>3</sub>	C <sub>org</sub>
- pteropods	CaCO <sub>3</sub>	C <sub>org</sub>

Therefore, CaCO<sub>3</sub> dominant over C<sub>org</sub>

The Plants:

	skeleton	soft
	constituent	parts
- coccoliths	CaCO <sub>3</sub>	Corg
- diatoms	SiO <sub>2</sub>	Corg
- dinoflagellates	Chitin	Corg

Therefore, Corg dominant over CaCO<sub>3</sub>

Given these differences, changes in surface water over the site might be expected to lead to different patterns of carbon and carbonate sedimentation with time as the ratio of the two populations changes. This can be shown using the simplistic diagram below.

If the western boundary of the current shifts westwards then the plants will be more abundant and so Corg will increase with respect to CaCO<sub>3</sub>. If that boundary shifts eastwards then the grazers become more abundant and so CaCO<sub>3</sub> will increase with respect to Corg.

### 3.2.3 Results and Discussion

The results of coulometric analysis of core PC12 and the pilot core PG12 are shown in Fig. 10.

About 1 in 10 samples were analysed in duplicate and the average precision of these duplicate values for calcium carbonate and total carbon was  $\pm 1.04\%$  and  $\pm 0.79\%$  respectively. Accuracy was calculated from replicate analysis of bulk samples of standards, and found to be  $\pm 1.21\%$ . See later for a discussion of the methods of calculations used.

Before interpreting the down-core patterns of carbon and carbonate it is important to bear in mind that fluctuations in carbonate may not simply reflect the abundance of plankton of one kind or another. It is also possible that the influx of carbonate did not change at all, but rather that the influx of terrestrial material changed, causing changes in the relative proportions of calcium carbonate down-core (see Fig 11). Alternatively, carbonate lows could represent periods of carbonate dissolution in acidic water. These different possibilities are considered in the interpretation (see later).

Note, also, that each centimetre down the core does not necessarily represent the same amount of time. Sediment accumulation rates can vary quite a bit with time, which means that the gradients of many of the carbon and carbonate peaks could change dramatically if the data were plotted on a time axis rather than a depth axis.

The first and most obvious observation to be made is that for all three profiles, the pilot core data is displaced from the piston core data. The possible reasons for this are discussed later in the section entitled "Problems encountered with coulometrics and the resultant data".

An important step in the interpretation of this data is to decipher "real" events (ie. events in the profiles which represent actual occurrences in the environment) from "unreal" events. For example, on the organic carbon profile for PC12 from 19 to 34cm, all the points show a smooth downward curve and, therefore, seem to represent a "real" event causing decreased carbon.

In contrast, the point at 141cm is much lower than any of its neighbours in all three of the profiles. Anomalies like this are unusual in the sediment record. Reference to the observations made when grinding this sample shows that it contained a large amount of shell, which, if it were silicified, might explain the uncharacteristic drop in carbonate and organic carbon.

The data obtained from PC12 at 13cm shows the importance of the carbonate-free organic carbon plot. The organic carbon for this sample seems abnormally low for this section of the core but when expressed as a percentage of the non-carbonate part of the sample, it differs only slightly from its neighbours. This shows that there was no decrease of organic carbon input to the sediment at the time, but rather an increase in carbonate sufficient to make the organic carbon appear depleted.

Changes in organic carbon in the core can represent changes in upwelling patterns. High carbon suggests increased upwelling of cold, nutrient-rich water giving higher productivity. Low carbon suggests decreased upwelling resulting in warmer, nutrient-depleted surface waters.

Discussion of two sections of the core, below, show how the three coulometric profiles can be used to interpret the upwelling patterns in the area. More extensive interpretations are presented later (Interpretation of all Results section).

#### **PC12 Core Section 280-300cm.**

The strong decrease in organic carbon over this section could mean decreased upwelling and warmer waters. However, the carbonate is also depleted down this section which suggests a greater influx of terrestrial matter diluting the signal of the other sediment constituents. This section, therefore, probably represents a combination in changes of the two factors, upwelling and input of terrestrial matter.

## PC12 Core Section 400-440cm.

A steady increase in organic carbon, suggests more upwelling currents. The carbonate percentage stays relatively static over this period which means there is no increase in terrestrial matter diluting the carbonate signal. Also, the calculation of carbonate-free organic carbon hardly changes the pattern of the profile (ie. there is no dilution effect from the carbonate). Therefore, this is probably a real signal of decreased upwelling and warmer, nutrient-depleted surface waters.

### 3.2.4 Problems Encountered with Coulometrics and the Resultant Data

The main problems I met with the coulometric methods and data are listed below:

- i) Technical problems with the apparatus
- ii) Deliquescence of sediment samples
- iii) Contrasting pilot and piston core data
- iv) Suspicion of high organic carbon values

#### i) Technical Problems with the Apparatus

This is rather a general heading since problems of this nature were quite frequent and cover a wide range of possibilities.

The first step towards solving such problems is to acknowledge their existence. Faults such as no reading on the display unit, or wildly high blank readings, are easily recognised, but leaks, or a build up of pressure in the system, may not be noticed for some time and may show up in the bulk readings only subtly if at all.

The next stage is to isolate where and what the problem is. Again, this may be obvious, but sometimes requires logical, step-by-step investigation. Leaks in the system can be detected by applying soapy water with a pipette to all of the joints; foaming will occur where there is a leak. If there are no leaks, then the fault may be in the coulometer or in the acidification/furnace apparatus. The chemistry laboratory has two coulometers, which helps answer this question. For example, if the furnace apparatus gives bad results when attached to one coulometer, but good results when attached to the second coulometer, one assumes that the fault was in the original coulometer. And so the elimination of possible causes of the problem continues until, hopefully, the fault is found.

Once isolated, the fault must be corrected. This could mean anything from adjusting the gas flow rate or tightening an electrode connection to changing an exhausted scrubber solution or cleaning a blocked frit by soaking in chromic acid. It is important to remember that if solving the problem took a lot of time or involved opening of the system to the air or changing a piece of glassware, then the apparatus may have to be allowed to run for some time before correct bulk readings can be achieved. This is because carbon dioxide from the air is absorbed on to the glass surface and would consequently interfere with the readings.

## ii) Deliquescence of Sediment Samples

During analysis of the first 100cm section of the piston core I began to suspect that the samples had absorbed water after they had been dried and ground. There were three main reasons why I thought this. The samples had become cakey and clung to the sides of the vials; the samples were more dense than they had been originally; and the magnesium perchlorate scrubber on the coulometric furnace was being used up at an abnormally fast rate.

The high organic content meant that the samples were likely to absorb water from the atmosphere. To investigate whether or not this had happened, some of the samples already analysed were dried in the oven at 100°C overnight and re-analysed. They all gave higher carbonate and total carbon values than before (See Appendix 1).

To check that this discovery was not merely a result of the coulometer producing high results on that particular day, I took one sample, PC12 104-105cm, and dried only half of it. When it was dry, I analysed the dried half and the original half for total carbon. The samples that were dried gave higher values than those that were not (see Appendix 2). This was evidence that samples were absorbing water and consequently giving incorrect (low) results. The percentage change in all values before and after drying, and the mean and standard deviation of this percentage change, were calculated for total carbon and carbonate (see Appendix 1). Because the change seemed to be consistent and had a low standard deviation it was agreed that the inorganic carbon and total carbon values for the core section from 0-1cm to 99-100cm should be corrected using the mean percentage change.

To prevent this problem recurring, all samples were re-dried and kept in desiccators before analysis.

### iii) Contrasting Pilot and Piston Core Data

One of our main concerns after I had completed coulometric analysis of the pilot core and the top of the piston core was that the results did not match. The carbonate was considerably higher and the organic carbon lower in the pilot core than in the piston core (see coulometric results: Fig. 10).

Our first concern, was that we might have the wrong pilot core. Several cores were taken during the cruise and it is remotely possible that the pilot and piston were numbered incorrectly. By studying the cruise report (Summerhayes, 1974), we found that no other pilot cores were the same length as PG12 so confusion of cores would have been highly unlikely. To confirm this, we analysed a separate set of PG12 samples (sent to us from Bornhold in Canada and analysed in the 1970s) to check that these were the same. The results were similar enough for us to conclude that the samples were from the same core (see Appendix 3). This meant that the core sampled for our work was the same one analysed shortly after the core had been obtained.

Other evidence to verify my results could be found by looking at other cores taken close to PC12. We found data from three cores collected by Bremner of the University of Cape Town from near Walvis Bay - cores 4778, 4805 and 4804 (see Fig. 12). All three show a pattern like that in PC12-PG12, with high carbonate at the top of the core dropping sharply to lower carbonate at core depths of between 80cm and 120cm. Similar evidence can be seen from the percentage organic carbon plots (see Fig. 13).

This was reassuring. Nevertheless, the drop in carbonate from PG to PC is dramatic. It may indicate a loss of some sediment: ie. when the piston corer hit the sediment surface more than 82cm (the pilot core length) was wafted away and therefore not collected. Alternatively, the top part of the sediment column sampled by PC12 was lost by some other means. Dating of the core (in progress) may give an indication of how much sediment may have been lost.

### iv) Suspicion of High Organic Carbon Values

As mentioned earlier, a crude analysis had been performed on this core soon after its collection in 1975. Comparison between the coulometric data and the previous data showed that whilst my carbonate data agreed fairly well with the previous data, my organic carbon values were consistently higher than those previously obtained (see Fig. 14). It was therefore important to check that my data were correct. The organic carbon values are a product of the carbonate and the total carbon data. Since the new and old carbonate data agreed fairly well, we assumed that any error would have to be in the new or old total carbon data.

First, I checked to see if the problem was just an error in the calculation of the organic carbon percentage; it was not. This meant that the fault had to be in the coulometric equipment or in the analyses made by previous investigators. To test these ideas I collected various samples of known total carbon content. I analysed three sediment samples that the chemistry group had run on a modern LECO system. My results were very close to those obtained on the LECO (see Appendix 4(i)).

Two geostandards, MESS-1 - a marine sediment, and NBS88a - a adomitic limestone, also gave correct results on the coulometer. However, another geostandard, SGR-1 - an oil shale, gave a very much higher result than the literature value. This was thought to be caused by the oil in the shale interfering with the total carbon signal (see Appendix 4(ii))

Next, I took some organic compounds from the chemical store and calculated the theoretical percentage of total carbon by using the relative molecular masses. My coulometric analysis of these yielded results very close to those expected for all five compounds. (see Appendix 4(iii)).

As a final check on the validity of my organic carbon data, I organised some inter-laboratory comparisons. First I asked two independent scientists to analyse a few of my samples. The School of Chemistry, University of Bristol, already had some PC12 samples for UK37 analysis and they agreed to check Corg% for some samples down the core. Their results agreed very well with my own (see Appendix 4(iv)). Then I sent four PC12 samples, plus the standard MESS-1, to BP Research for them to analyse by the LECO method. In turn, they sent me five of their standard samples for carbonate and total carbon analysis. Our results agreed reasonably well for organic carbon content, but there did seem to be a discrepancy with the carbonate data. In general, the IOS carbonate values were slightly lower than those obtained at BP Research (see Appendix 4(v)).

With the cumulative evidence pointing towards my coulometric data for carbon being correct, I began to research the two analytical techniques used previously to see if there was any reason why their carbon results were so much lower. The previous organic carbon data were obtained by Bremner at the University of Cape Town, and Summerhayes at Woods Hole Oceanographic Institution in the 1970s.

Bremner used a method called Morgans Wet Chemical Technique (Morgans, 1954). This involved addition of excess oxidising agent - potassium dichromate ( $K_2Cr_2O_7$ ), in a sulphuric acid medium, to a known mass of sediment sample (in mg), and then back titrating to null point with ferrous sulphate ( $FeSO_4$ ). Assuming that 1 ml  $K_2Cr_2O_7$  is equivalent to 3mg of organic

carbon, we can calculate the dry weight percentage of organic carbon in the sediment by the following equation:

$$\% \text{ Corg} = \frac{V_1 - V_2}{M} \times 0.003 \times 100\%$$

where  $V_1$  = volume of N  $\text{K}_2\text{Cr}_2\text{O}_7$  (10.5ml)

$V_2$  = volume of N  $\text{FeSO}_4$  (ml)

$M$  = sample mass (mg)

It is assumed that there are no other substances in the sediment that could be oxidised by the potassium dichromate and that the nature and oxidation state of the organic matter is constant.

There is a risk in this method of losing organic carbon during the effervescence caused by addition of the acid. Morgans quoted an organic carbon recovery of only 75%. These factors might explain why Bremner's data did not agree with my own.

Summerhayes analysed core PC12 using the LECO system. This works in a similar way to the coulometrics method, in that carbon in the sediment is converted to carbon dioxide which is then measured. We do not have an exact account of what method Summerhayes used to prepare his samples, but it was quite common for organic carbon to be analysed in the following way: an acid (often hydrochloric or phosphoric acid) was added to a known mass of sample to remove all the carbonate carbon, then the residual sediment was burnt in a furnace to convert all the organic carbon to carbon dioxide which was then measured.

Several references suggest that this method is unreliable. Telek and Marshall (1974) state that "because of the organic coating that may form around carbonate nuclei (Chave 1965, Suess 1970) such acid treatment may not be completely or consistently effective." Others suggest that organic carbon is dissolved and lost to the acid, so that the result can be only 55% of the true value if the spent acid is discarded without analysis (Roberts et al, 1973; Hedges et al 1984; Froelich, 1980).

We are now confident that the coulometric results for organic carbon are correct.

## Inductively Coupled Plasma-Atomic Emission Spectroscopy

### 3.3.1 The Apparatus and Analytical Technique

#### Atomic Emission Spectroscopy

In atomic emission spectroscopy (AES) the atomic spectra emitted by a sample are used to determine its qualitative or quantitative elemental composition. The method works because excited atoms and ions emit radiation of a characteristic wavelength when electrons return from the excited state to ground state. AES uses the wavelength range 170nm to 780nm, which covers the visible, near ultra-violet, and some of the vacuum ultra-violet regions on the electromagnetic spectrum.

Glass absorbs radiation below 310nm, so optical lenses and prisms in the spectrometer should be made of quartz (which absorbs only below 160nm). Also, oxygen in air absorbs radiation below 200nm, so for detection of any elements that also absorb below this wavelength (such as arsenic, mercury and gold), the optical path of the spectrometer must be evacuated and filled with a non-absorbing gas such as argon. For ICP-AES, the system is always run with argon gas, regardless of the sample components.

Identification of the wavelengths present in an atomic emission spectra permits the qualitative analysis of a sample. Intensity (energy per unit time) of the spectral lines allows quantitative analysis of the sample.

#### The Inductively Coupled Plasma System

To excite atoms in a sample so that they emit spectra, there must be an excitation source which, for the spectrometer at IOSDL, is the inductively coupled plasma or ICP (Fig. 15).

This excitation depends on the interaction between the magnetic field of an oscillating radio-frequency current and the charged species present in the argon plasma. The current flows through a copper coil which is wound around the ICP tube. When the argon passes through the magnetic field, an annular (doughnut-shaped) plasma is formed at temperatures of more than 5000°C. The charged species within the plasma become highly accelerated.

When the sample solution is introduced, these particles collide with the gaseous sample atoms thus transferring energy to them and causing excitation of the sample atoms. The radiation is

emitted from the ICP "flame" when the atoms return to ground state and is analysed by the spectrometer.

## Sample Introduction

The sample to be analysed is in solution (see "Sample Preparation" below), but if this were injected directly into the ICP, the plasma would be extinguished and analysis would be impossible. Therefore, the sample must be passed through a nebuliser to convert it into an aerosol. There are two main types of nebuliser: the concentric design (Fig. 17) and the crossflow design. Both work to the same principle, and utilise the Venturi effect in which reduced pressure resulting from a fast moving gas jet causes solution to be drawn into the gas and broken up into droplets. Ideally, these droplets should be less than  $10\mu\text{m}$  diameter. In practise, however, many larger droplets are produced which must be drained away. Consequently, only 0.5 - 1.5% of the sample solution reaches the excitation source. A pump is used to control the flow rate of the liquid entering the nebuliser.

## Summary

Fig. 17 summaries the ICP-AES system.

### 3.3.2 Sample Preparation

There was not time to analyse the whole core for inorganic constituents. We were particularly interested in seeing what changes might occur in these constituents when there was an environmental change, so we used the carbon and carbonate data to suggest what would be a good core section to analyse.

It was decided that the core section 264-354cm would be used for detailed mineralogical study using ICP-AES. This particular section was chosen because in this area the organic carbon profile showed a deep and quite sharp trough (coulometric data, Fig. 10). We suspected that the carbon data represented an environmental change from upwelling (carbon-rich) to non-upwelling (carbon-poor) and back to upwelling (carbon-rich). Such changes might be expected to be accompanied by changes in wind strength and direction, reflected in the mineralogy and inorganic geochemistry of the sediment.

The samples had already been dried and ground prior to coulometric analysis. Because of a shortage of available sediment it was decided to analyse samples at 2cm intervals (instead of 1cm) and to get enough sample by combining adjacent 1cm samples. Rather than begin the

lengthy process of mixing two powdered samples from adjacent core depths to make them homogenous, and then weighing out the 0.5 grams needed for the analysis, 0.25 grams of each 1cm sample was weighed out and then placed with its neighbouring sample in a clean, glass vial. Since the next stage of the sample preparation was dissolution, homogeneity was assured. Note, that this meant the two samples (for example) 266-267cm and 267-268cm became 266-268cm and, after analysis, was plotted as the intermediate value, 267cm.

### **Acid dissolution**

The samples had to be in liquid form in order to be analysed by the ICP-AES. This meant dissolving the samples in acid. Nitric acid, perchloric acid and hydrofluoric acid were used.

**Safety note:** Perchloric acid is highly oxidising and if it comes into contact with any organic matter explosions may occur. Hydrofluoric acid is extremely poisonous by inhalation and on contact with skin causes severe burns.

### **Procedure**

The weighed samples (0.5g) were put into labelled PTFE beakers. Glass could not be used as it is eroded by hydrofluoric acid. A small amount of double distilled water was added to a sample. The beaker was agitated so that all sediment was wet. This helped to prevent excess effervescence and consequent loss of sample when the acid was added.

The samples had to be treated with nitric acid before addition of the perchloric acid because they contained a high amount of organics. Concentrated nitric acid (10ml) was added to the sample and heated slowly to evaporation and dryness of sediment on a hot plate. It was then allowed to cool. This was repeated using 5ml nitric acid instead of 10ml. All carbonate and organic matter should now be removed.

Hydrofluoric acid (5ml, 48%) and perchloric acid (4ml, 70%) were added to the sample which was placed on hot plate at the maximum setting. The beakers were gently swirled to break up the sediment and to wash away any from the sides, then were left on the hot plate for 30-60 minutes until the sample had been reduced to a thick, sticky residue. This was left to cool. Perchloric acid (3ml) was added and heated to leave a residue as before. This was to ensure that all the hydrofluoric acid had been removed. When the sample was cool, nitric acid (10ml, 5N) was added and the sample was left to stand overnight to dissolve the residue. Each sample solution was made up to 50cm<sup>3</sup> with double distilled water and transferred to plastic bottles.

These samples were then run through the ICP-AES.

### 3.3.3 Results and Discussion

Fig. 18 shows the coulometric data for this core section on the same scale as the ICP-AES data for easy comparison.

A total of 24 profiles of element or mineral composition against depth of core were produced by the AES. Five of these (As, Co, Pb, Na and Zr) are not shown with the rest of the results as they are believed to be unreliable or meaningless (see 3.3.4 Problems and Limitations).

I have separated out the rest of the data into two groups. The first group all show similar characteristics and include lithium, scandium and the oxides of aluminium, iron, potassium, magnesium and titanium (Fig. 19). The carbonate-free plots of some elements, and any other data manipulations for these elements are also shown in Fig. 19. All of these elements are usually unaffected by diagenesis (changes that take place in the sediment after its deposition, often involving oxidation) so are good indicators of the character of their geological sources, problem rocks and soils on land nearby. The profiles all show a very similar pattern, except for magnesium, which remains relatively constant. Magnesium is a constituent of the authigenic mineral dolomite, which might explain its independence from the other elements in this group. The pattern of the other elements in this group is approximately inverse to the  $\text{CaCO}_3$  profile (Fig. 18.1). This shows that the shape of the profiles is to some extent the product of dilution by carbonate, the major constituent present. The carbonate-free plots support this as the profiles are straightened out slightly. The extent to which these profiles are related to each other is demonstrated in Fig. 19.3 in which the strong linear relationship between aluminium and iron is clear. Fig. 19.12 shows that there is some relationship between scandium and carbonate.

Fig. 20 shows all the rest of the elements/minerals analysed. They are discussed individually below.

#### Barium (Fig. 20.1, 20.2 and 20.3)

This plot shows a trough at the same point as the organic carbon but to a much greater extent. The profile changes very little when plotted on a carbonate-free basis so there does not appear to be a dilution effect. A cross-plot of  $\text{Corg}\%$  against Ba ppm shows some relationship between the two but I do not feel confident that it is a linear relationship.

### **Calcium (Fig. 20.4 and 20.5)**

The calcium oxide in this core section does not vary greatly and has a very good linear relationship with the calcium carbonate data obtained from the coulometer.

### **Chromium (Fig. 20.6 and 20.7)**

These are quite high levels for chromium (the average value for shales is 90 ppm) which is often associated with sulphides. The C.F. plot enlarges a dip at 300cm.

### **Copper (Fig. 20.8 and 20.9)**

This profile appears more varied than many of the other plots showing a fluctuating input of copper in terrestrial matter. The C.F. profile does not change it significantly.

### **Manganese (Fig. 20.10)**

The manganese levels are very low. This suggests that most of the manganese was in solution in the pore waters. Dissolution of manganese by diagenetic processes is to be expected in the reducing environment of this organic rich core.

### **Molybdenum (Fig. 20.11 and 20.12)**

These very high values suggest a sulphidic environment. Again, the C.F. plot shows little change.

### **Nickel (Fig. 20.13 and 20.14)**

This profile is fairly constant although there does seem to be a slight gradient. As with chromium, the C.F. plot highlights a dip at 300cm.

### **Phosphorus (Fig. 20.15 and 20.16)**

Both the original and C.F. plot show no significant variations with depth. Phosphate could be present as fish teeth, which might be expected to follow other productivity indicators. There is no sign that phosphorus follows organic carbon. Alternatively, phosphate grains may be washed seawards by bottom currents from the shelf after storms resuspend phosphatic shelf sediments. In this case the phosphate could fluctuate independently of iron alumina silicates which may

come from dust falls or (less likely in view of the desert coast) from rivers. Phosphate may have precipitated in the sediment diagenetically. Further examination is needed to check this.

### **Strontium (Fig. 20.17 and 20.18)**

Sr correlates very well with  $\text{CaCO}_3\%$ , as illustrated by the cross-plot (Fig. 20.18). This was to be expected, as strontium substitutes for calcium in carbonates. Sr also substitutes for calcium in the apatite in fresh teeth and in phosphorite grains, so where strontium diverges from the carbonate plot (such as 266 to 279cm), this could be an apatite signal.

### **Vanadium (Fig. 20.19 and 20.20)**

These levels are lower than might be expected for a highly organic sediment (the average value for a shale is 120-130 ppm). The C.F. plot shows an unexplained dip at 317cm.

### **Yttrium (Fig. 20.21)**

These levels are as expected for sediments of this type.

### **Zinc (Fig. 20.22 and 20.23)**

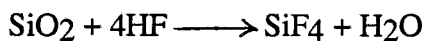
Zinc can sometimes be associated with organic matter but there does not seem to be a relationship between the two here.

The sample preparation did not allow analysis of silicon (see 3.3.4 Problems and Limitations). However, a silicon dioxide plot was estimated as follows, by using some of the other data sets. An average shale composition of silica, aluminium oxide, ferric oxide, magnesium oxide and potassium oxide was determined from three different literature sources (see Appendix 5). The ratio of silica to the four other minerals was then determined.

Since we knew the PC12 values for these four minerals, the silica could be calculated from this average ratio. Thus, Fig 21, silicon dioxide percentage against depth was produced. Also, from this, the silica-free organic carbon plot (Fig. 21.1) was produced, removing the silica dilution effect from the organic signal in the same way as the carbonate-free plot.

### 3.3.4 Problems and Limitations

As mentioned earlier, silica could not be analysed using this method. This is because the hydrofluoric acid reacts with the silica in the sediment which is lost as tetrafluorosilane gas.



Five elements for which values were obtained (Fig. 22) were found to be of no use for various reasons discussed below.

#### **Arsenic (Fig. 22.1)**

This plot does give the approximate amount of arsenic in the sediment but it is unreliable and the precision is bad. This is because a specific sample preparation, hydride generation, is needed. Hydride generation is also needed to obtain bismuth and celerium data.

#### **Cobalt (Fig. 22.2)**

Good precision and reliable data cannot be obtained for cobalt when it is at such low levels (4-5 ppm) in the sediment.

#### **Sodium (Fig. 22.3)**

This is an indicator of the salt content but is only useful if the samples had been washed before analysis which the PC12 samples had not.

#### **Lead (Fig. 22.4)**

These levels of lead are very close to the detection limit and the values are consequently very imprecise and unreliable.

#### **Zirconium (Fig. 22.5)**

This profile was considered unreliable as the ICP-AES was giving incorrect values for zirconium in standard samples.

### 3.4 Statistics

Various statistical manipulations of the analytical data were carried out in order to aid its interpretation and also to check its reliability. The types of statistics used are summarised in three parts below.

#### 3.4.1 Accuracy and Precision

Accuracy for the coulometer and for the ICP-AES were calculated from replicate analyses of standard bulk samples. Precision was calculated from duplicate and replicate analyses of randomly selected samples in the core, as described below.

##### Calculation from duplicate analyses.

The percentage deviation of each duplicate analysis from the mean of each pair of determinations is given by:

$$X_{pi} = \left[ \frac{X_i - X_{ii}}{2} \middle/ \frac{X_i + X_{ii}}{2} \right] \times 100$$

where  $X_i$  and  $X_{ii}$  represent the two determinations. The mean percentage deviation for all duplicates is given by:

$$X_p = \sum \frac{X_{pi}}{N}$$

where  $N$  represents the number of duplicate pairs. The standard deviation of the individual percentage deviations ( $X_{pi}$ ) about the mean percentage deviation ( $X_p$ ) is given by:

$$\sigma^2 = \frac{\sum (X_{pi} - X_p)^2}{N - 1}$$

At the 95% confidence level, if individual percentage deviations are normally distributed about the mean, the precision may be estimated thus:

$$P = \pm (X_p \pm 2\sigma) \%$$

##### Calculation from replicate analyses

Where five or more replicate determinations were carried out on one sample, precision (or accuracy) was calculated at the 95% confidence level thus:

$$P = \pm \frac{200}{X} \sqrt{\frac{\sum X^2 - N \cdot \bar{X}^2}{N - 1}}$$

### 3.4.2 Fast Fourier Transform

We suspected that while some of the high frequency signal in the carbon and carbonate data might be noise, some represented cyclicity at one or more periods. To check this hypothesis we analysed the data sets by fast fourier transform (f.f.t.). This is a mathematical method of analysing a data series that contains periodic variations such as seasonal precipitation. These can be represented by a series of sine or cosine functions.

The data sets were transferred on disc from the Apple Mac to an IBM mainframe computer where David Carter at IOSDL ran them through a f.f.t. package. The method he used assumes that all the data points were equally spaced. Although this is true in the depth sense, it may not be true in the time domain if the rate of sedimentation varied down core. Not having precise age information the data were kept as profiles against depth in centimetres and conversion to time in years was not attempted until after the fourier transform was completed.

## Results

Fig. 23, 24 and 25 show respectively the carbonate, organic carbon and carbonate-free organic carbon (CF) plots with the linear trend superimposed on them. Below each plot is the analysis of residuals. Note, at the  $N$ th frequency, frequency =  $N/400$ , wavelength =  $400/N$ . The analysis of residuals shows a large energy component at the first and second frequency.

Removing these components by least squares fit gave the results shown in Figs 26, 27 and 28. Carbonate has a peak at  $N = 5, 9$  and  $12$ . The corresponding wavelengths are shown on the data plots.

Fig. 29 shows the wavelengths remaining when the first five components ( $N = 1, 2, 5, 9$  and  $12$ ) are removed from the CF organic plot. This leaves peaks at  $N = 4$  and  $N = 7$  which appear to be significant. This suggests a broad band, low frequency spectrum rather than a few discrete frequencies.

Removing all the low frequencies up to  $N = 14$ , gives the spectra shown in Figs 30, 31 and 32. Whilst the carbonate plot shows peaks at  $N = 15, 17, 18$  and  $30$ ; the organic carbon and carbonate-free plots show a significant peak only at  $N = 28$ . Removal of this component ( $N = 28$ ) from the CF plot shows that any signal above this frequency is just noise (Fig. 33).

## Interpretations

If we assume that the sedimentation rate was constant, and that 400cm represents 100,000 years (estimated from the biostratigraphic data) then depth can be converted to time. Also, each significant frequency peak from the f.f.t. can be expressed as a time period. For example, the wavelength,  $N = 28$  represents a 3571 year cyclicity ( $100,000/N = 3571$ ). Below is a list of the significant wavelengths produced from the f.f.t. and the time that each represents using the above assumptions. Note, the most significant features are those with lowest value of  $N$ .

		Plots in which the peak is observed		
N	Years	CaCO <sub>3</sub>	C <sub>org</sub>	CF
1	100,000	*	*	*
5	20,000	*	*	*
9	11,100		*	*
12	8,300			*
15	6,700	*		
28	3,600			*
30	3,300	*		

The Milankovitch hypothesis states that the variations in the Earth's climate on the scales of  $10^4$  to  $10^5$  years are in a large part due to variations in the Earth's orbit around the sun. The orbital variations have three main components:

- changes in eccentricity (95,000 year cyclicity)
- changes in tilt of the Earth's axis (41,000 year cyclicity)
- changes in precession variation of longitude of the perihelion relative to the equinox (23,000 year cyclicity)

These variations produce changes both in total amount of radiation per annum received by the earth and in its distribution according to hemisphere and season.

The f.f.t. data appears to follow this hypothesis only in part. That is, the first and third components may be represented in our data by  $N = 1$  (100,000 years) and  $N = 5$  (20,000 years) but there does not seem to be a wavelength corresponding to the changes in tilt of the earth's axis at 41,000 years. I believe this highlights the weakness of the assumptions made: ie sedimentation rate may not be constant, and 400cm does not necessarily represent 100,000 years.

However, this analysis was successful in showing that there were several significant cyclic features in the coulometric data for both carbon and carbonate. Many of the wavelengths detected probably represent periodic changes in upwelling that were forced by periodic changes in winds in the South Atlantic.

### 3.4.2 Factor Analysis

Factor analysis is a statistical method for studying the interrelations between various trace elements in order to discover whether certain correlations allow an explanation in terms of one or more common factors.

This analysis was applied to the ICP-AES data to decipher how the elements and minerals were related to each other. Depth was included as a variable; the other 23 variables were:

$\text{Al}_2\text{O}_3$ ,  $\text{Fe}_2\text{O}_3$ ,  $\text{MnO}$ ,  $\text{MgO}$ ,  $\text{CaO}$ ,  $\text{Na}_2\text{O}$ ,  $\text{K}_2\text{O}$ ,  $\text{TiO}_2$ ,  $\text{Ba}$ ,  $\text{Co}$ ,  $\text{Cr}$ ,  $\text{Cu}$ ,  $\text{Li}$ ,  $\text{Mo}$ ,  $\text{Ni}$ ,  $\text{Sc}$ ,  $\text{Sr}$ ,  $\text{Y}$ ,  $\text{Zn}$ ,  $\text{P}_2\text{O}_5$ ,  $\text{V}$ ,  $\text{Corg}$  and  $\text{CaCO}_3$ .

The objective was to reduce the complexity represented by the 23 variables to a simple level (i.e. a few factors) representing highly correlated variables. These geochemical groupings, or factors, would be expected in turn to represent the mineralogy of the sediments (e.g. organic carbon, calcium carbonate, aluminosilicate clay minerals, and phosphorite - a natural phosphate rock made up principally of the mineral carbonate-fluorapatite). Principal components (factor) analysis is based on the correlation between the variables, so the first thing produced by the analysis is a correlation matrix (not reproduced here). The factors, which are statistically the dominant features of the data variation, are derived from the correlation matrix. The principal factor matrix is rotated to produce what is termed a varimax orthogonal solution in which each factor represents a single dimension in the data.

Ordering the variables within factors we find that factor 1 is dominated by one group that are positively correlated and another that is negatively correlated (table 1).

Factor 1      +     $\text{P}_2\text{O}_5$ ,  $\text{MnO}$ ,  $\text{TiO}_2$ ,  $\text{Co}$ ,  $\text{Na}_2\text{O}$ ,  $\text{Y}$ ,  $\text{Sc}$ ,  $\text{Mo}$ ,  $\text{V}$ ,  $\text{Cr}$ ,  $\text{Li}$ ,  $\text{K}_2\text{O}$ ,  $\text{Cu}$   
-     $\text{Fe}_2\text{O}_3$ ,  $\text{Zn}$ ,  $\text{Corg}$ , Depth,  $\text{CaCO}_3$ ,  $\text{CaO}$ ,  $\text{Sr}$

We have to remember that the elemental analyses were carried out on sediments crossing a major event within the core; above and below the event the sediments were rich in organic matter and calcium carbonate, while at the peak of the event both of these components were reduced. Factor 1 reflects this major event. The negative group consists of organic carbon

(Corg) and calcium carbonate ( $\text{CaCO}_3$ ),  $\text{CaO}$  and  $\text{Sr}$  - which substitutes for  $\text{Ca}$  in carbonates). The association of  $\text{Fe}_2\text{O}_3$  and  $\text{Zn}$  with this group probably reflects the abundance of pyrite in the organic rich sediment, which was preserved under reducing conditions ( $\text{Fe}_2\text{O}_3$  in the print-out represents  $\text{Fe}$ , not iron oxides).

The positive group in factor 1 looks like a detrital mineral deposit associated with oxidising conditions.  $\text{P}_2\text{O}_5$  represents phosphorite, which is abundant at outcrop and in the sediment of the nearby continental shelf.  $\text{K}_2\text{O}$  and  $\text{Na}_2\text{O}$  are likely to represent clays like glauconite, another mineral common to shelves.  $\text{TiO}_2$  and  $\text{Cr}$  are likely to represent heavy minerals like rutile.  $\text{MnO}$  (representing  $\text{Mn}$ ) is commonly abundant in oxidised shelf sediments.

Ordering the variables within factor 2 we find that it is also dominated by two groups (table 1).

Factor 2	+	$\text{Al}_2\text{O}_3$ , $\text{K}_2\text{O}$ , $\text{Li}$ , $\text{V}$ , $\text{Cr}$ , $\text{Mo}$ , $\text{Sc}$ , $\text{Co}$ , $\text{Y}$ , $\text{P}_2\text{O}_5$ , $\text{TiO}_2$ , $\text{MnO}$
	-	$\text{Ba}$ , $\text{CaO}$ , $\text{CaCO}_3$ , $\text{Sr}$ , $\text{Zn}$ , Depth

The positive group is clearly dominated by an aluminosilicate group (clay minerals):  $\text{Al}_2\text{O}_3$ ,  $\text{K}_2\text{O}$ ,  $\text{Li}$ ,  $\text{V}$ ,  $\text{Cr}$ ,  $\text{Mo}$ ,  $\text{Sc}$ ,  $\text{Co}$ ) and has a weak association with phosphorite ( $\text{P}_2\text{O}_5$ ), heavy minerals ( $\text{TiO}_2$ ), and oxidising conditions ( $\text{MnO}$ ). This is opposed to a calcium carbonate group ( $\text{CaO}$ ,  $\text{CaCO}_3$ ,  $\text{Sr}$ ) representing calcareous plankton;  $\text{Ba}$  is commonly associated with these carbonates. This suggests that there is a natural interplay in these sediments between planktonic remains and detritus that could be blown in from the desert, or be winnowed off the shelf, or be supplied by rivers (less likely but not impossible).

Ordering the variables within factor 3 we find that it too is dominated by two groups (table 1).

Factor 3	+	$\text{Ni}$ , $\text{Cu}$ , $\text{Corg}$ , $\text{Cr}$ , $\text{Na}_2\text{O}$ , $\text{Mo}$ , $\text{Y}$ , $\text{V}$ , $\text{P}_2\text{O}_5$ , $\text{TiO}_2$ , $\text{Co}$ , $\text{MnO}$ , $\text{Sc}$
	-	Depth, $\text{Sr}$ , $\text{CaO}$ , $\text{CaCO}_3$ , $\text{Fe}_2\text{O}_3$

Taking the positively loaded variables first, it is common to find many minor elements, like  $\text{Ni}$  and  $\text{Cu}$ , associated with the organic factor (Corg) in these kinds of environments. Apart from Corg,  $\text{Ni}$ ,  $\text{Cu}$  and  $\text{Cr}$ , most other variables are very weakly loaded in this group (loadings of less than 0.4) and their presence may not be significant.

The negative loadings really all represent calcium carbonate, which we know from the coulometrics data is the inverse of Corg down core.

Factor 4 accounts for a very small amount of the variance (table 1). It is dominated by MgO, probably representing the mineral dolomite. Dolomite can form within the sediment by diagenetic processes, which may explain why it is not related to the five other major mineral components Corg, CaCO<sub>3</sub>, aluminosilicate clay minerals, phosphorite (P<sub>2</sub>O<sub>5</sub>) and pyrite.

**Table 1**

**Rotated factor pattern:**

**Only factors with eigen values greater than 1.0 and only factor loadings greater than 0.3 are regarded as significant.**

	Factor 1	Factor 2	Factor 3	Factor 4
Eigen value	17.69	2.38	1.91	1.19
variance	73.70	9.90	7.94	4.95
<u>Variable</u>				
Depth	-0.65	-0.35	-0.62	
Al <sub>2</sub> O <sub>3</sub>		0.97		
Fe <sub>2</sub> O <sub>3</sub>	-0.91		-0.34	
MnO	0.81	0.48	0.32	
MgO				0.92
CaO	-0.41	-0.77	-0.44	
Na <sub>2</sub> O	0.78		0.38	0.40
K <sub>2</sub> O	0.38	0.87		
TiO <sub>2</sub>	0.81	0.48	0.32	
Ba		-0.79		-0.32
Co	0.80	0.50	0.31	
Cr	0.74	0.53	0.40	
Cu	0.37		0.85	
Li	0.49	0.83		
Mo	0.75	0.53	0.36	
Ni			0.90	
Sc	0.79	0.51	0.31	
Sr	-0.41	-0.71	-0.55	
Y	0.79	0.50	0.33	
Zn	-0.81	-0.48		
P <sub>2</sub> O <sub>5</sub>	0.81	0.48	0.32	
V	0.75	0.56	0.32	
Corg	-0.80		0.47	
CaCO <sub>3</sub>	-0.49	-0.57	-0.43	

### **3.5 Use of Computers**

During my analytical work at IOSDL, I was able to gain experience of using various computer systems mostly for processing the data obtained from analysis. Listed below are the four main computer systems that were used.

#### **The Toshiba 2000 - lap-top computer**

The Toshiba was used at the beginning of my industrial placement to summarise all the previous data from the core that was available.

I wrote a short program using the "Quattro" package to enable me to do speedy precision calculations for duplicate analyses. The word processing package "Word" package was used to write correspondence to other members of the analytical team.

#### **The IBM Mainframe**

This was used to analyse my coulometric data by fast fourier transform (see "3.4 Statistics").

#### **The IBM personal computer**

This computer was connected to the ICP-AES and processed the data on Quattro. I was able to enter other information, such as the coulometric data, to compare with the mineralogy data.

#### **The Apple Macintosh**

Cricket Graph - this package was used extensively to store and plot the coulometric data. The previous data and all the other graphs in this report were stored and plotted from this package.

Mac Draw II - most of the diagrams in this report were produced from this drawing package.



Fig 6. The coulometer cell.

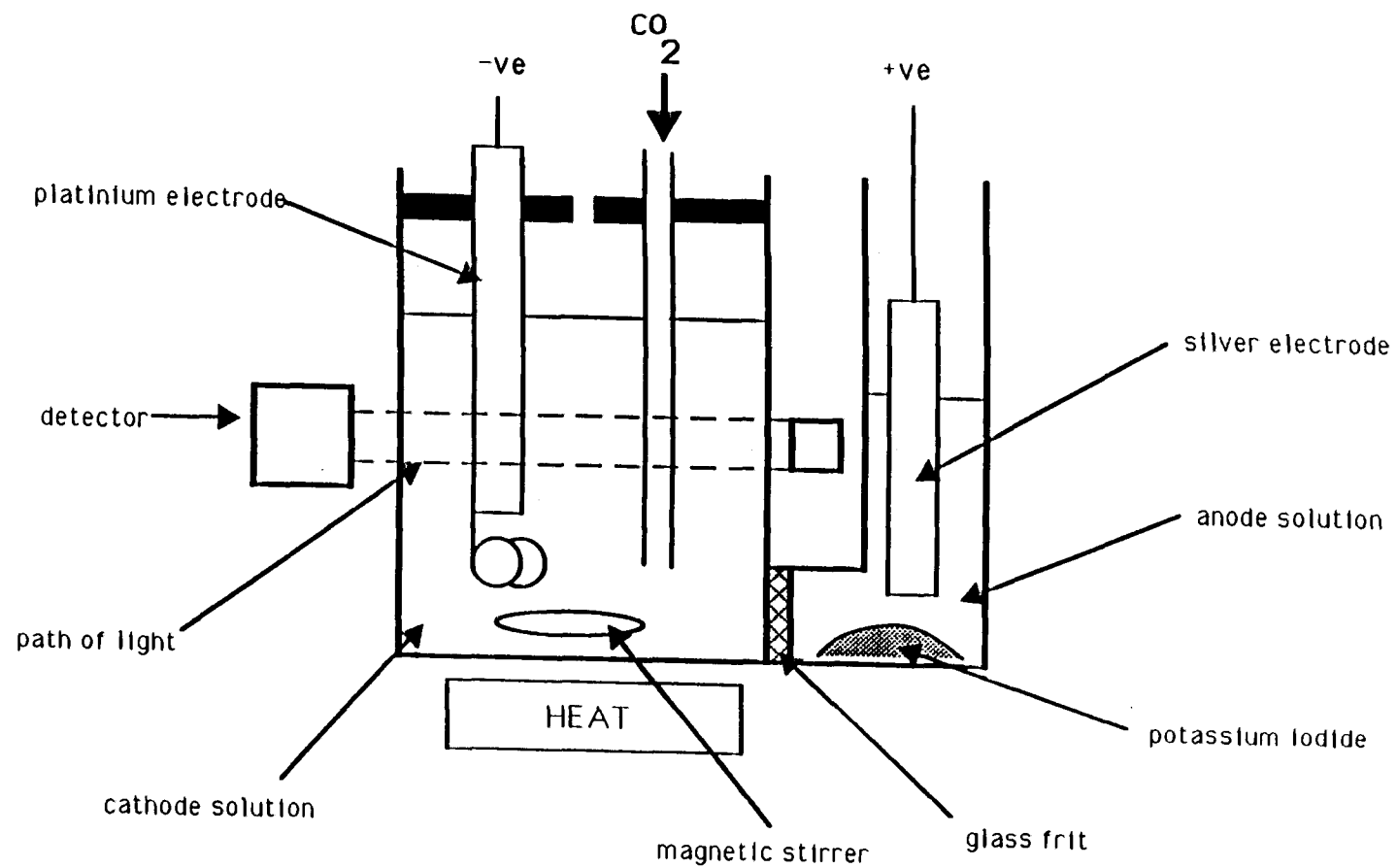


Fig 7. Acidification apparatus for carbonate analysis.

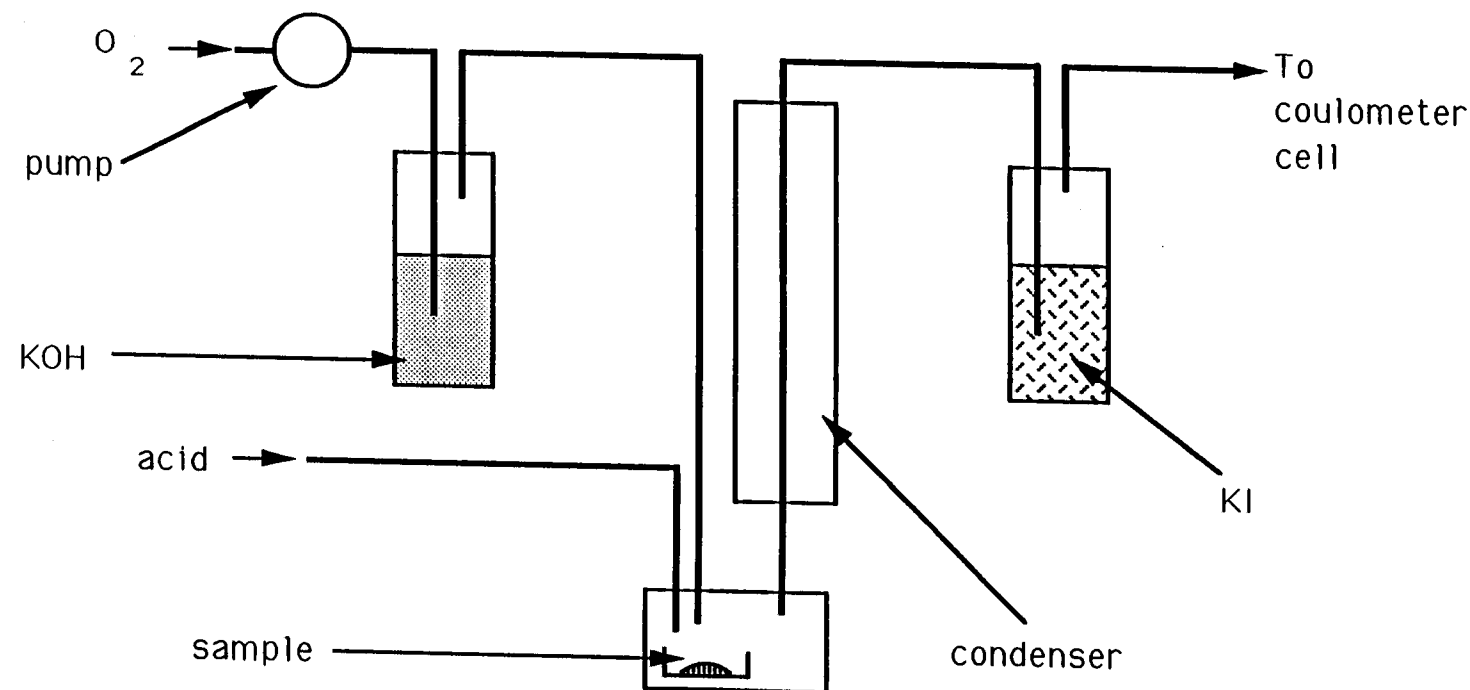
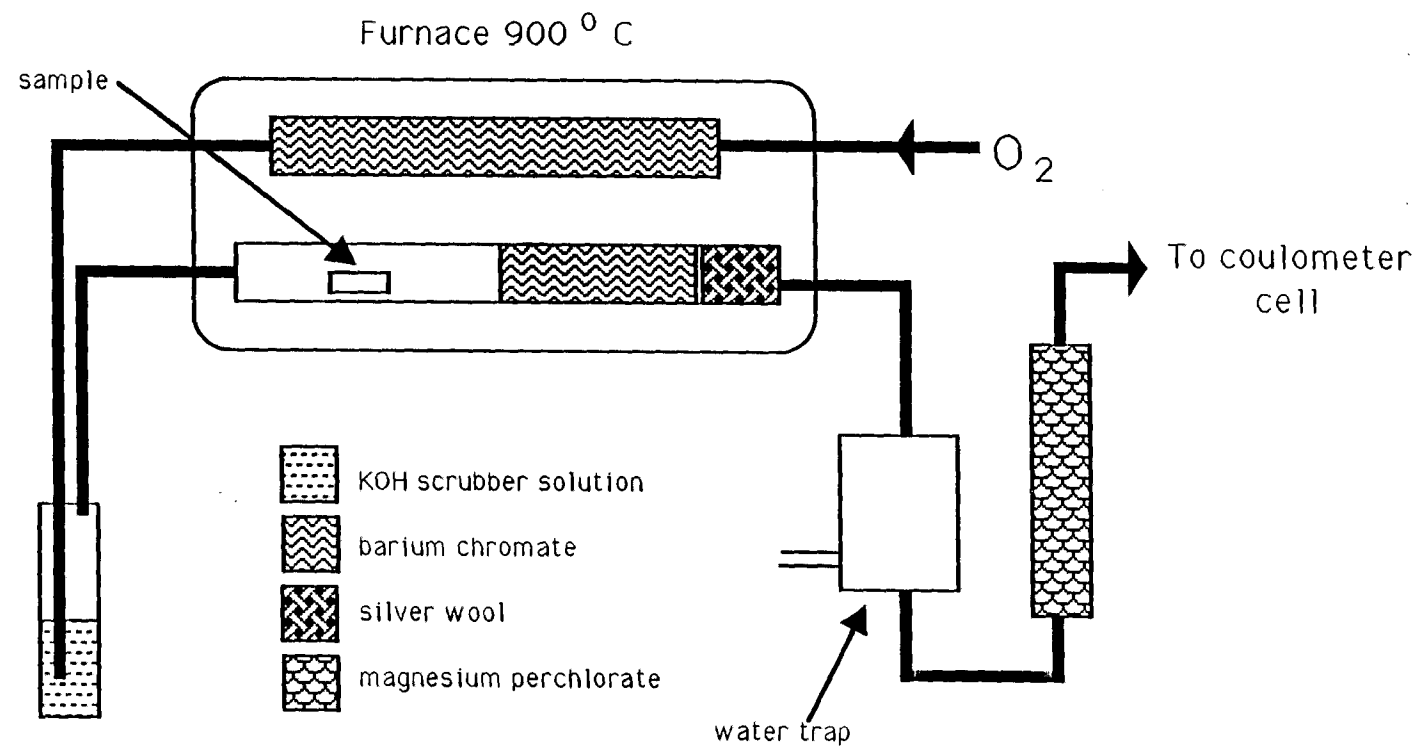
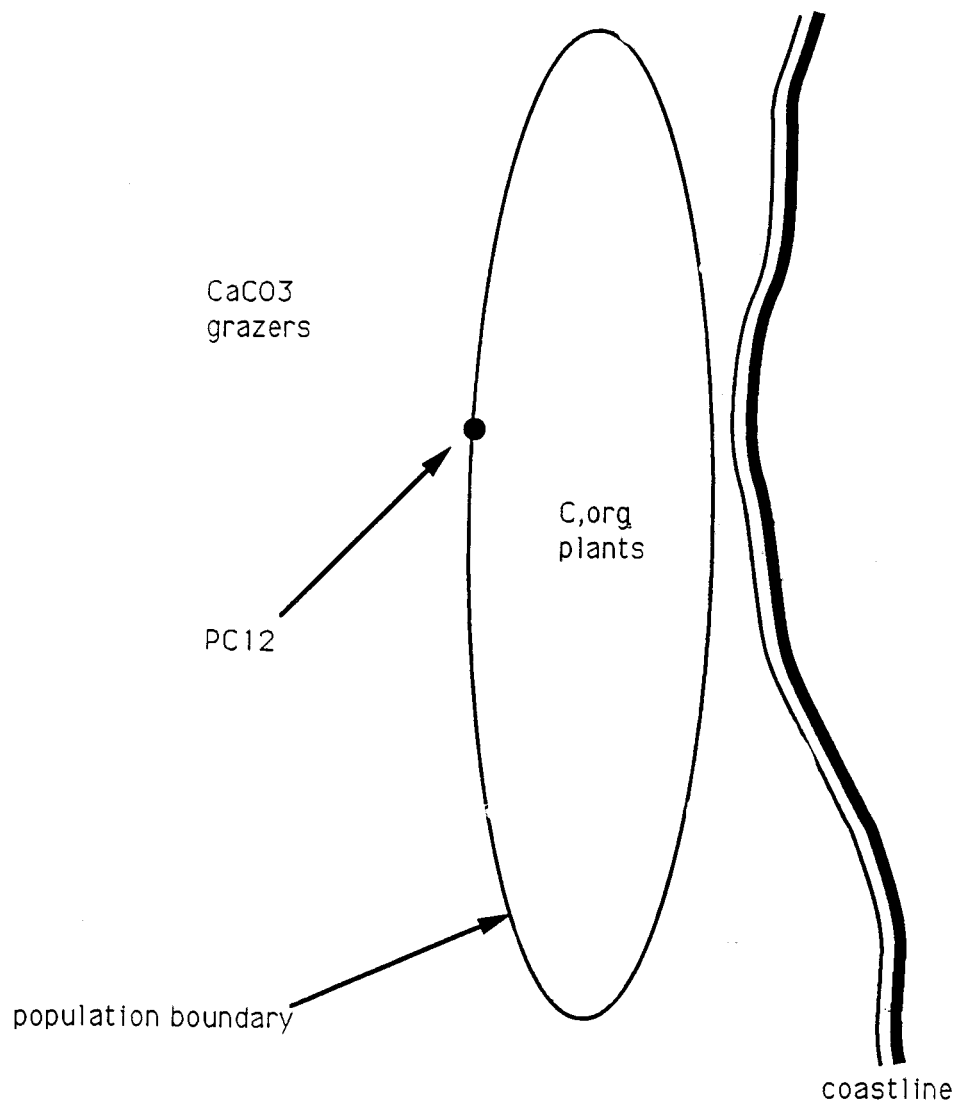


Fig 8. Combustion apparatus for total carbon analysis.



**Fig 9. Diagram to show the possible position of PC12 on the boundary of a current carrying plant populations.**





**Fig 10.** The coulometric data obtained from the pilot and piston core 12.

NB, Pilot core plotted from 0cm to 81cm.  
Piston core plotted from 82cm to 620cm.

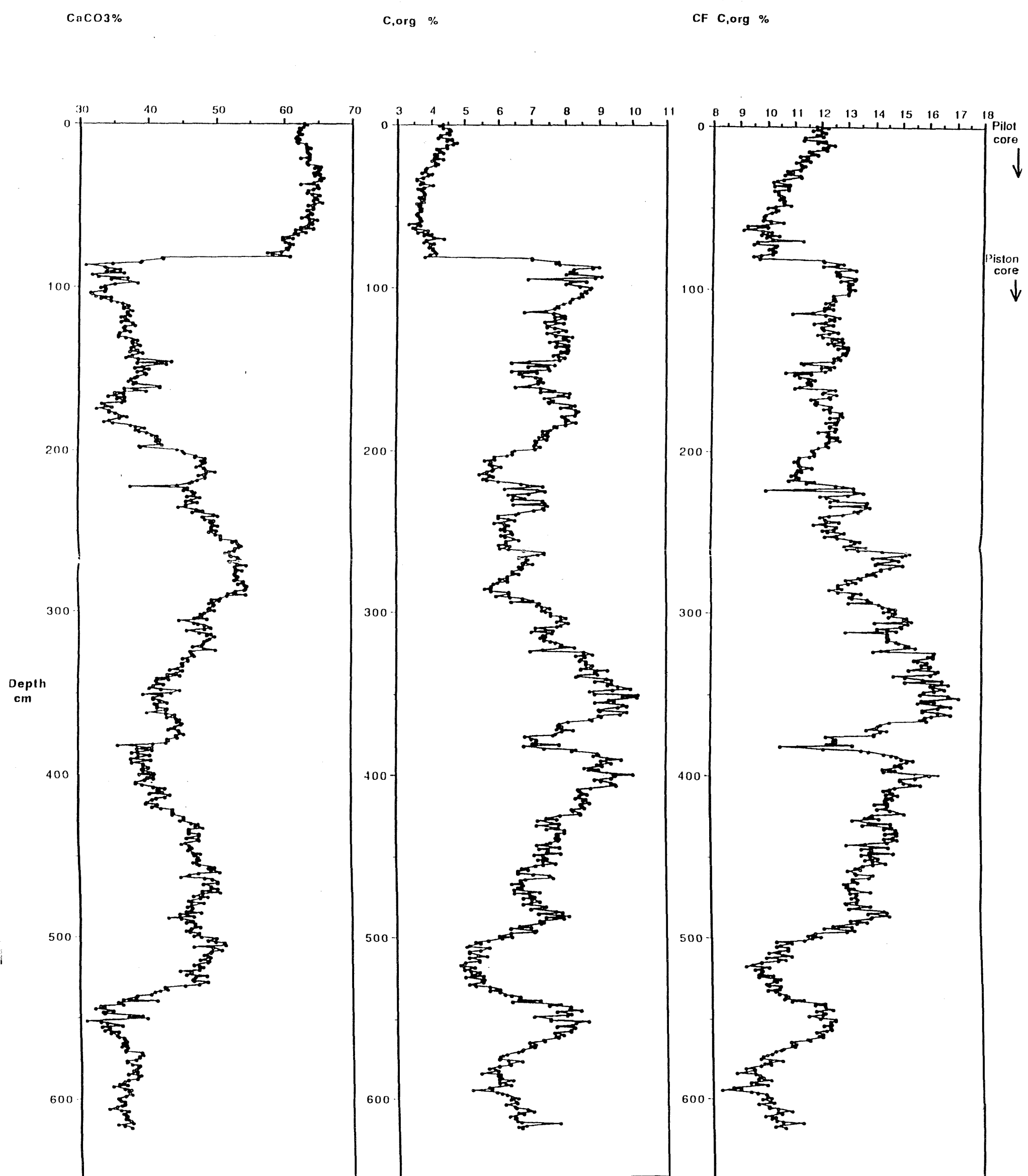


Fig 11. An example of how  $\text{CaCO}_3\%$  might vary with influx of terrestrial material.

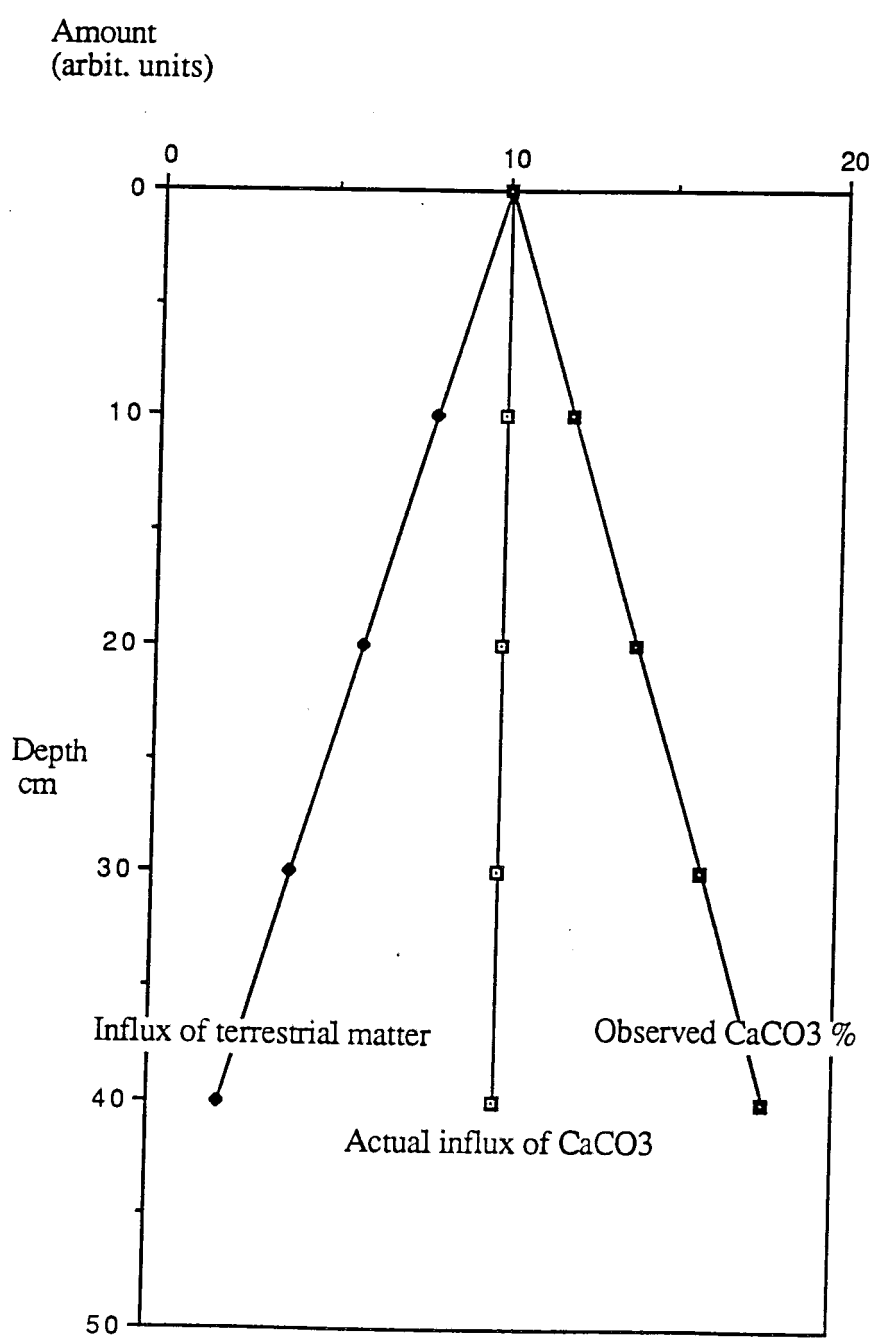
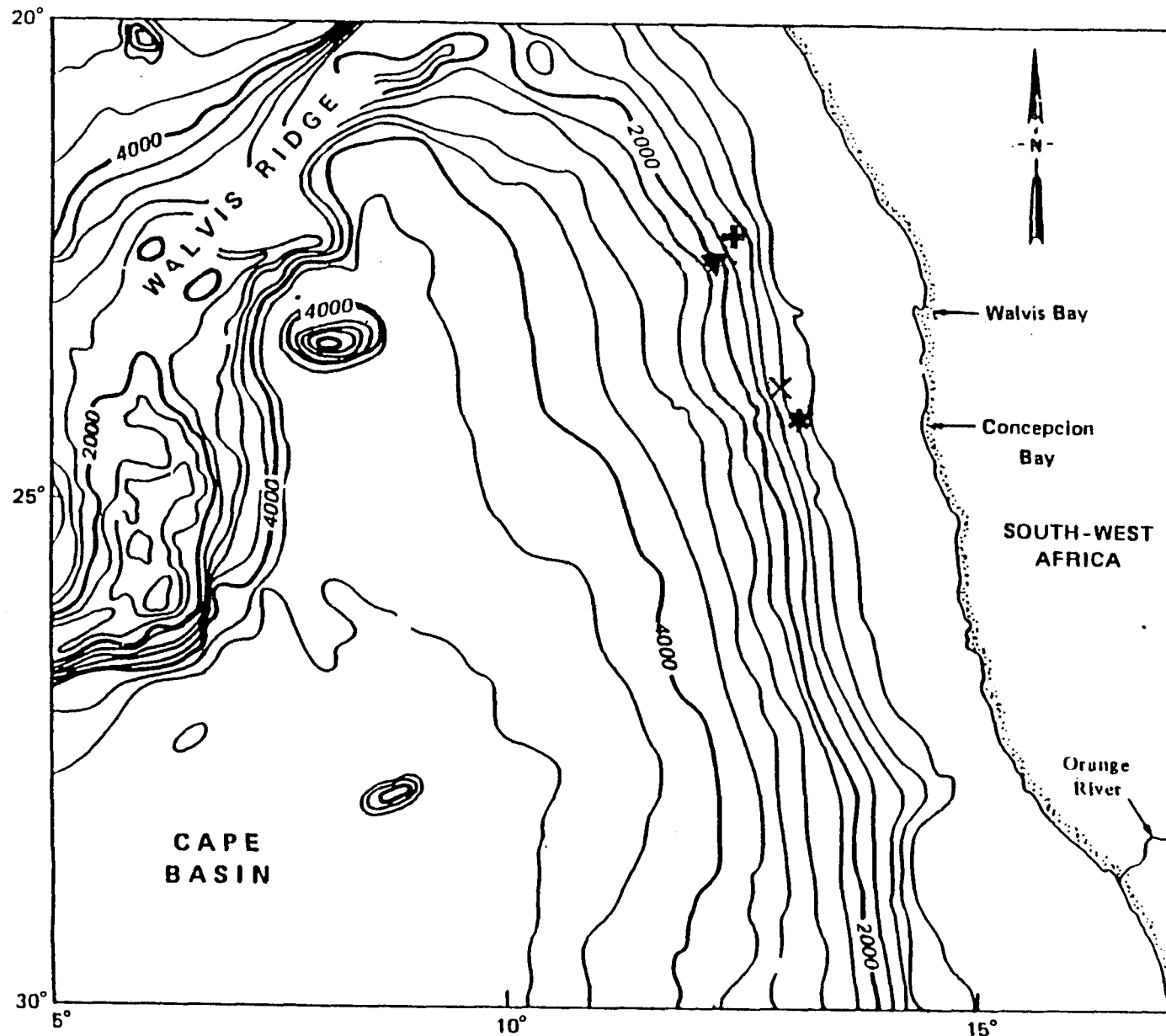
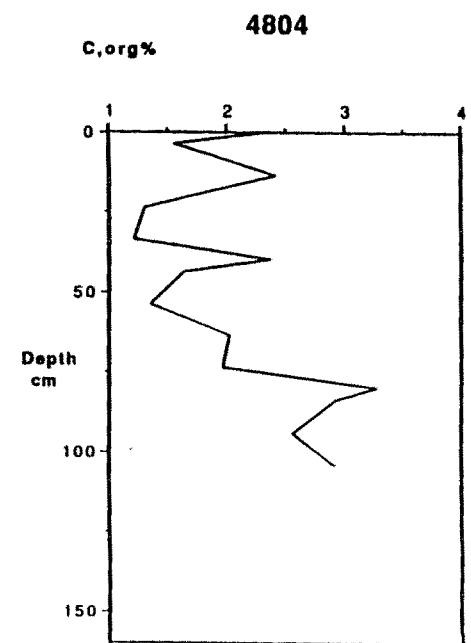
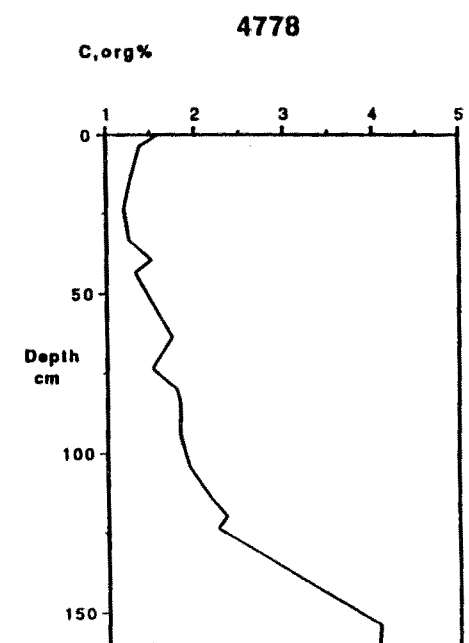
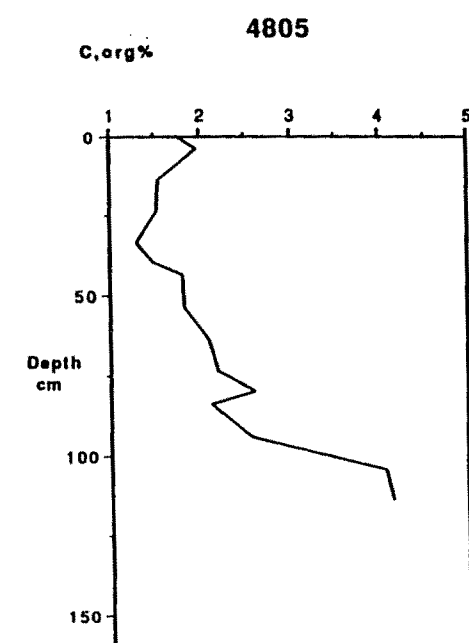
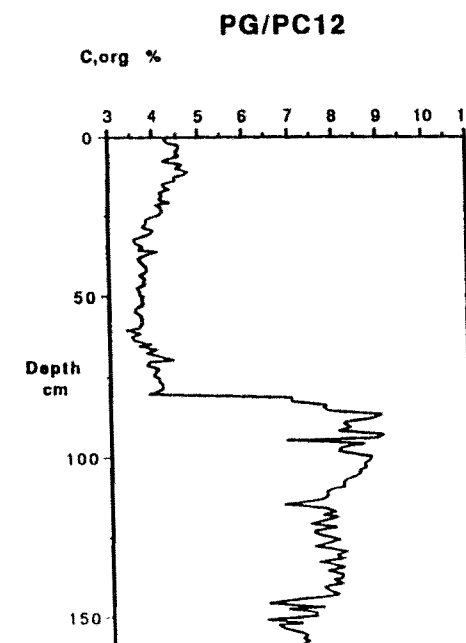
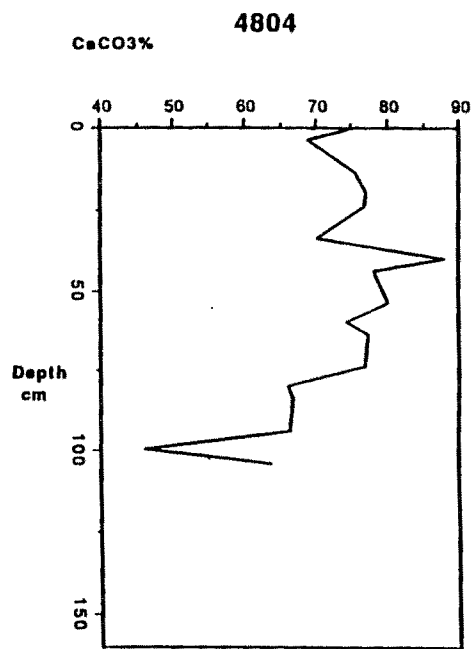
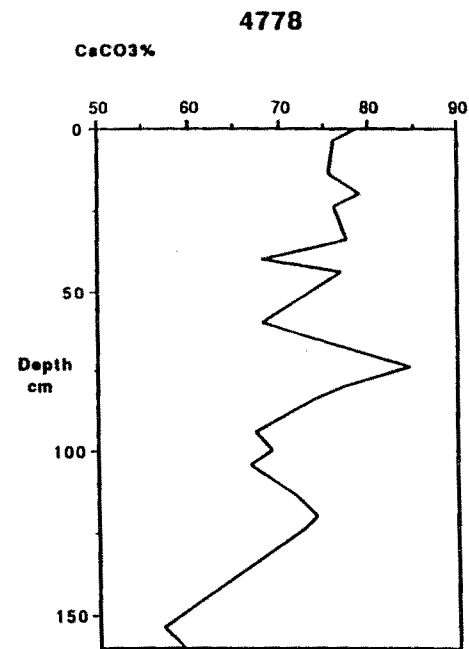
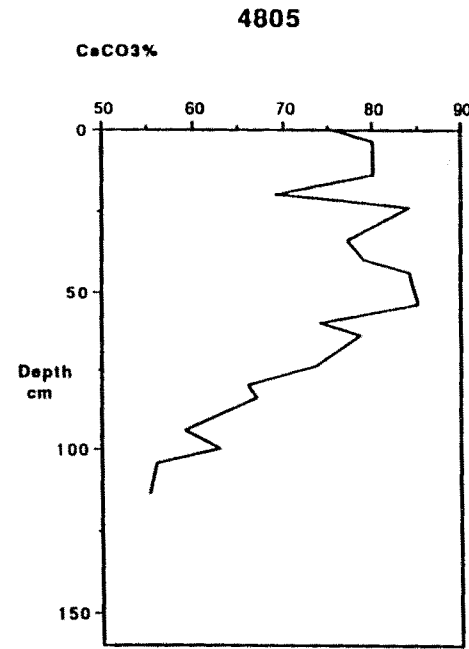
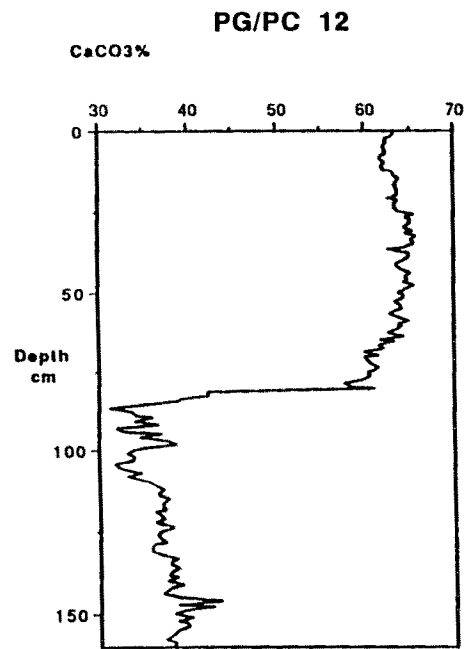


Fig 12. Map of the Walvis Bay area showing the locations of PC12 and three of the 4000 series.



⊕ PG/PC12  
⊗ 4805  
▽ 4778  
\* 4804

Fig 13. Comparison of the CaCO<sub>3</sub>% and Corg% profiles for PG/PC12 and three of the 4000 series cores.



**Fig 14. Comparison between C<sub>org</sub>% at IOS and at University of Cape Town**

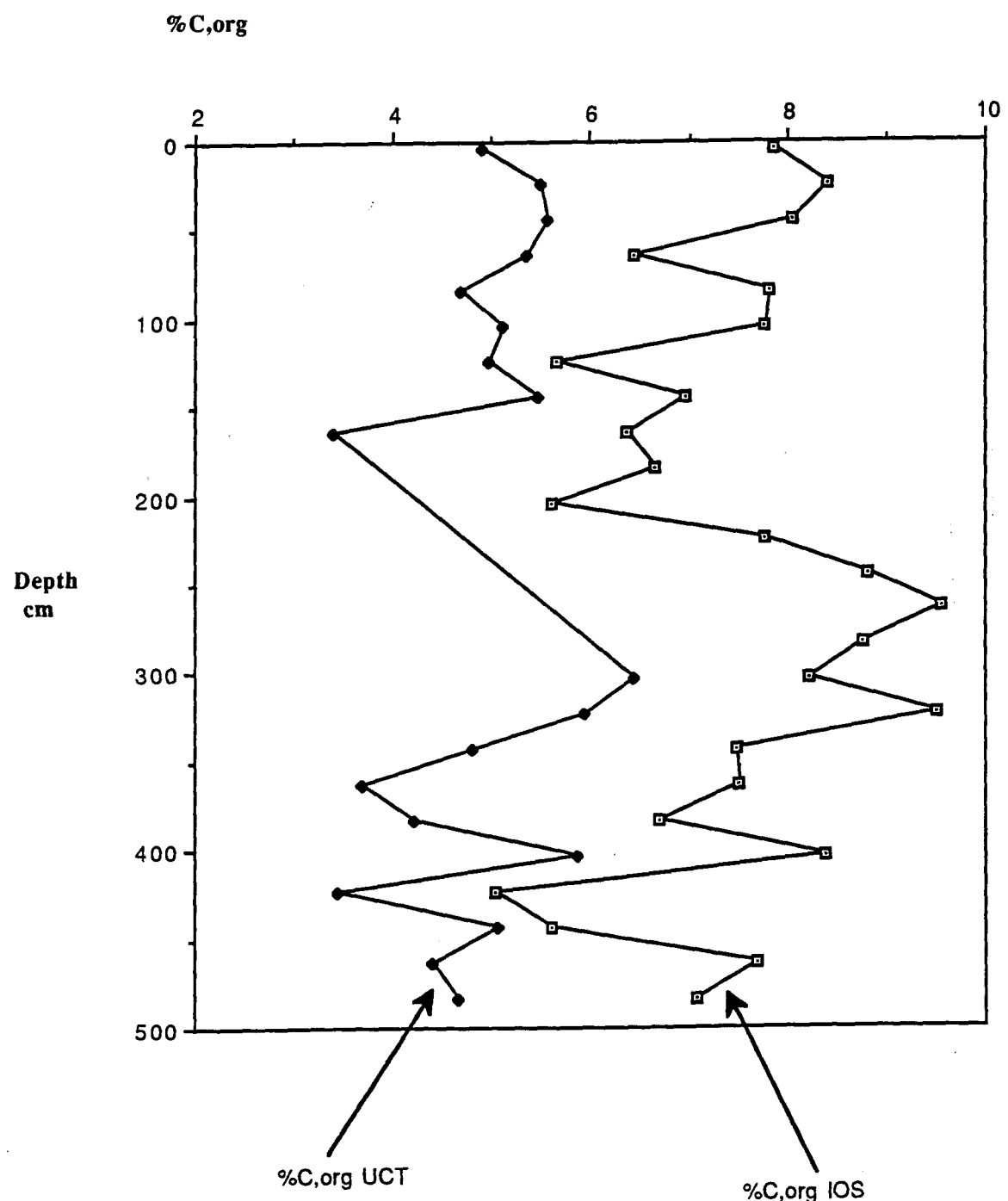


Fig 15. The ICP torch.

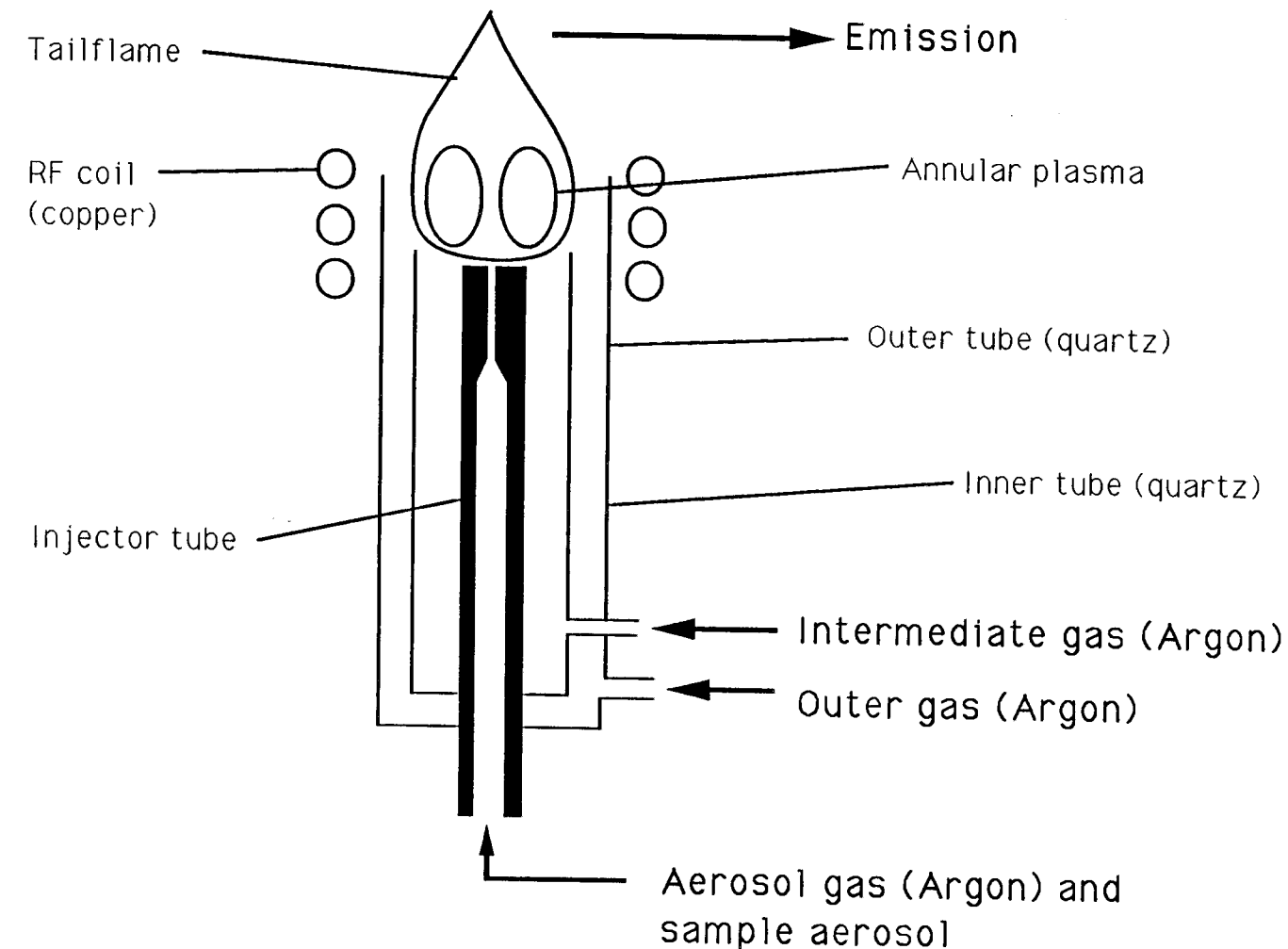


Fig 16. The concentric nebuliser.

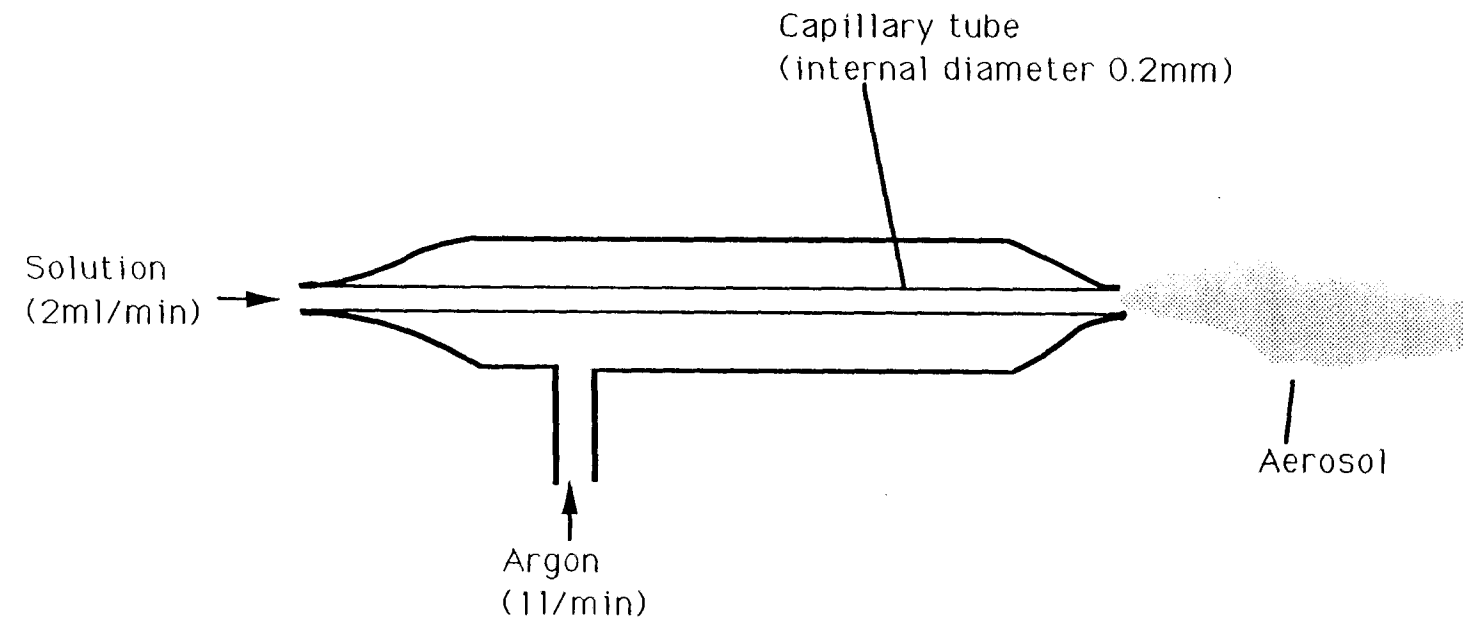


Fig 17. The ICP-AES system.

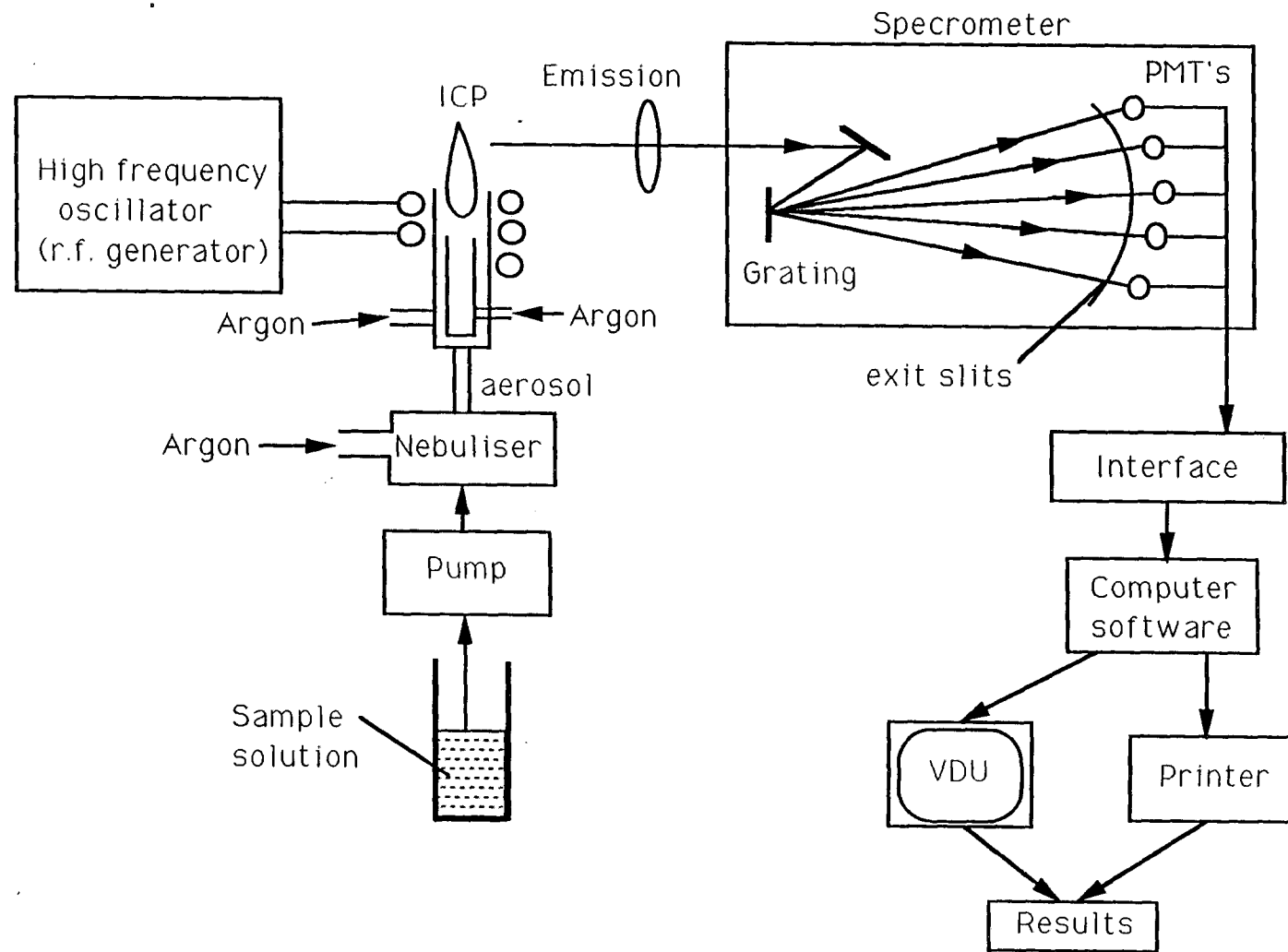


Fig 18.1

Fig 18. The coulometric data for core section 260-360cm.

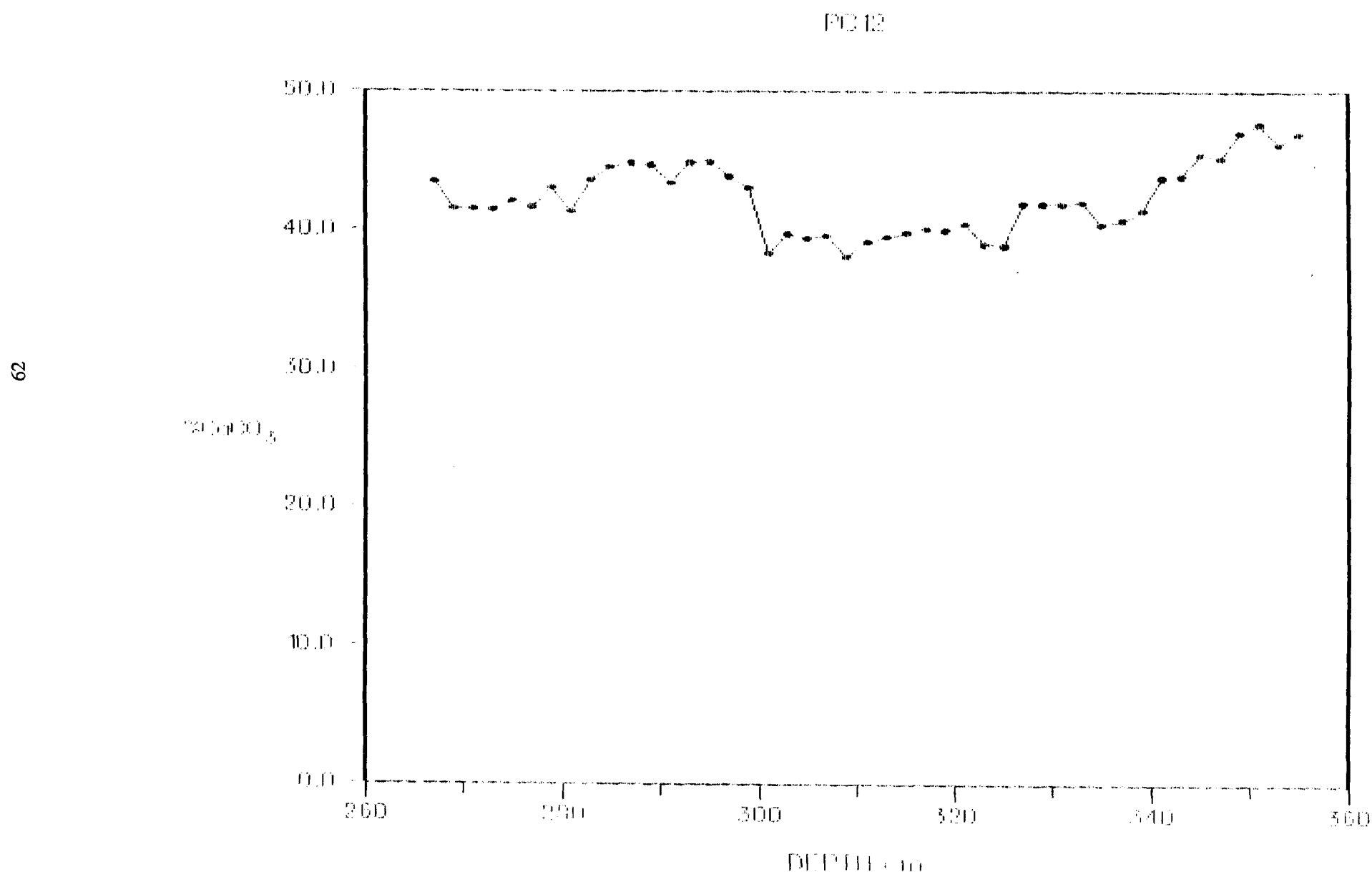


Fig 18.2

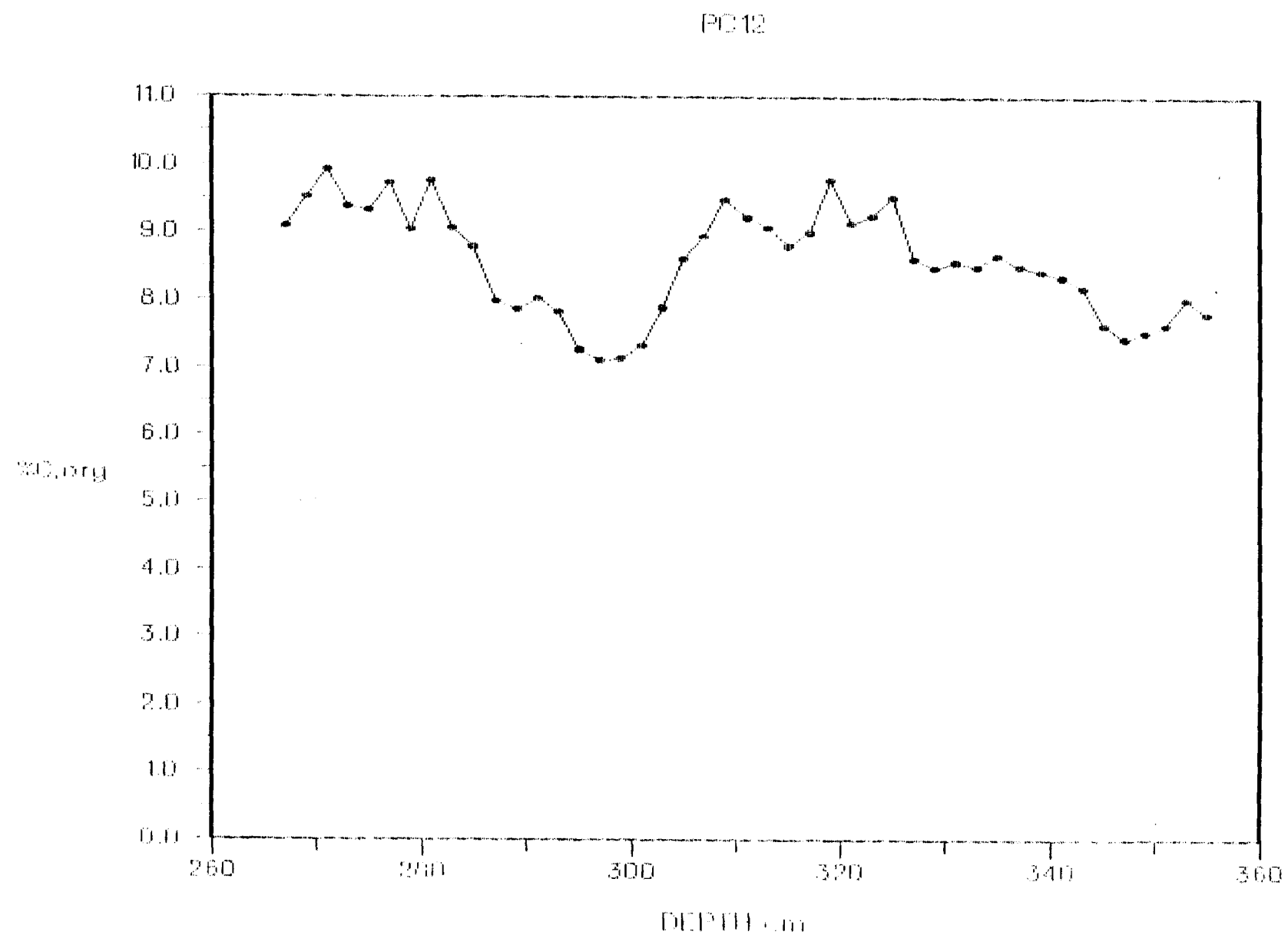


Fig 18.3

Fig 18.3

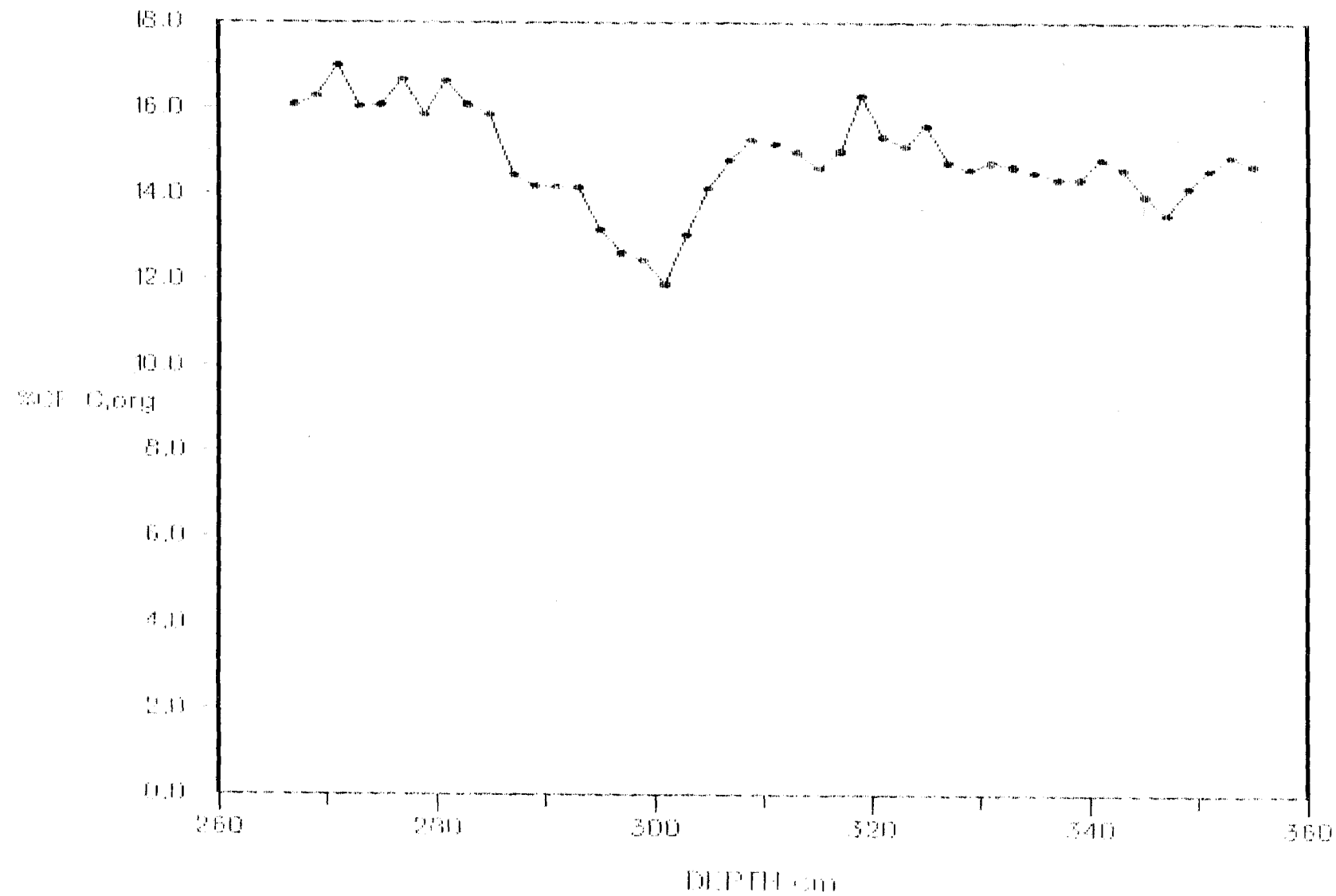


Fig 19.1

Fig 19. The first group of ICP-AES results.

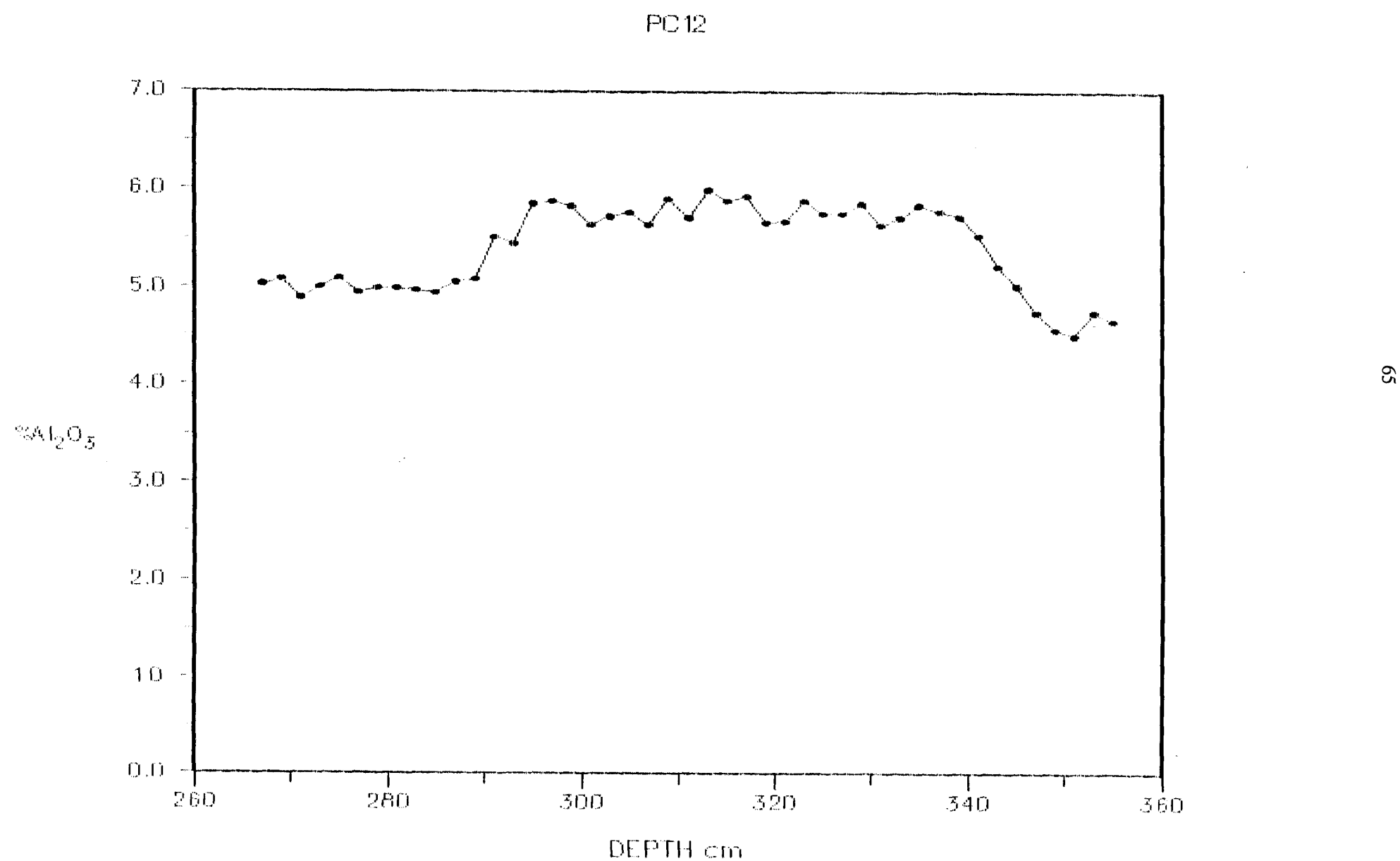


Fig 19.2

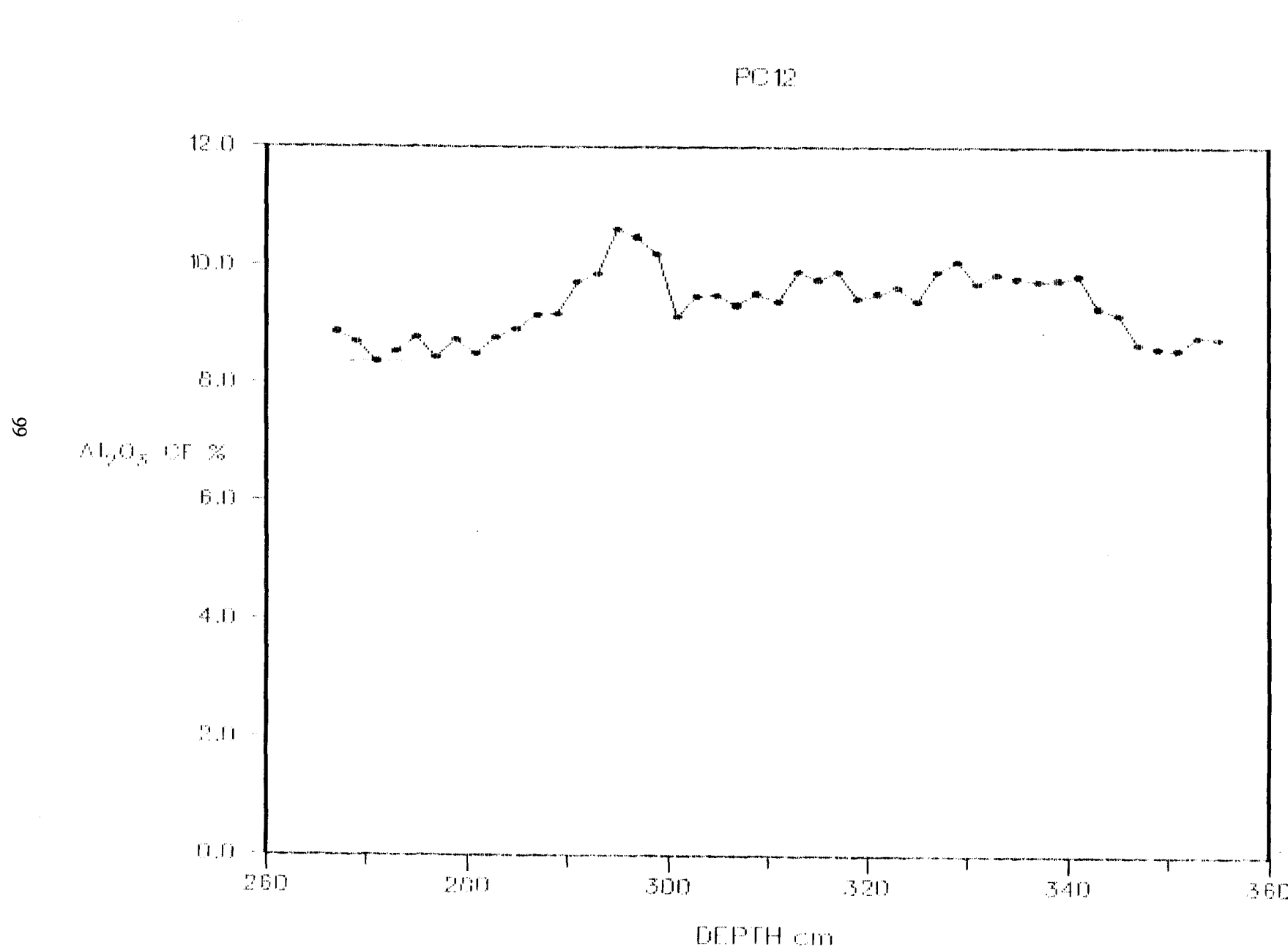


Fig 19.3

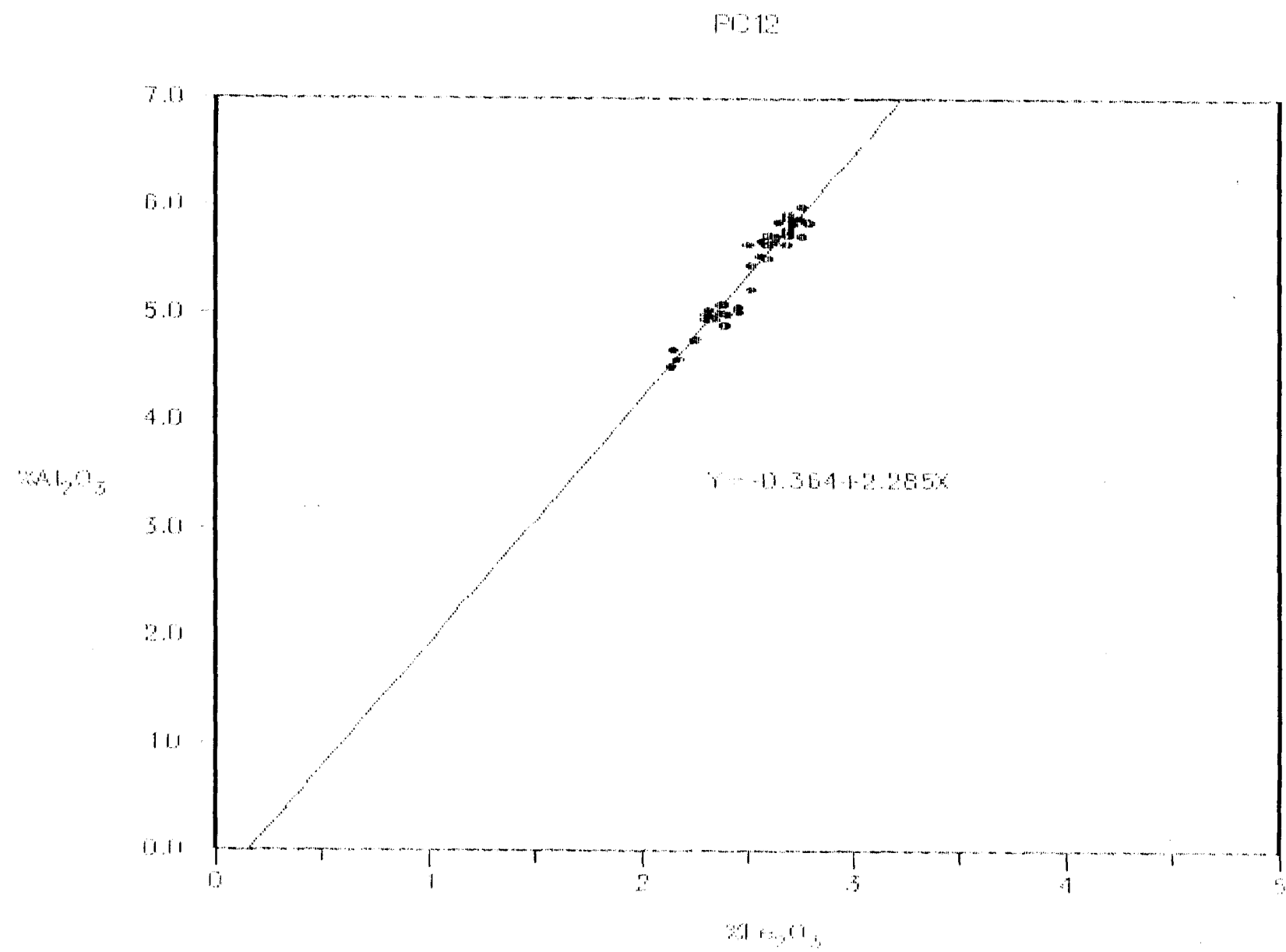


Fig 19.4

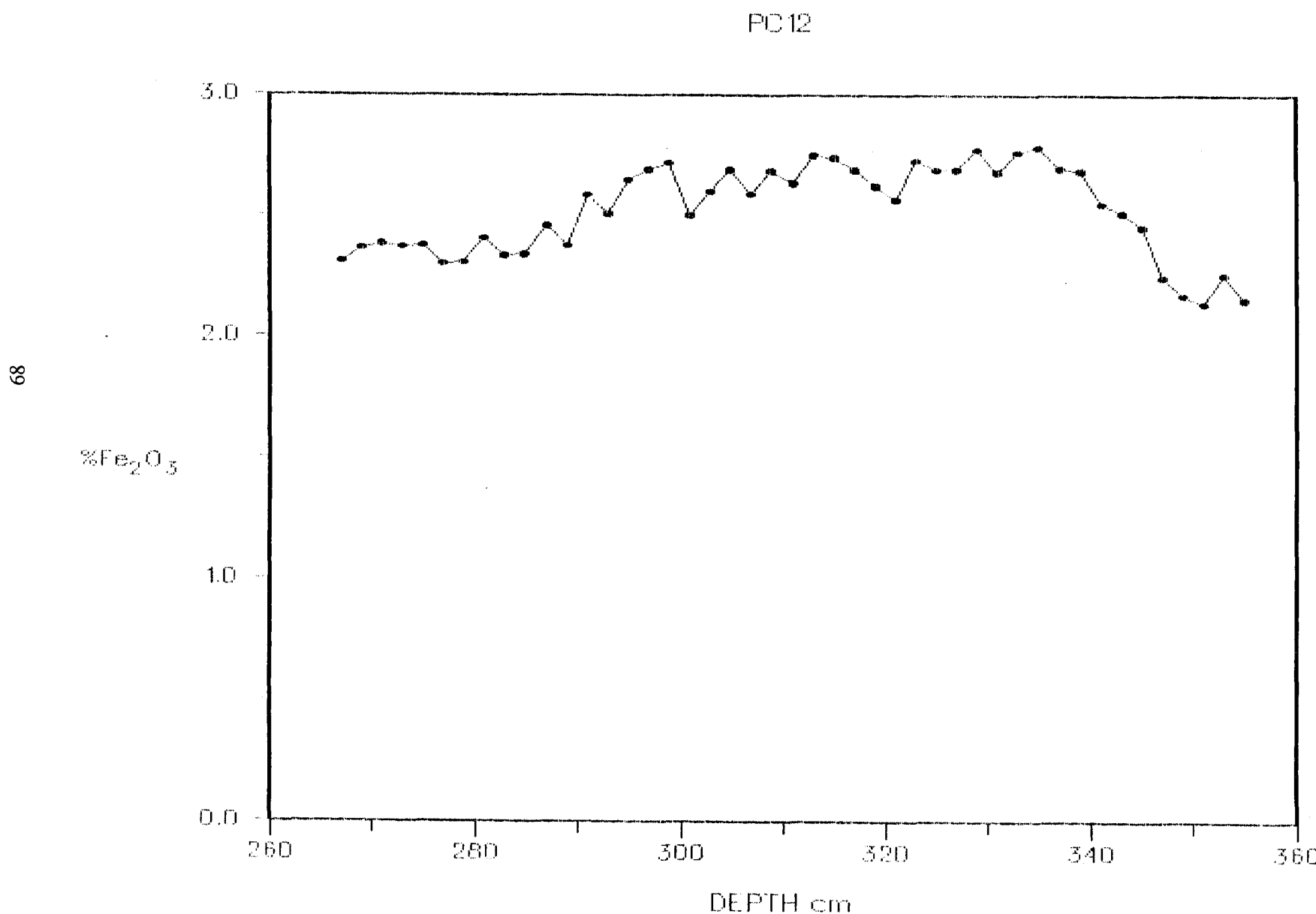


Fig 19.5

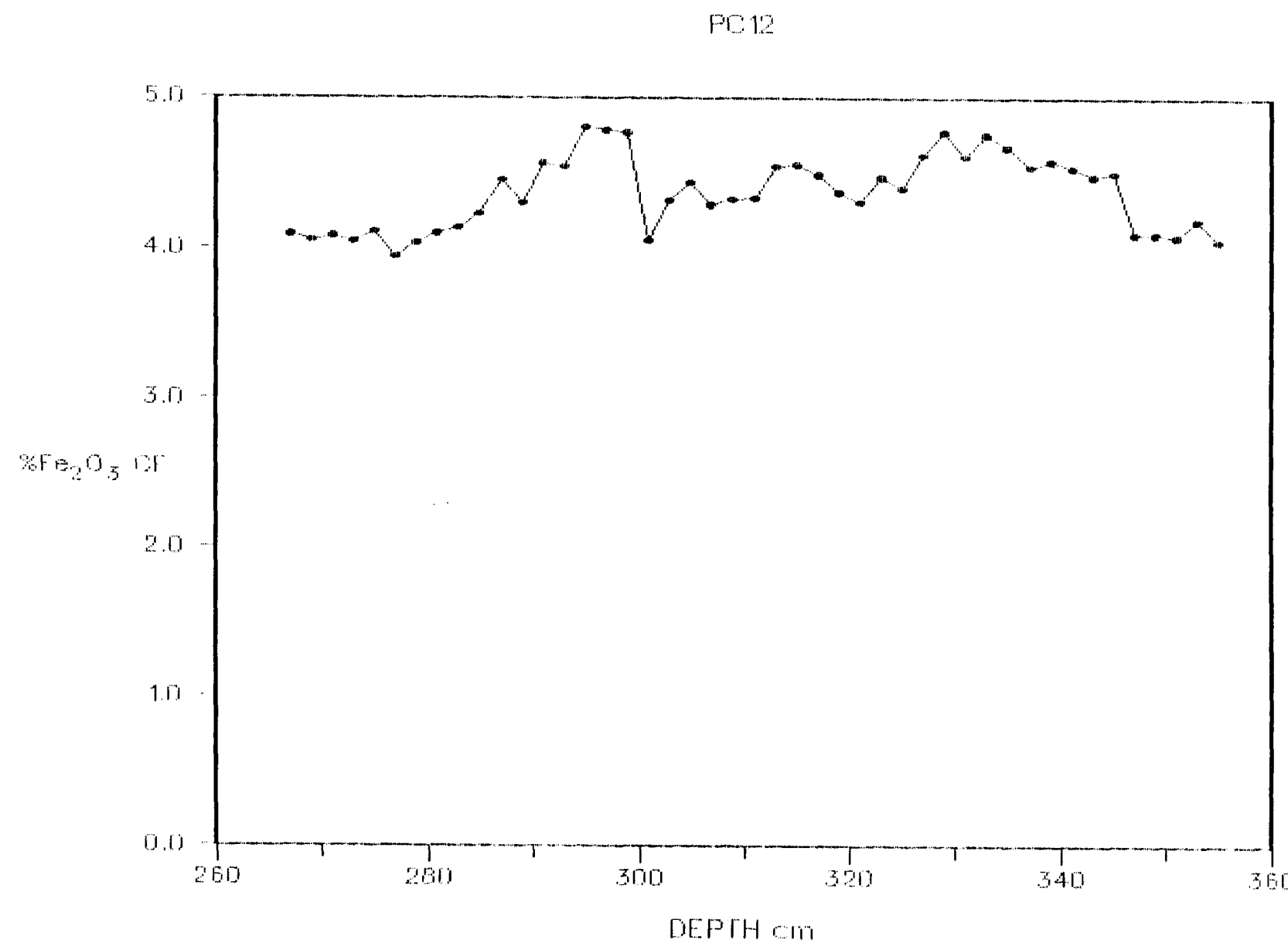


Fig 19.6

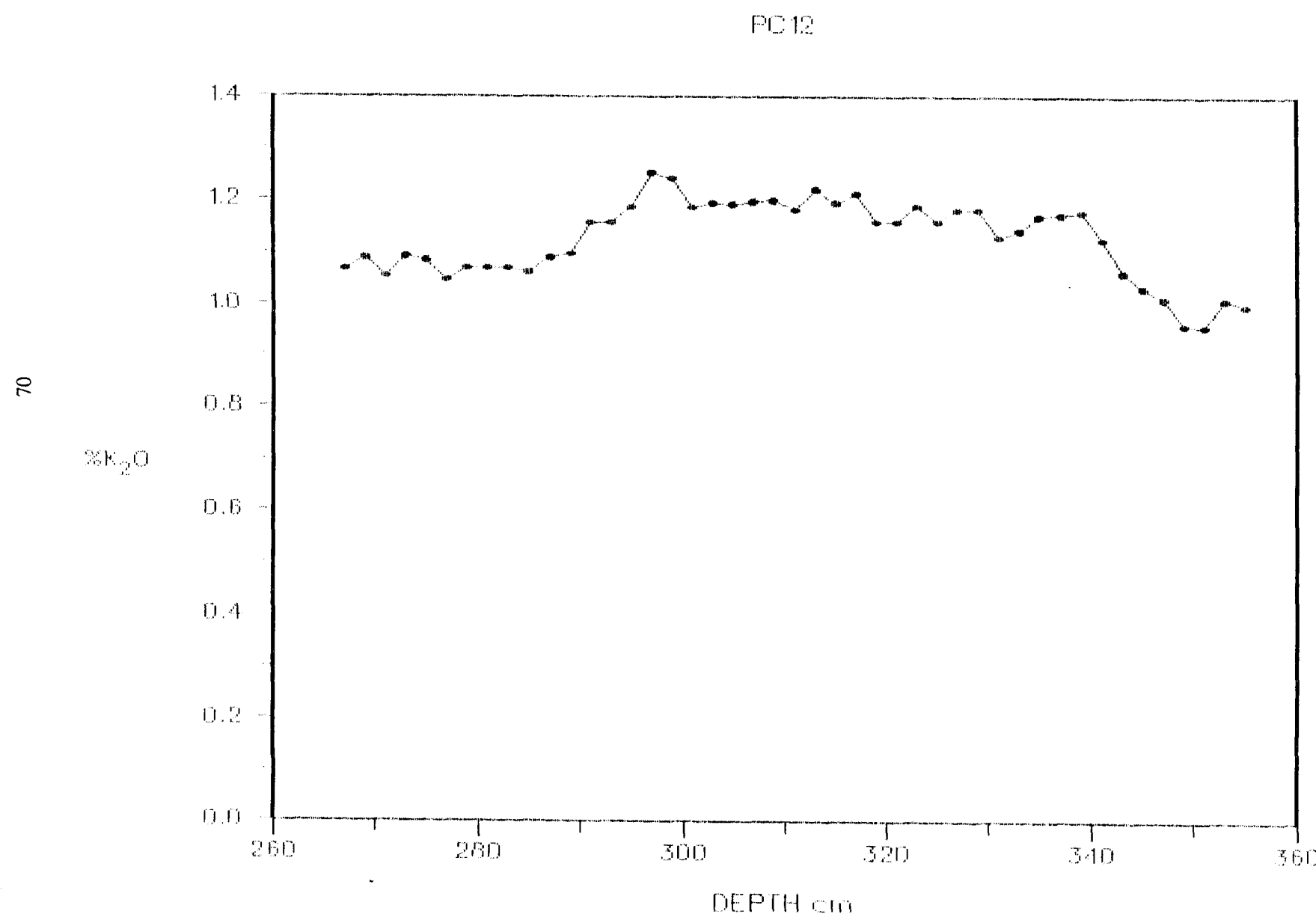


Fig 19.7

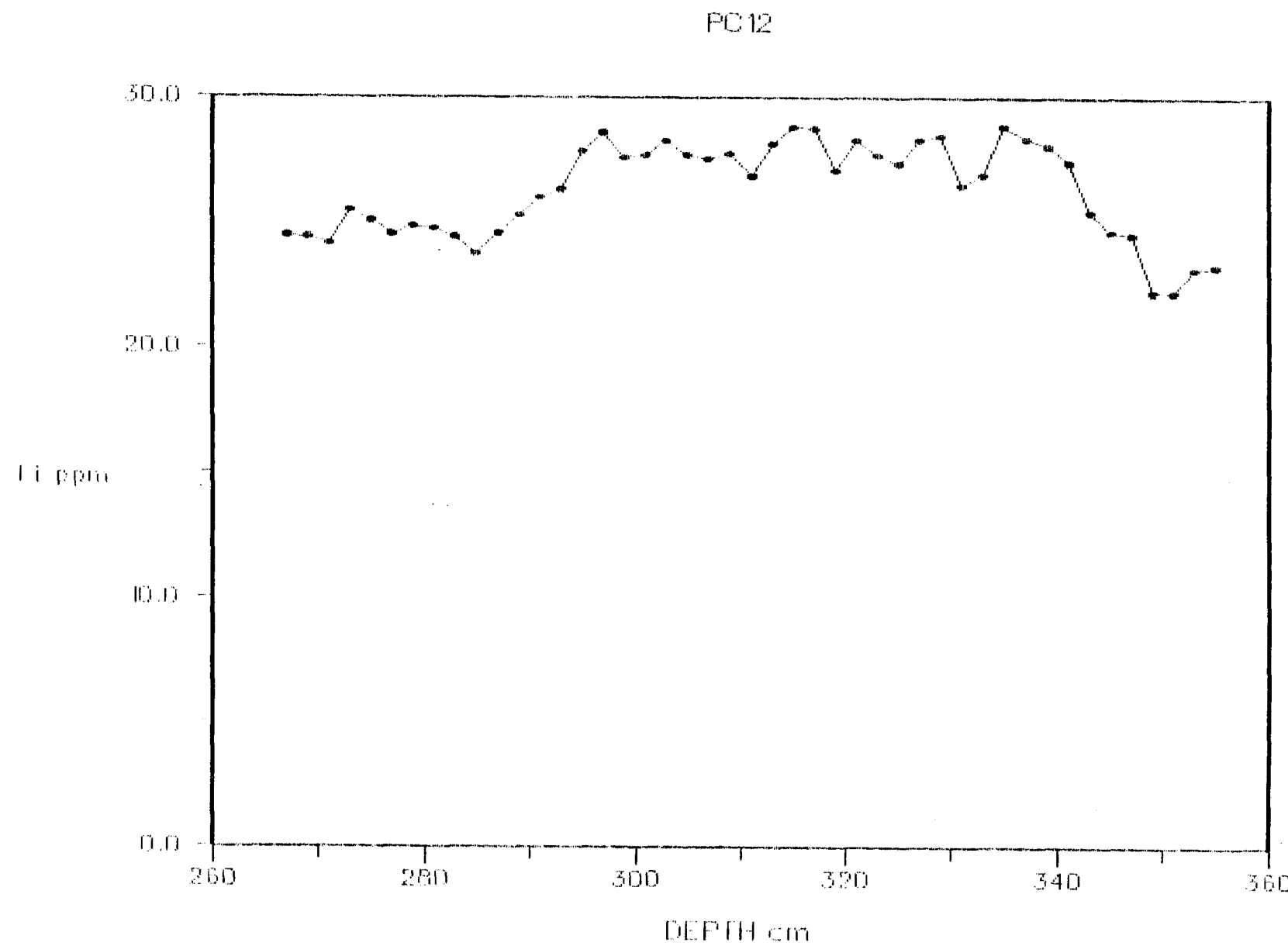


Fig 19.8

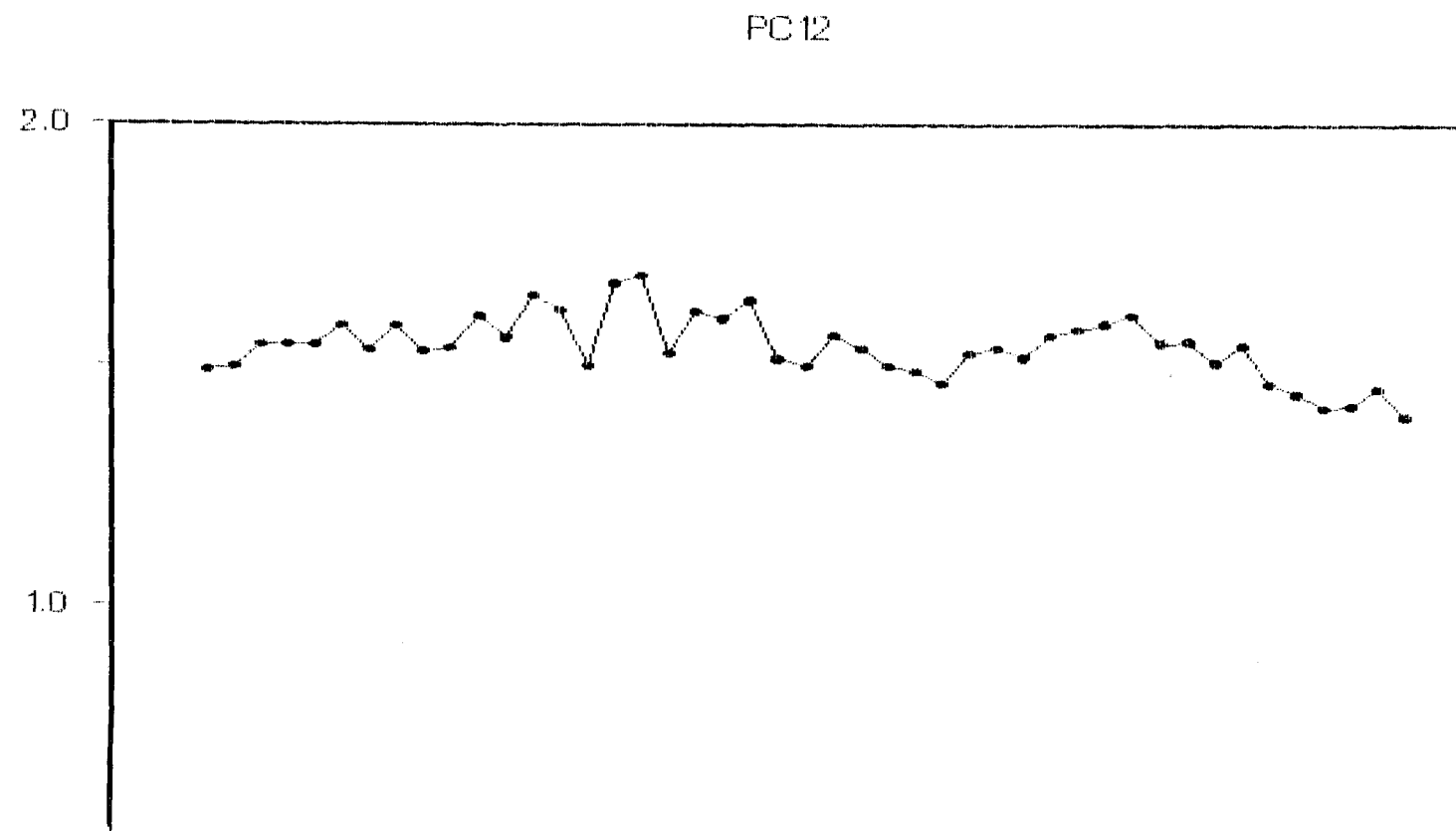


Fig 19.9

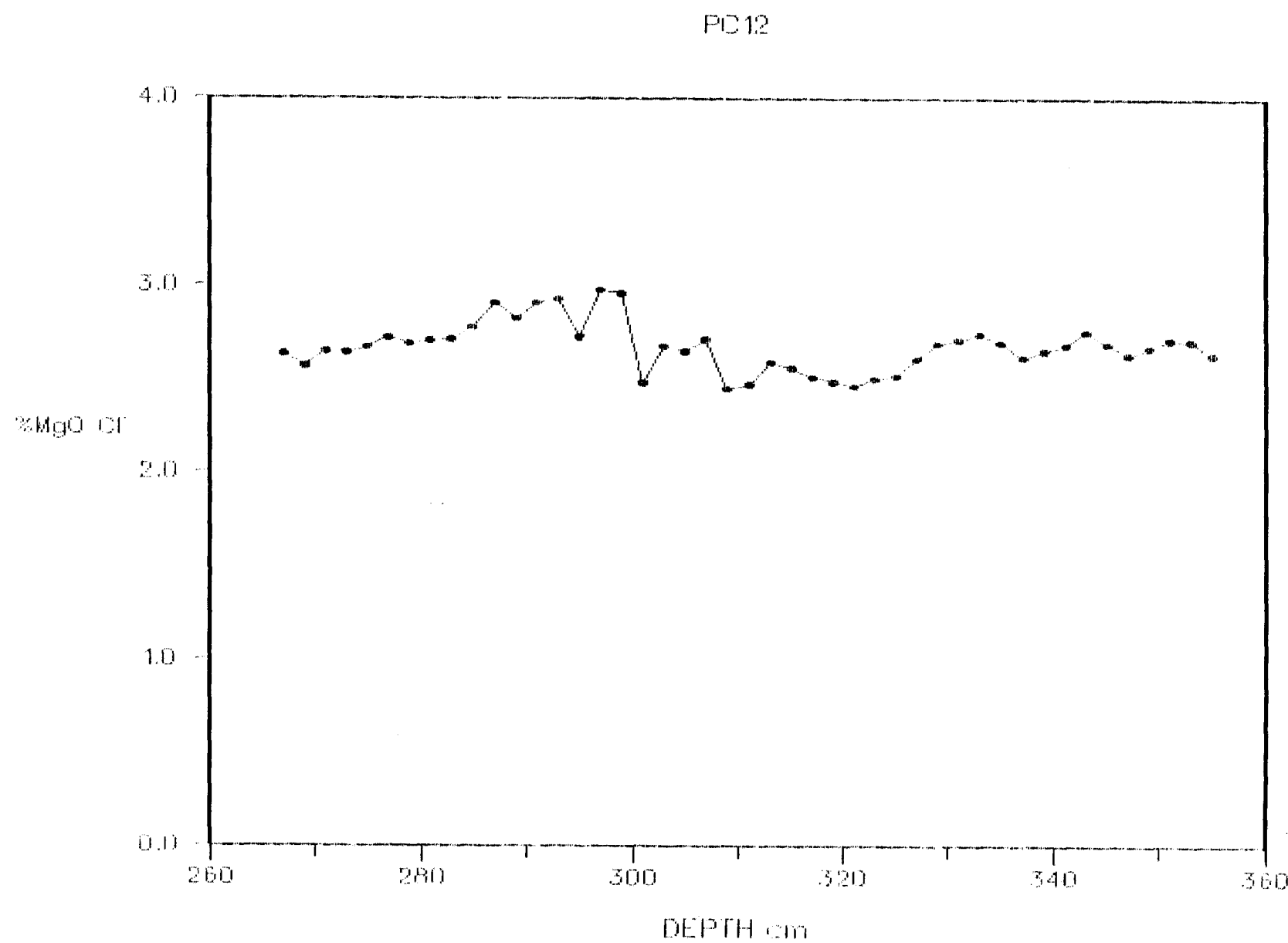


Fig 19.10

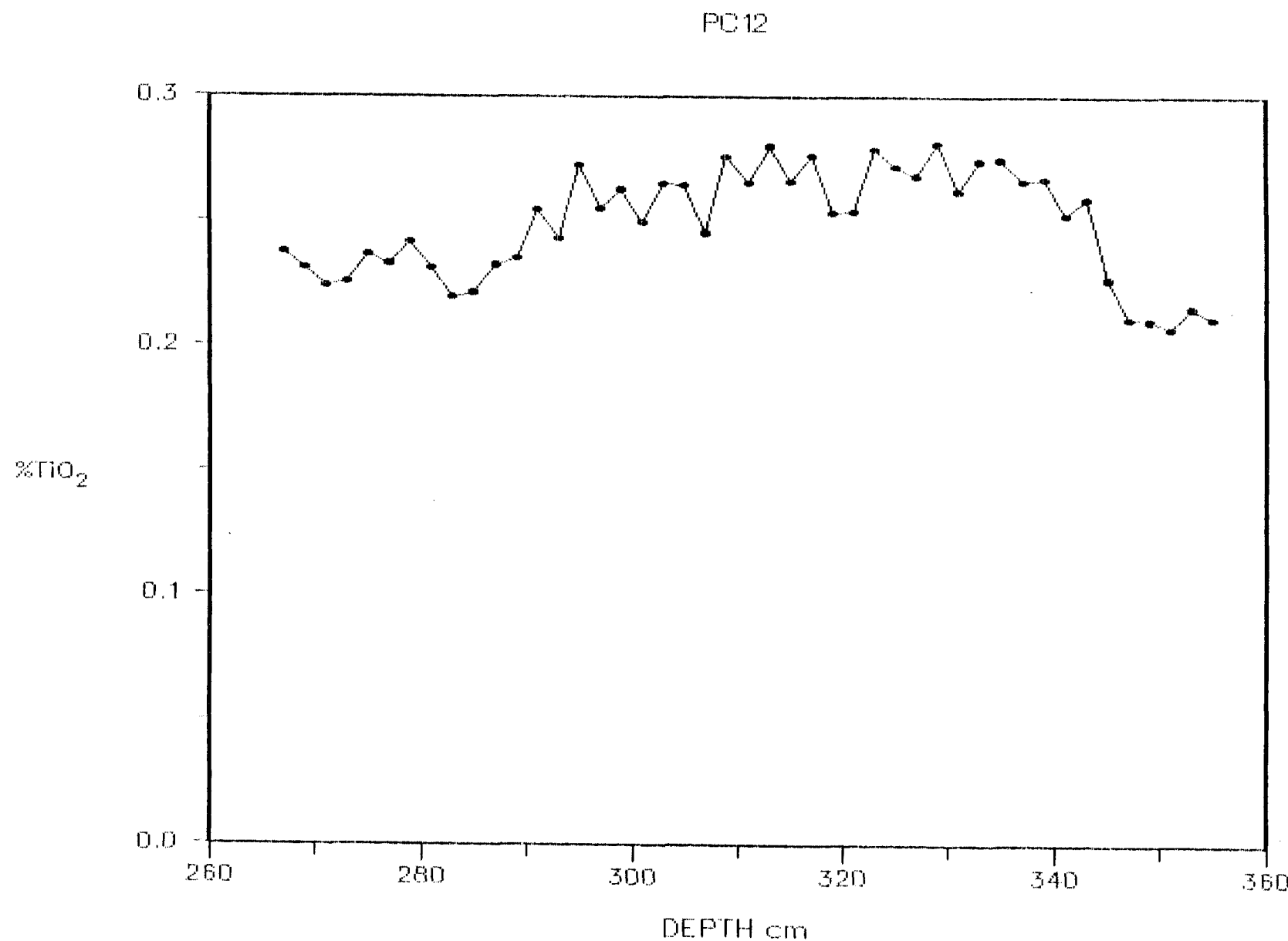


Fig 19.11

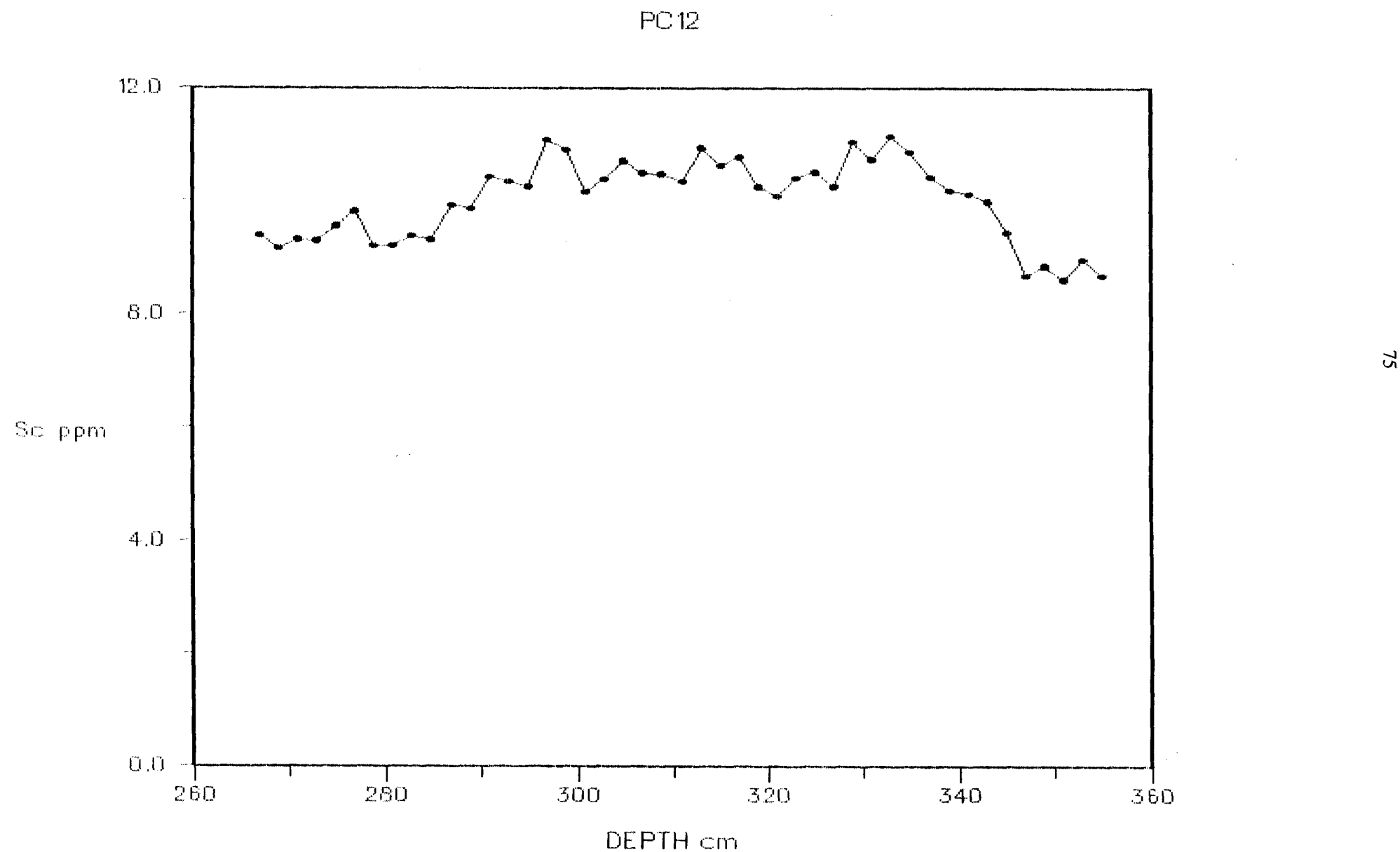


Fig 19.12

76

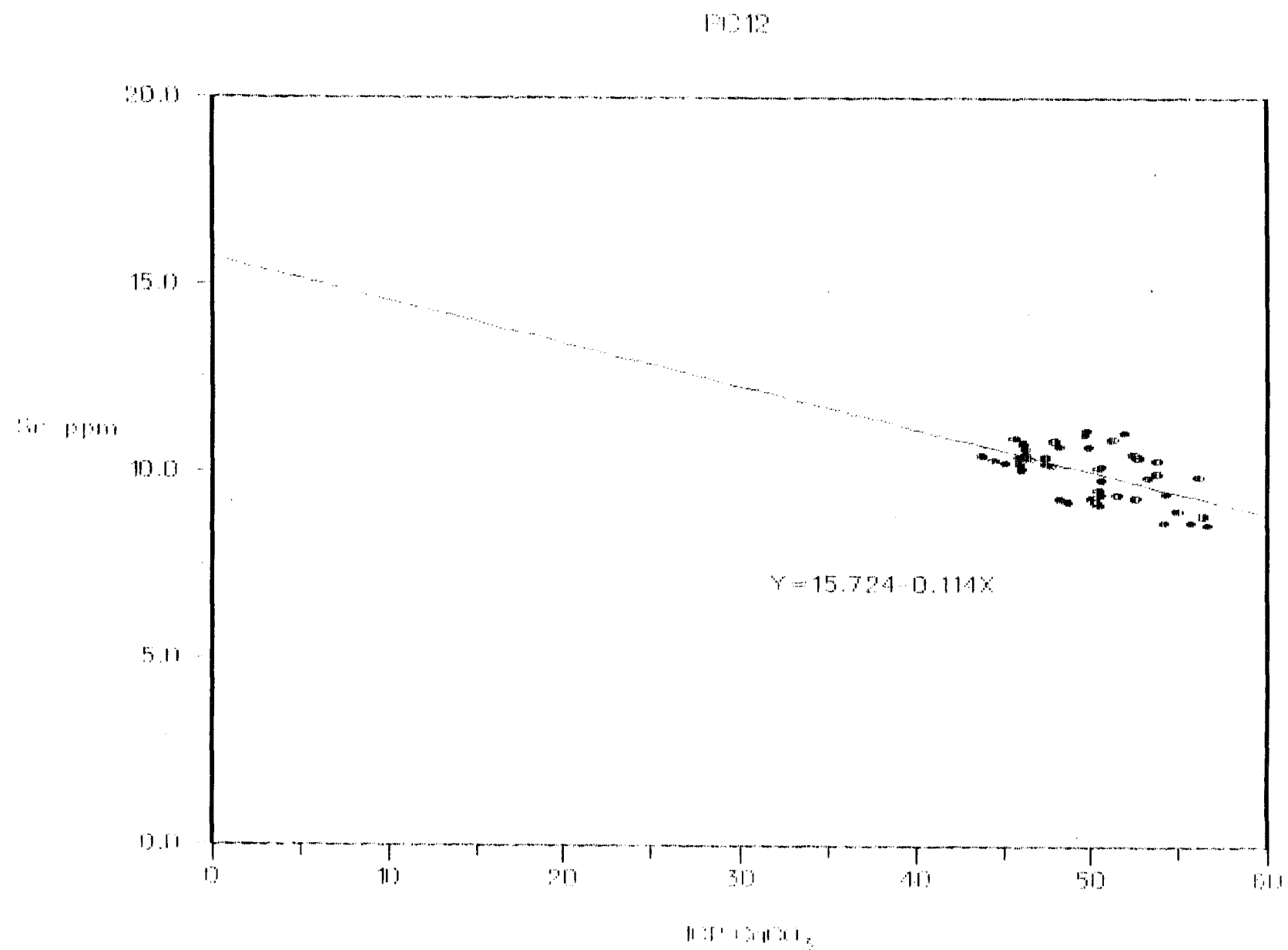


Fig 20.1

Fig 20. The second group of ICP-AES results.

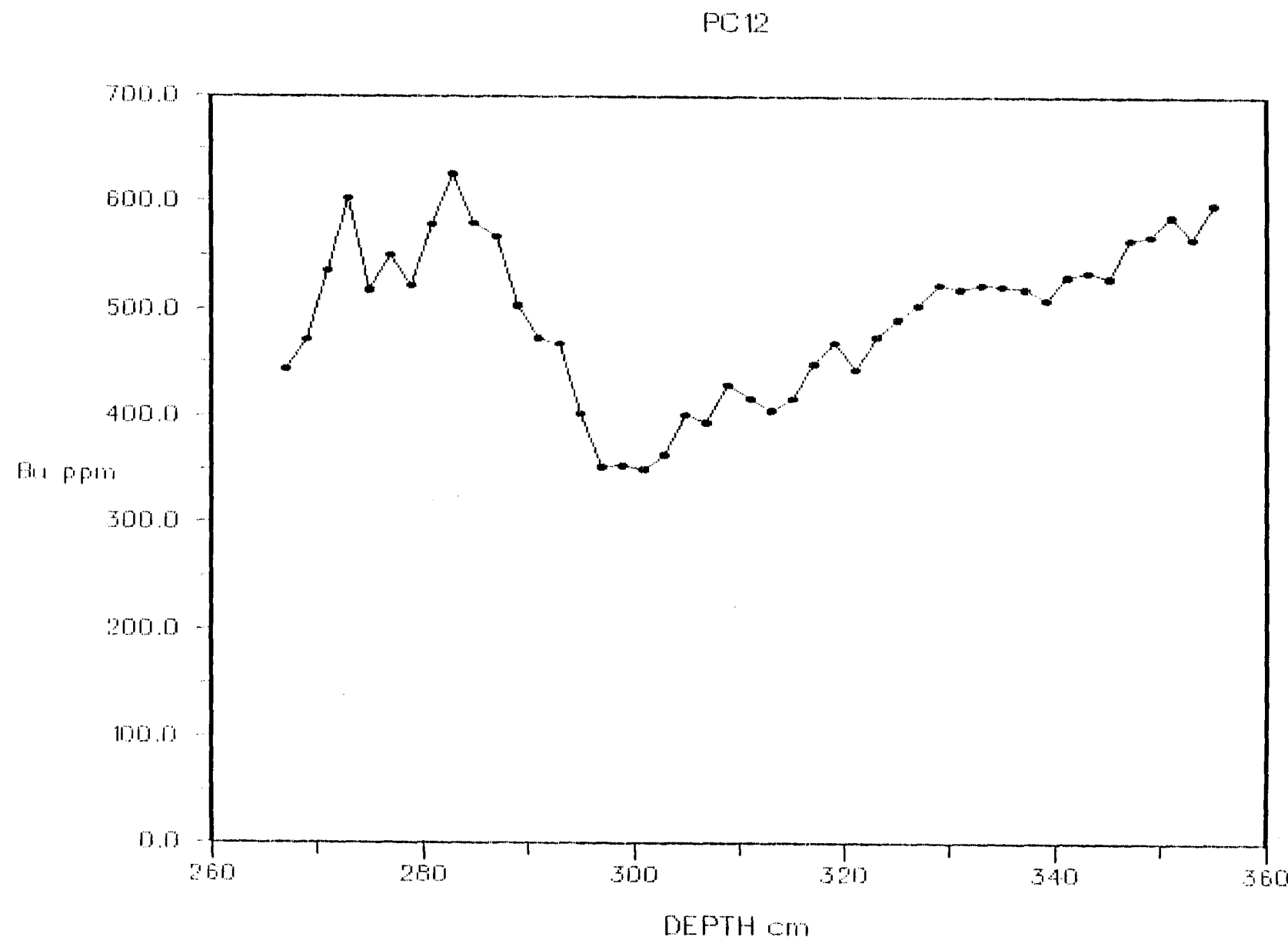


Fig 20.2

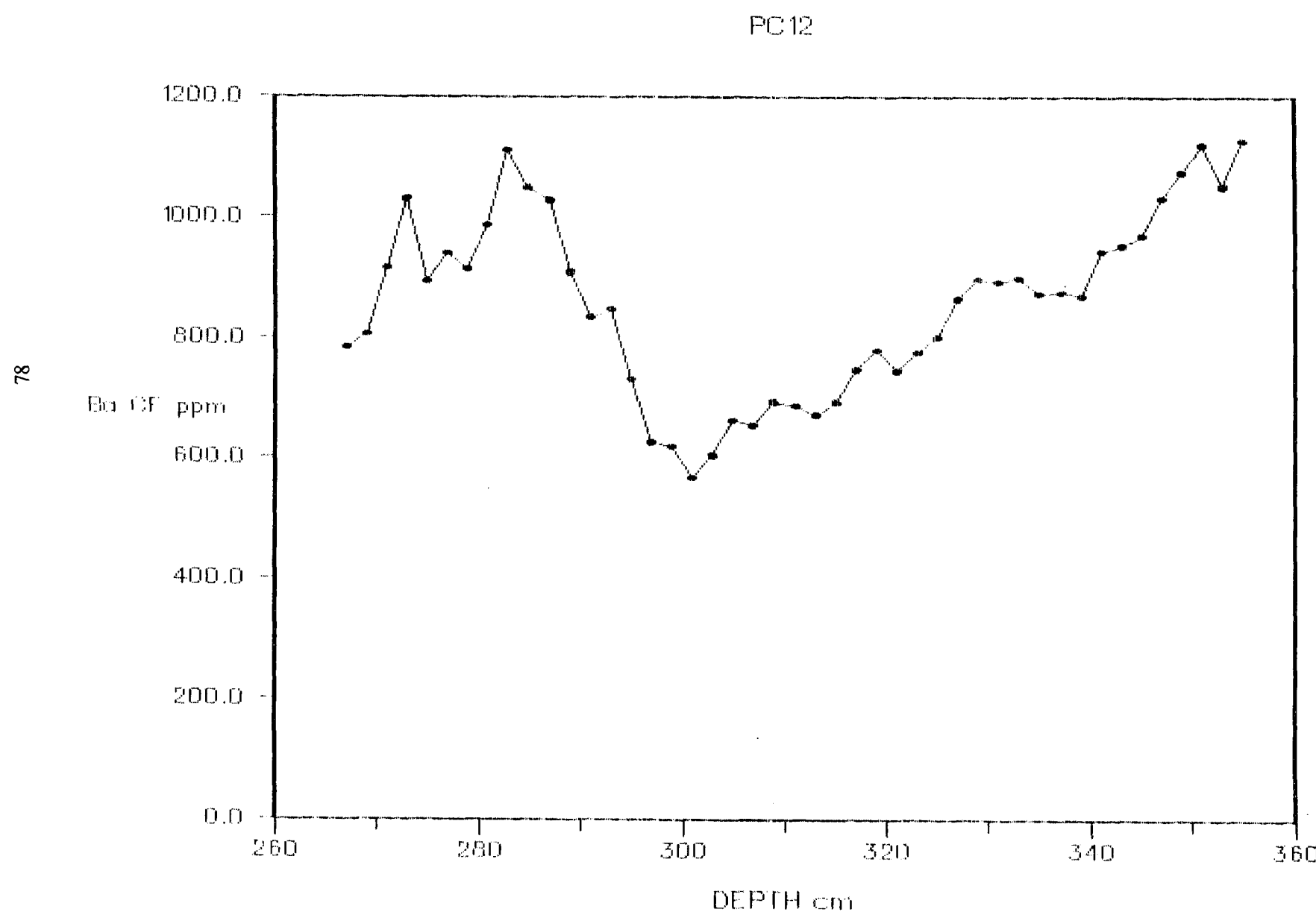
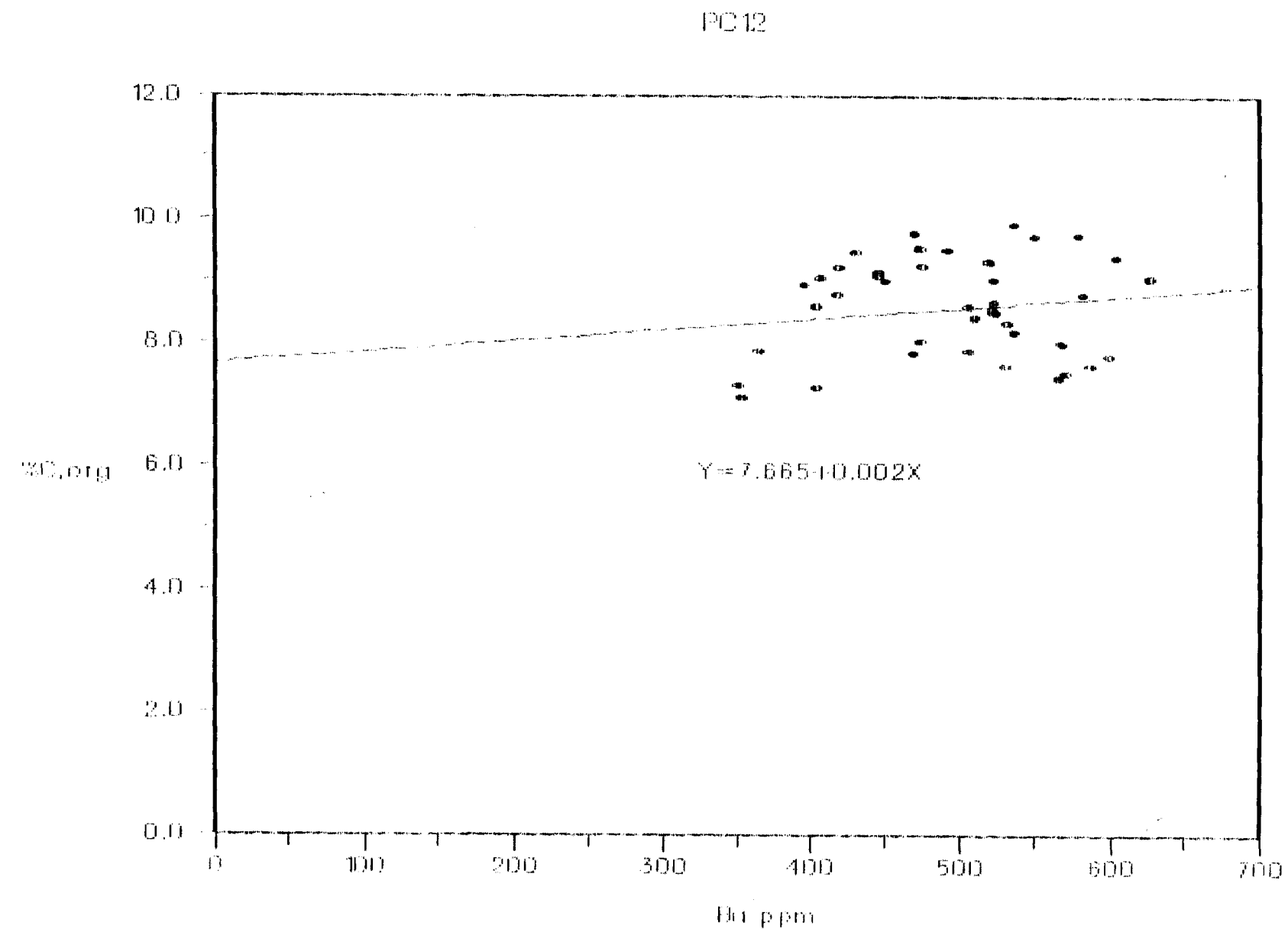


Fig 20.3



**Fig 20.4**

PC 12

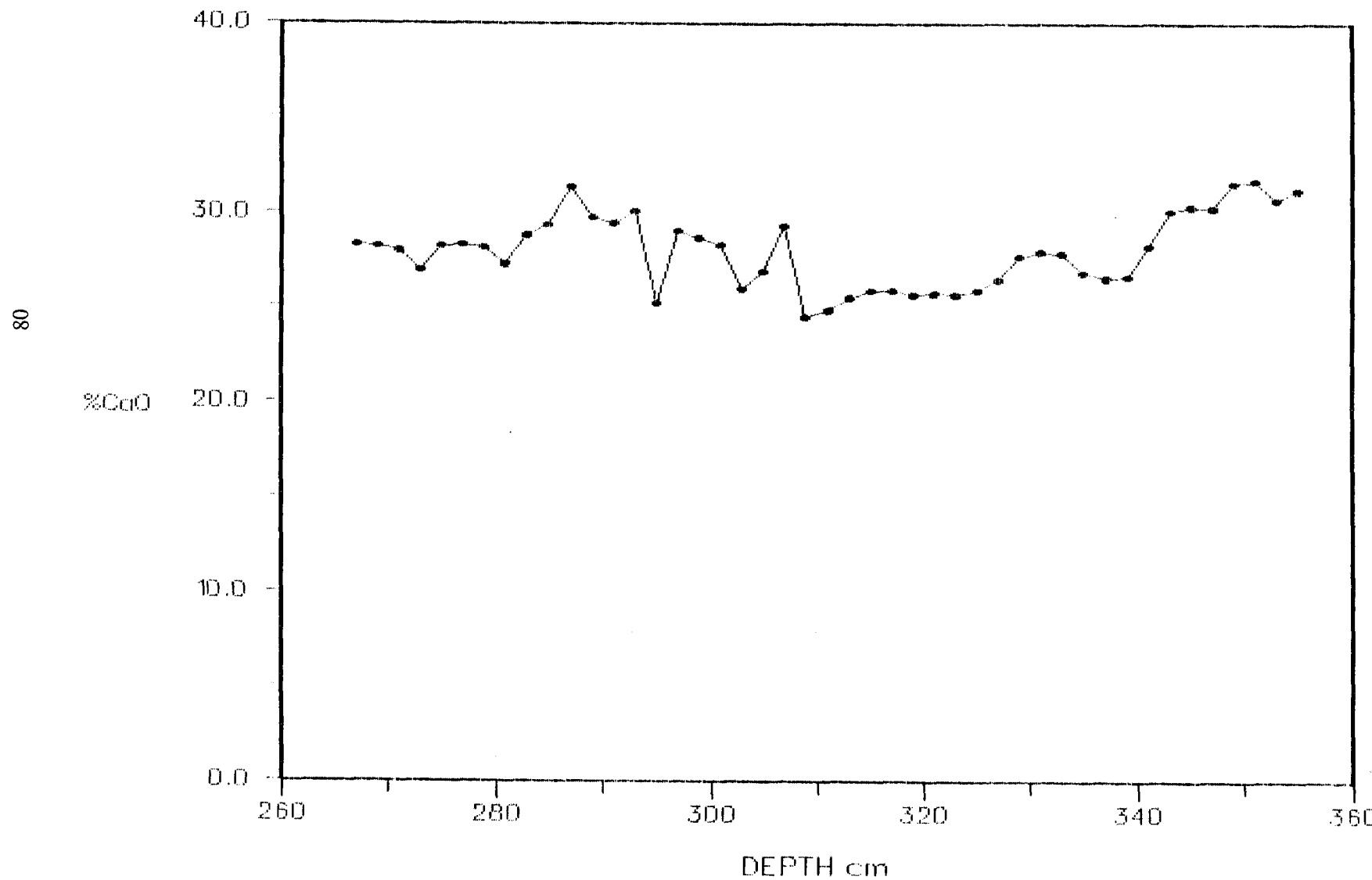


Fig 20.5

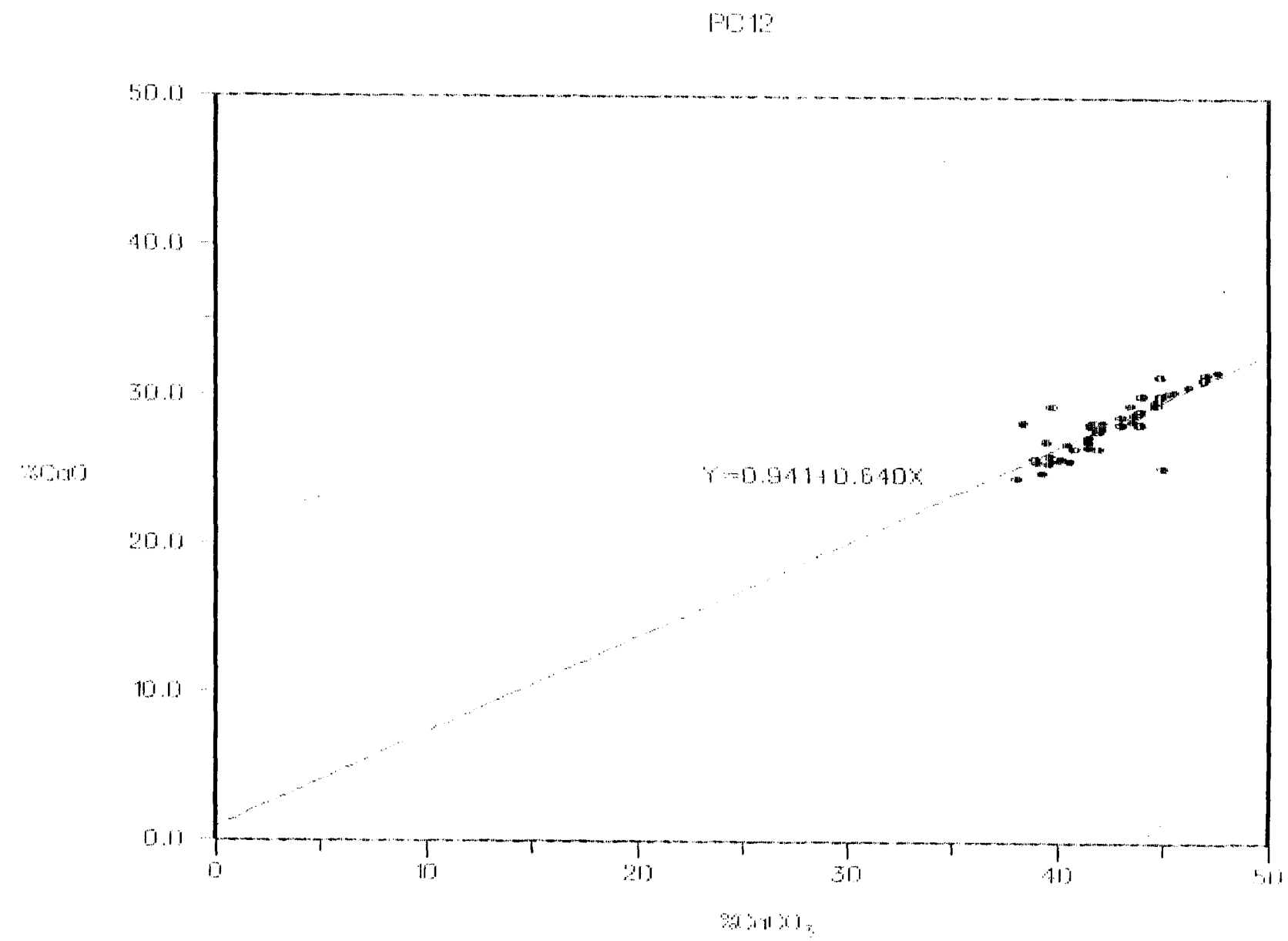


Fig 20.6

82

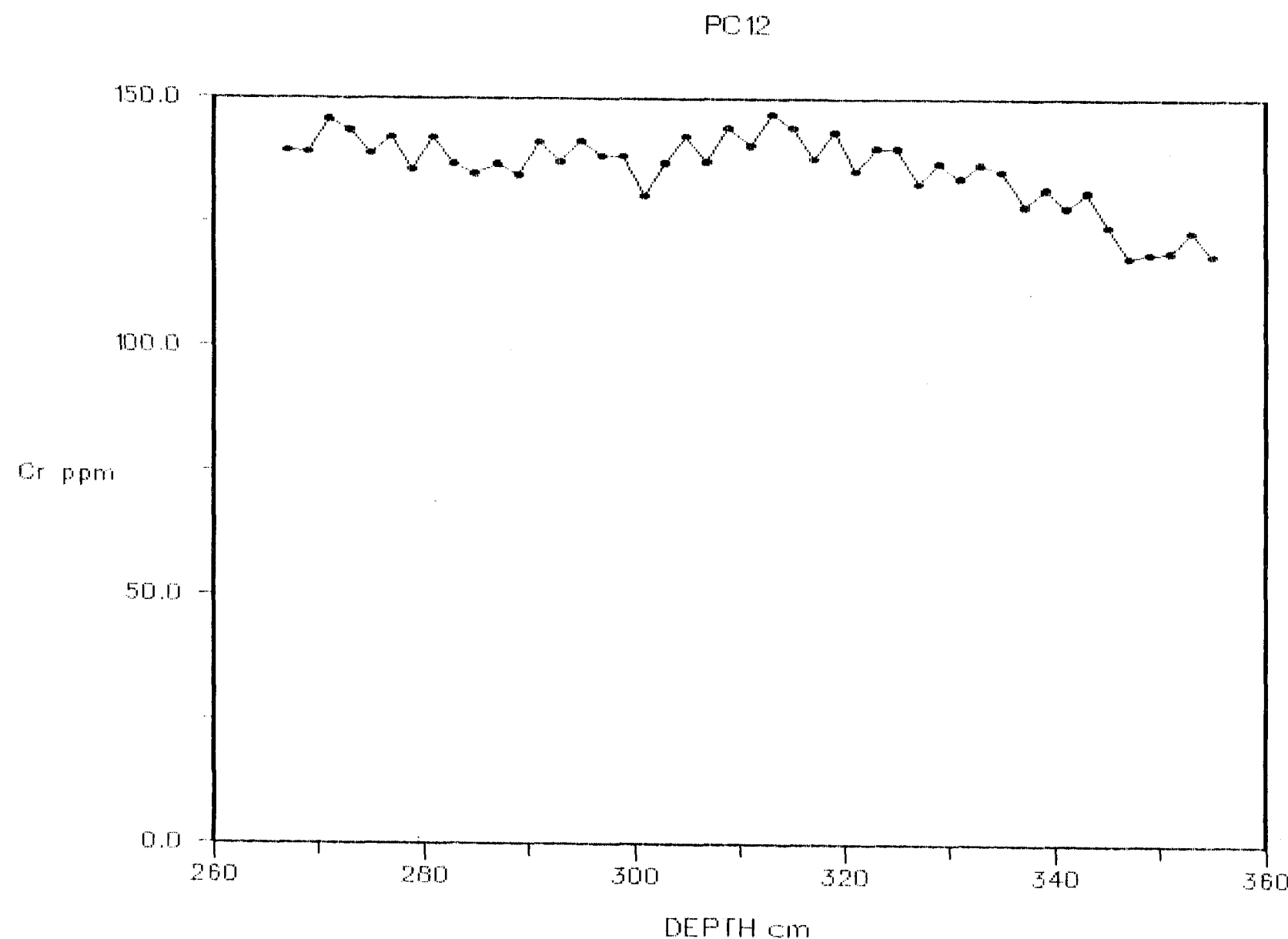


Fig 20.7

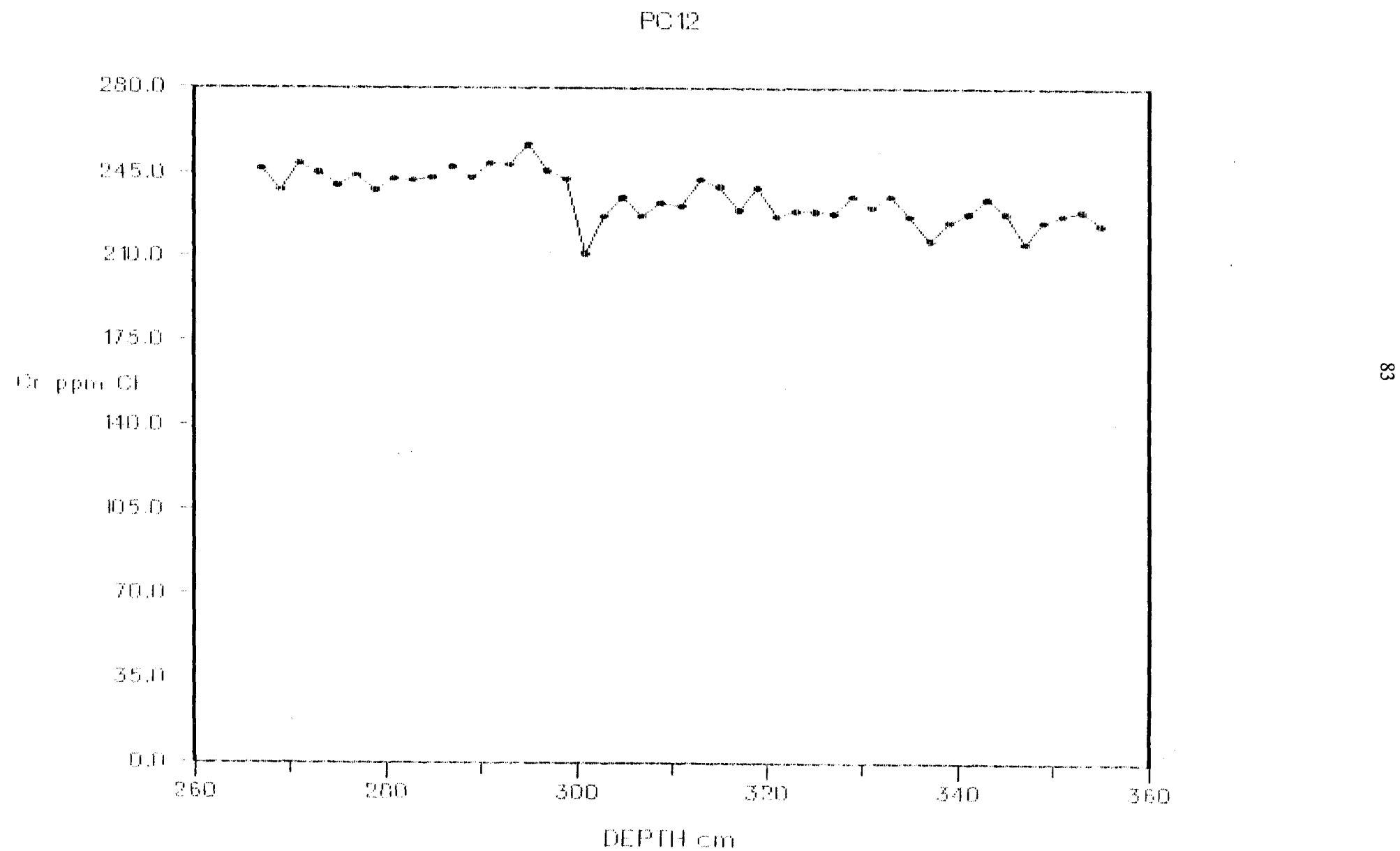


Fig 20.8

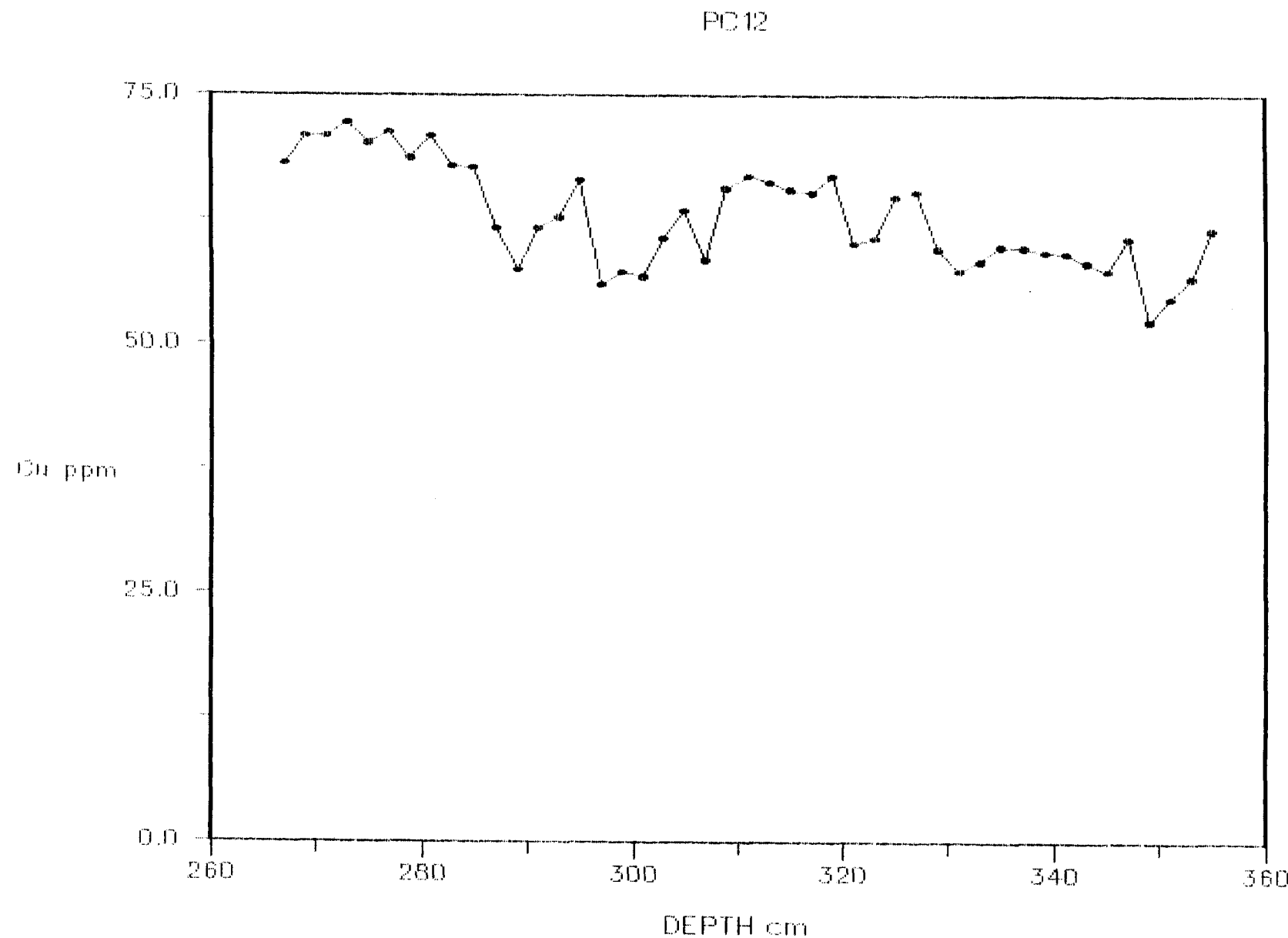


Fig 20.9

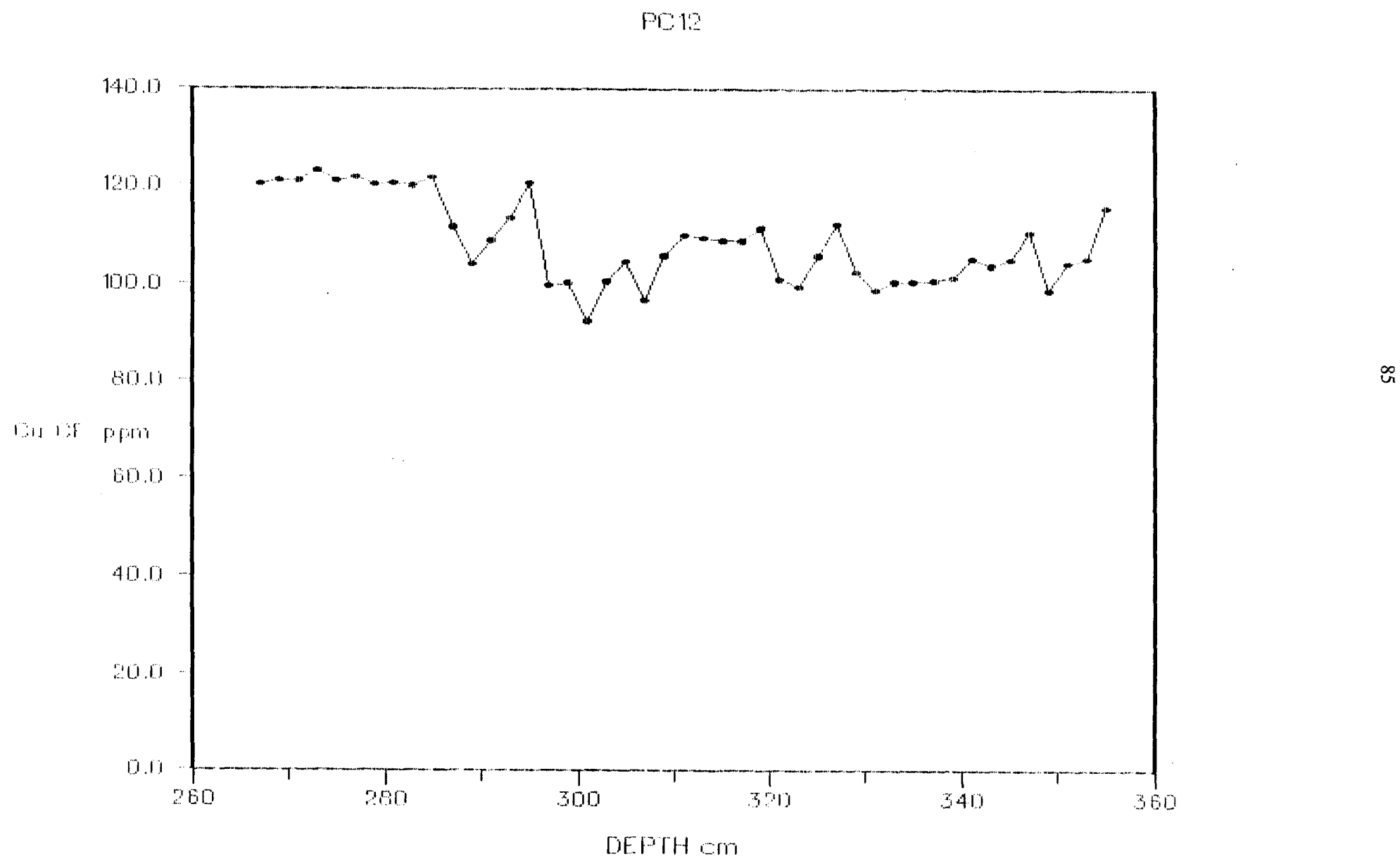


Fig 20.10

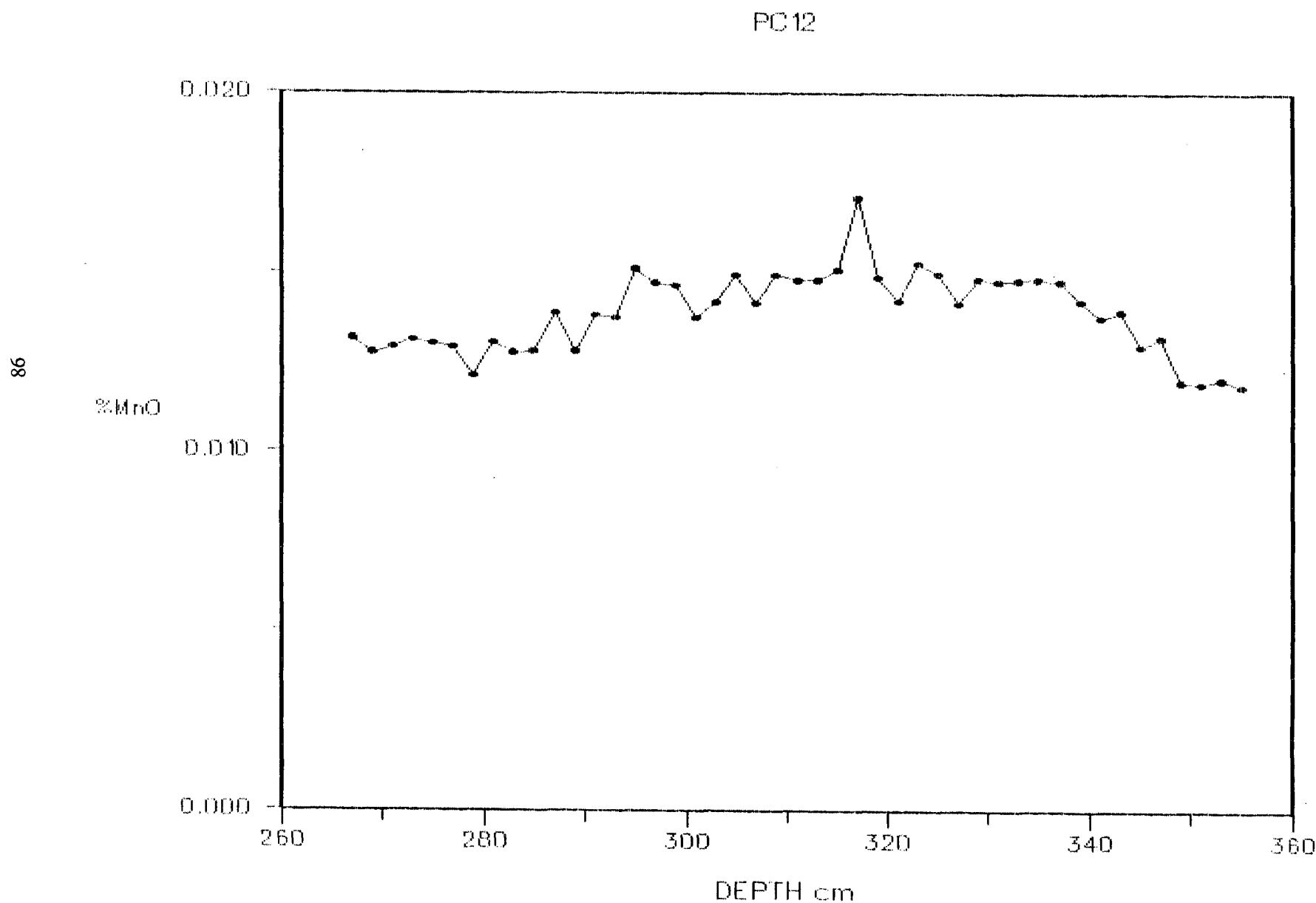


Fig 20.11

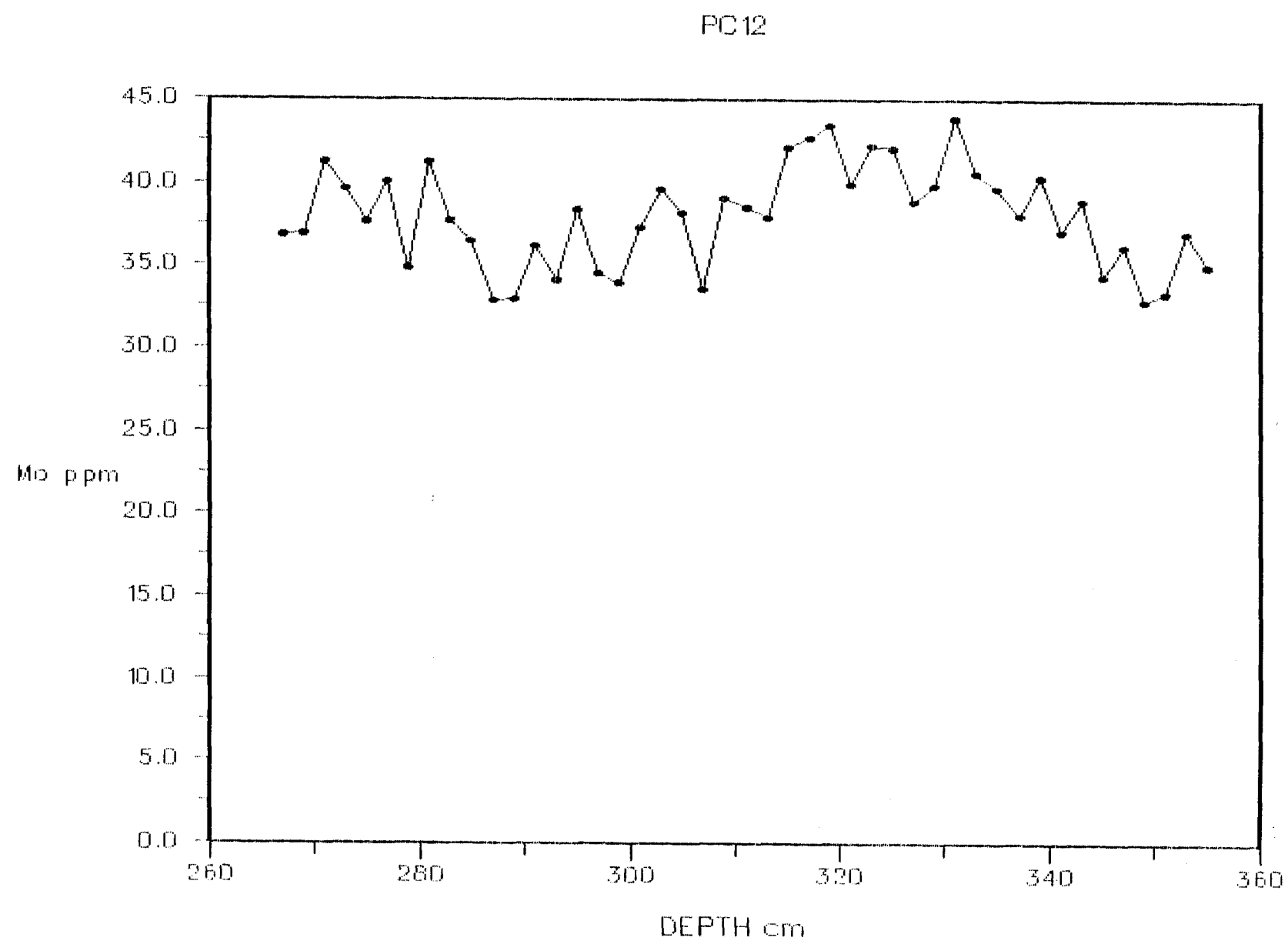


Fig 20.12

88

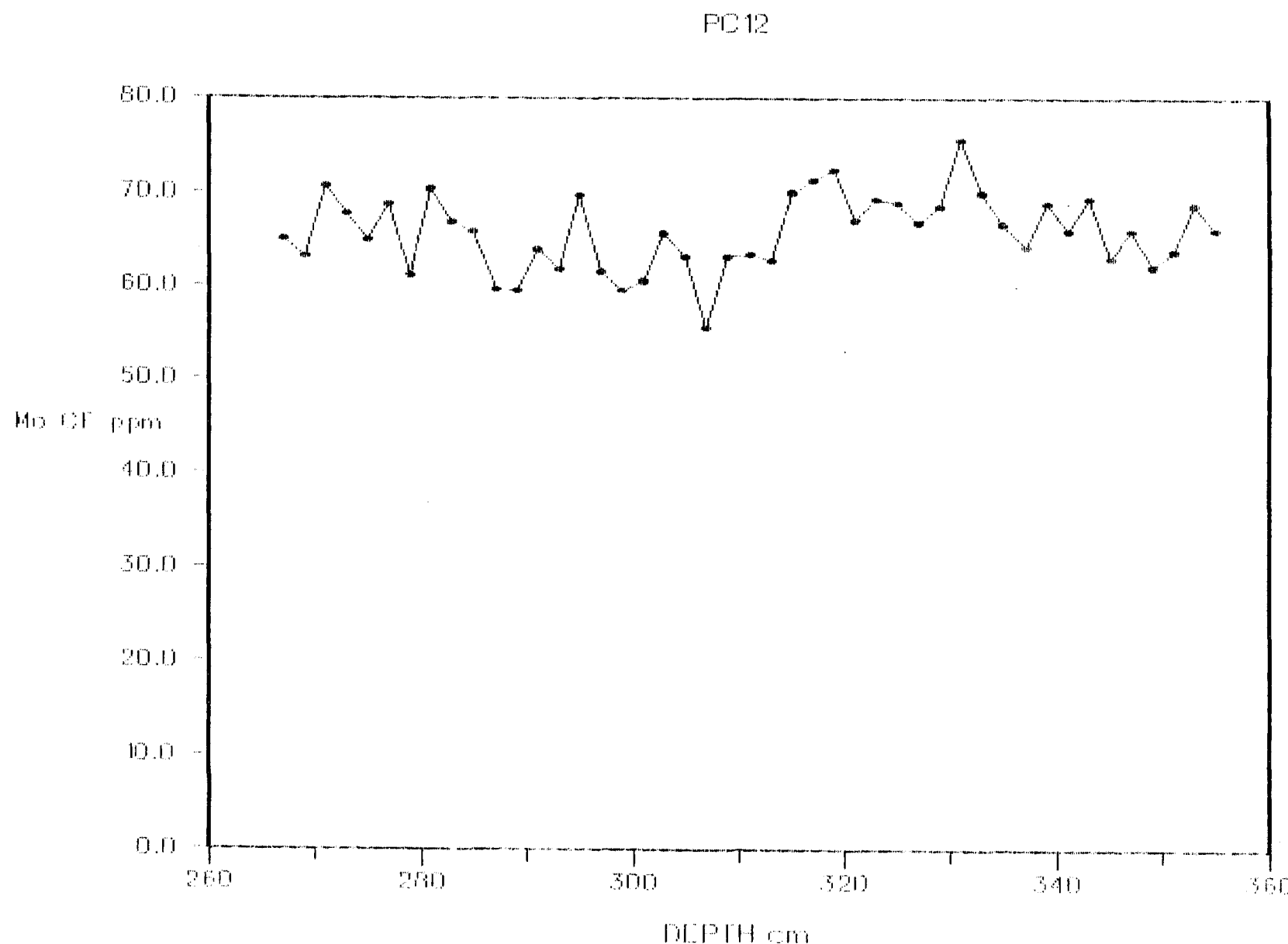


Fig 20.13

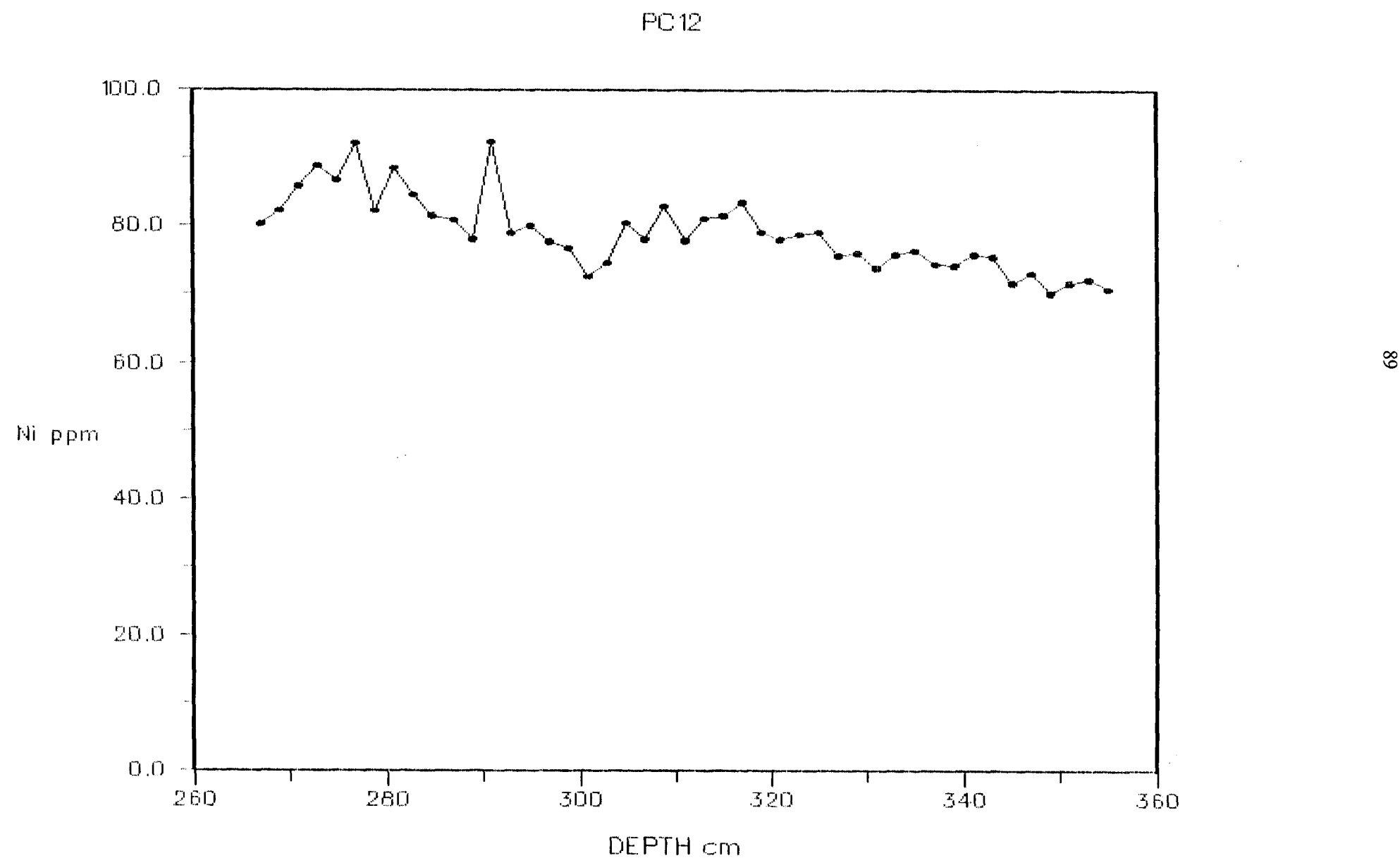


Fig 20.14

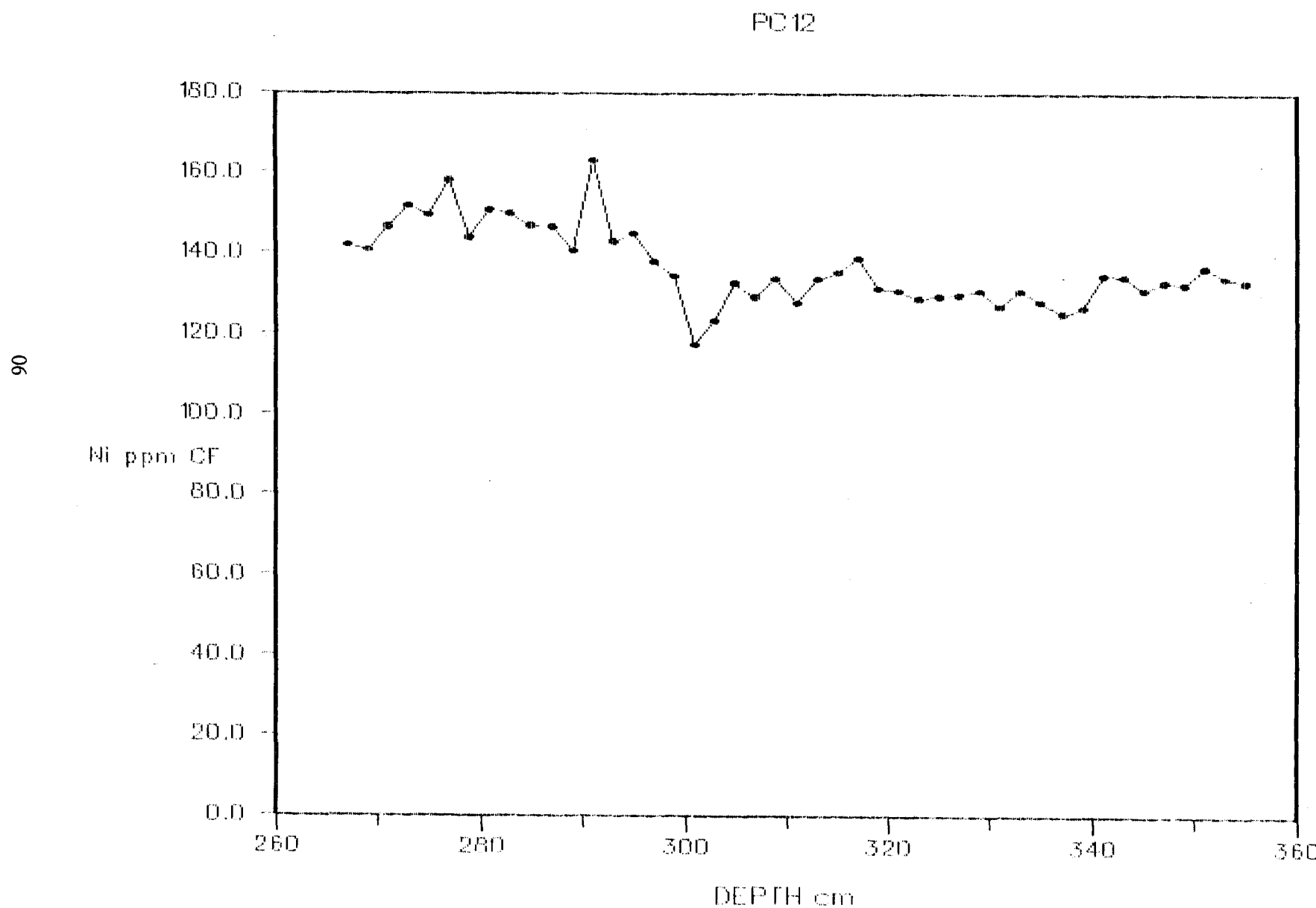


Fig 20.15

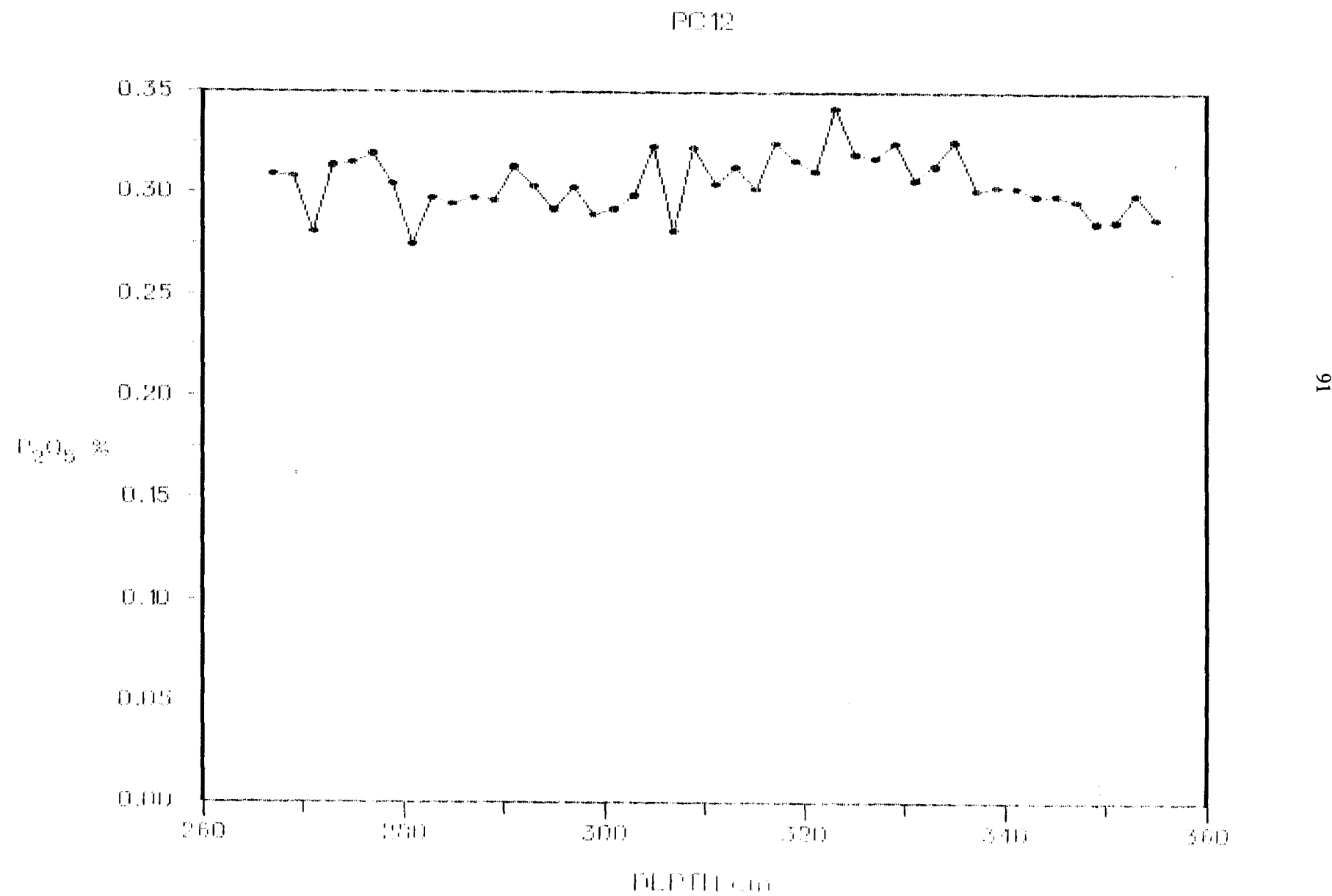


Fig 20.16

92

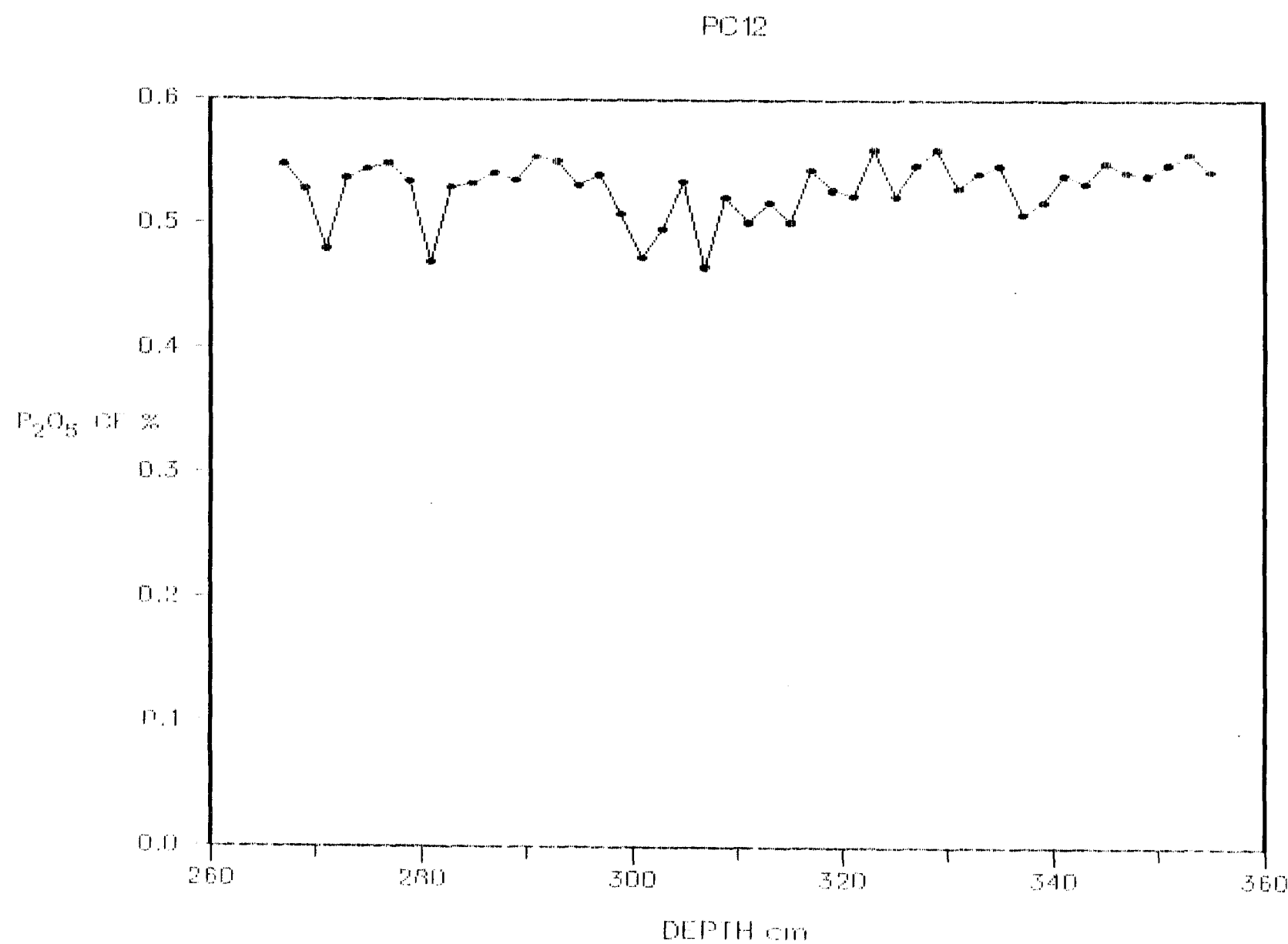


Fig 20.17

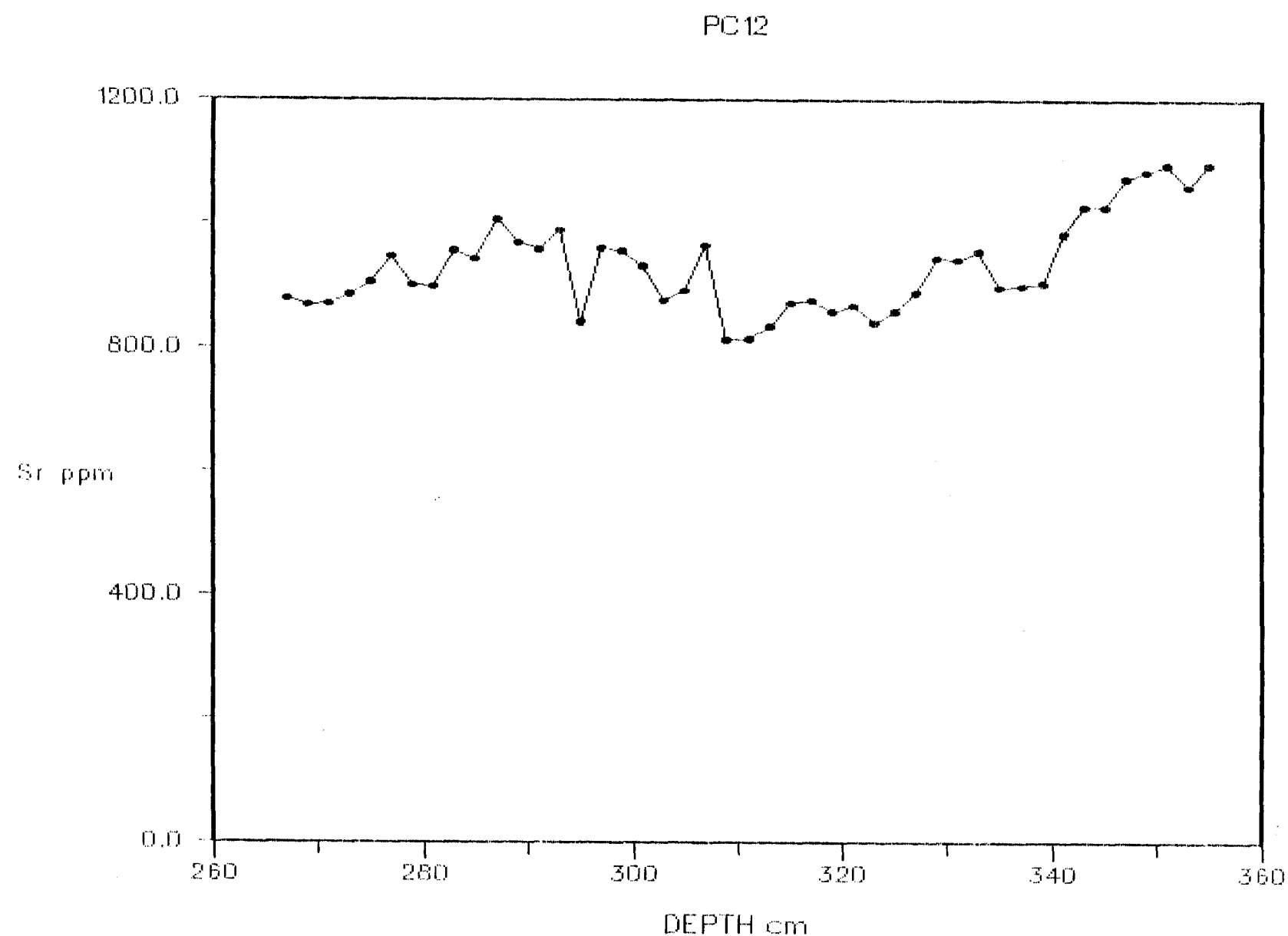


Fig 20.18

Fig 20.19

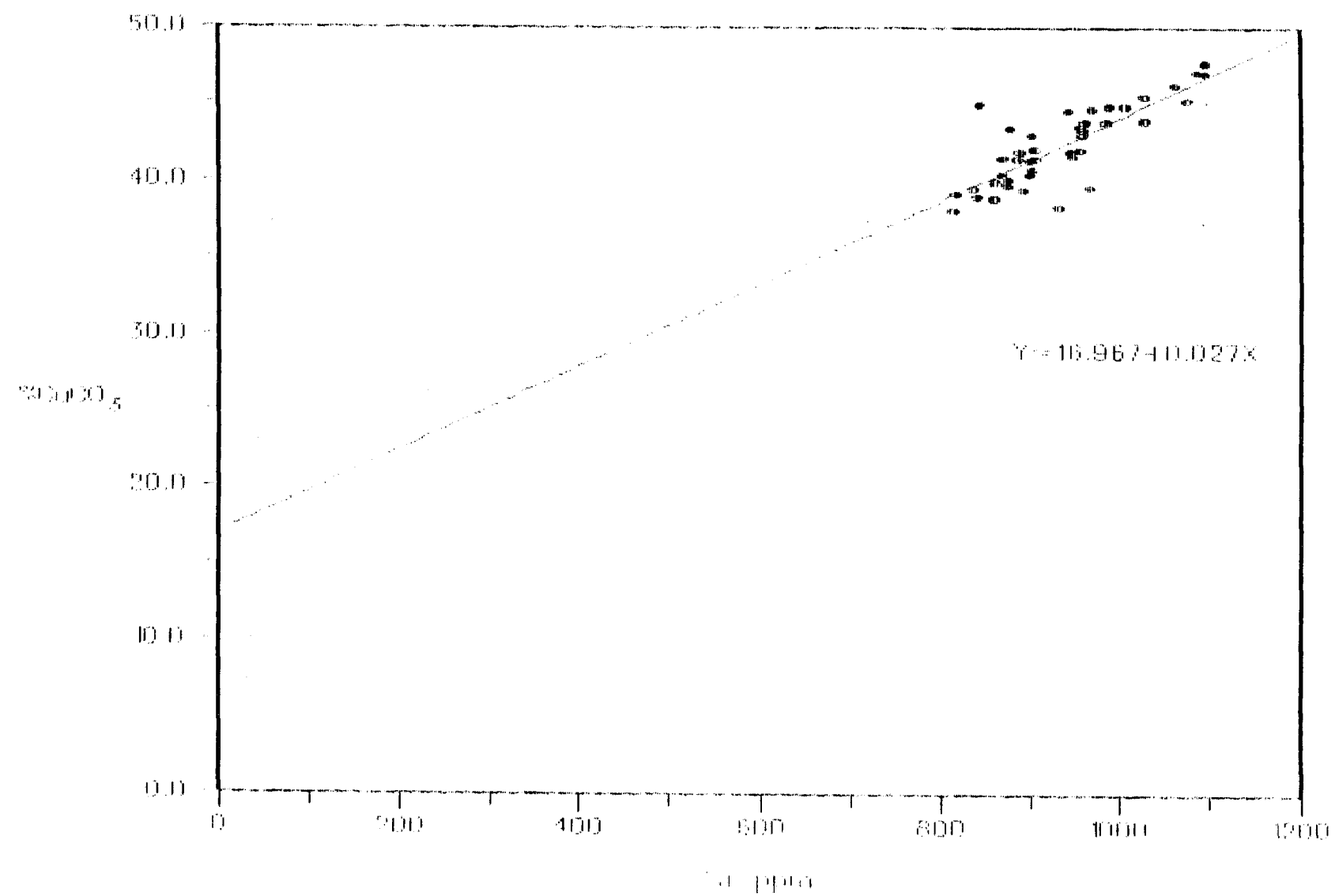


Fig 20.19

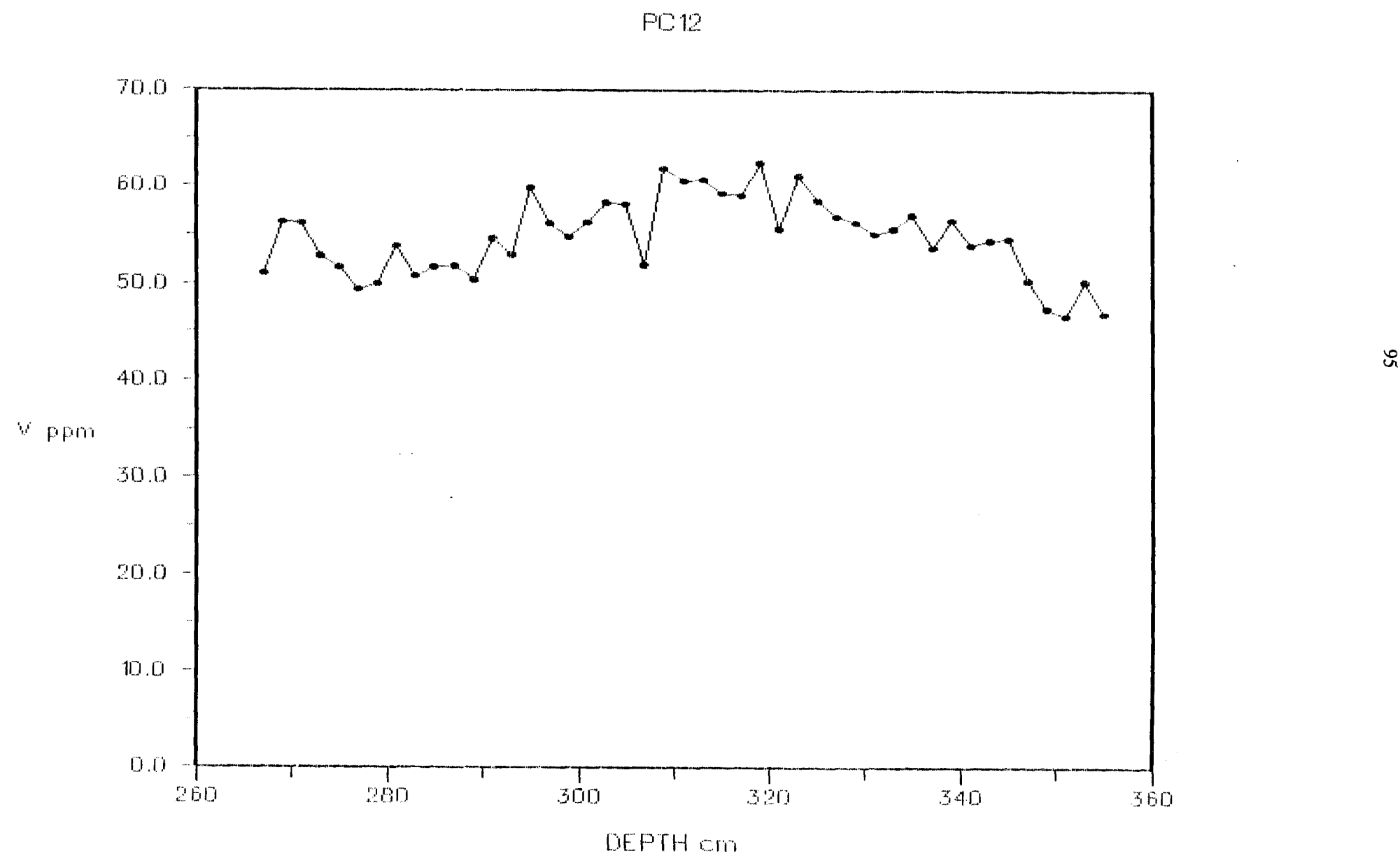


Fig 20.20

FIG 12

96

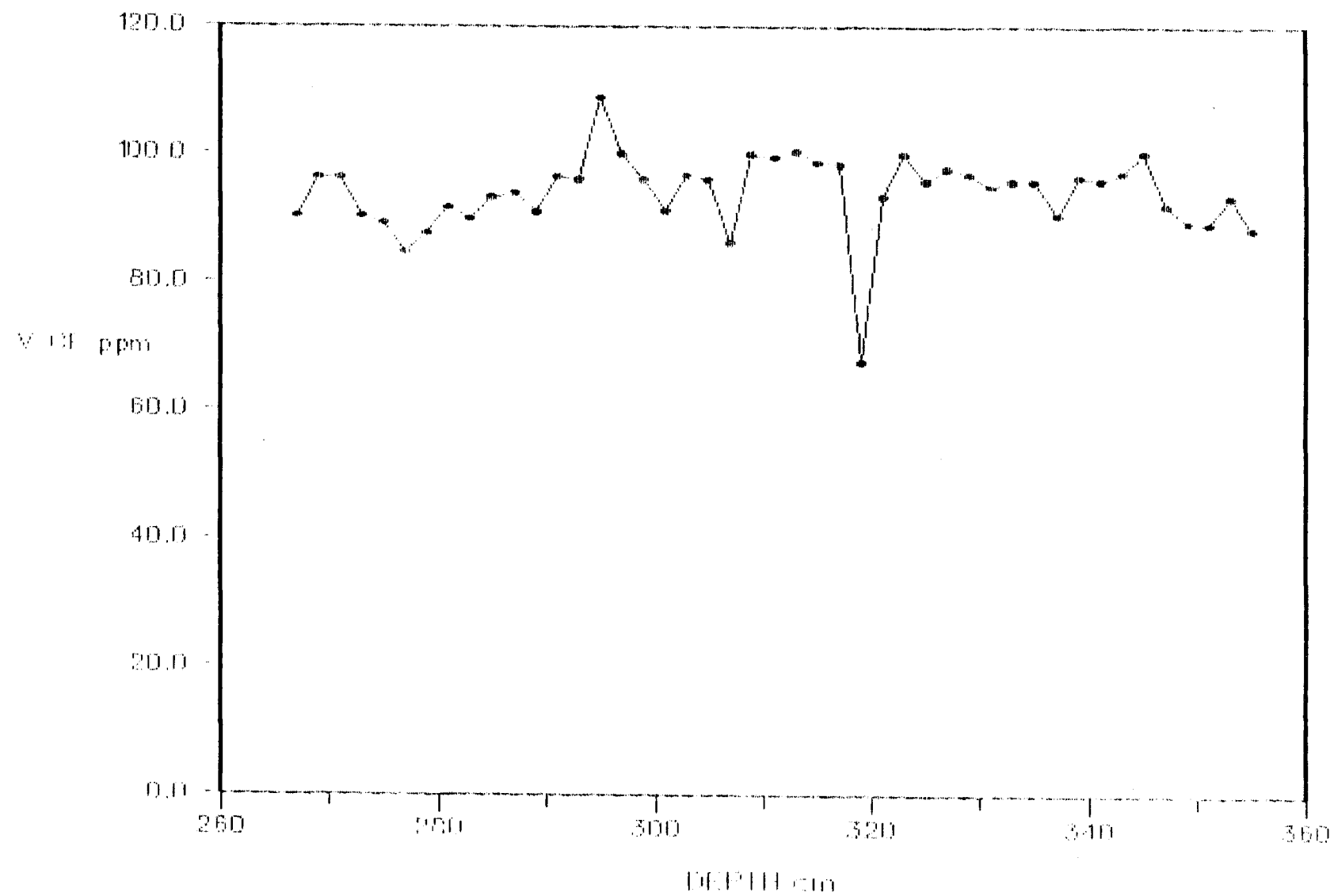


Fig 20.21

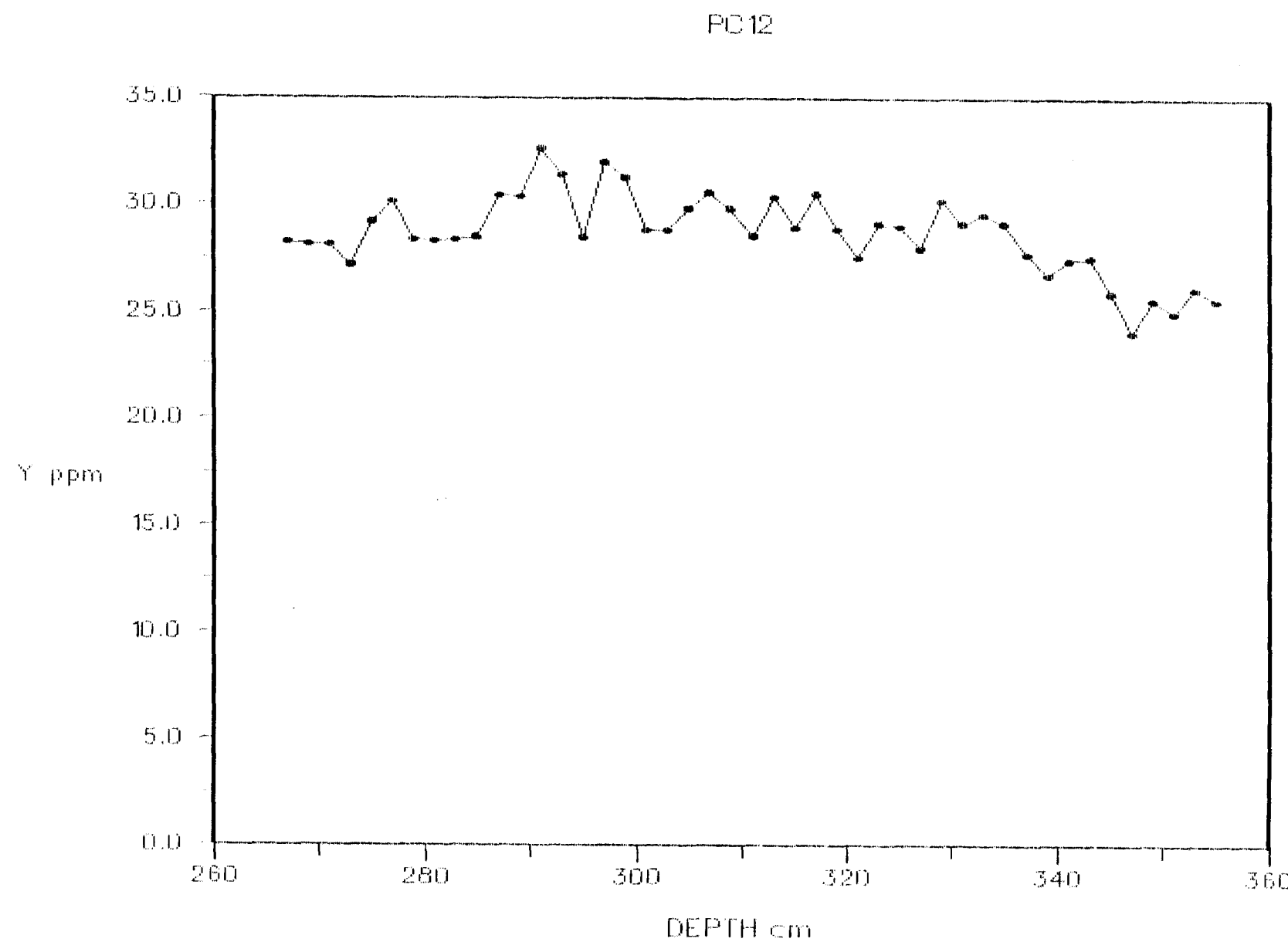


Fig 20.22

PC12

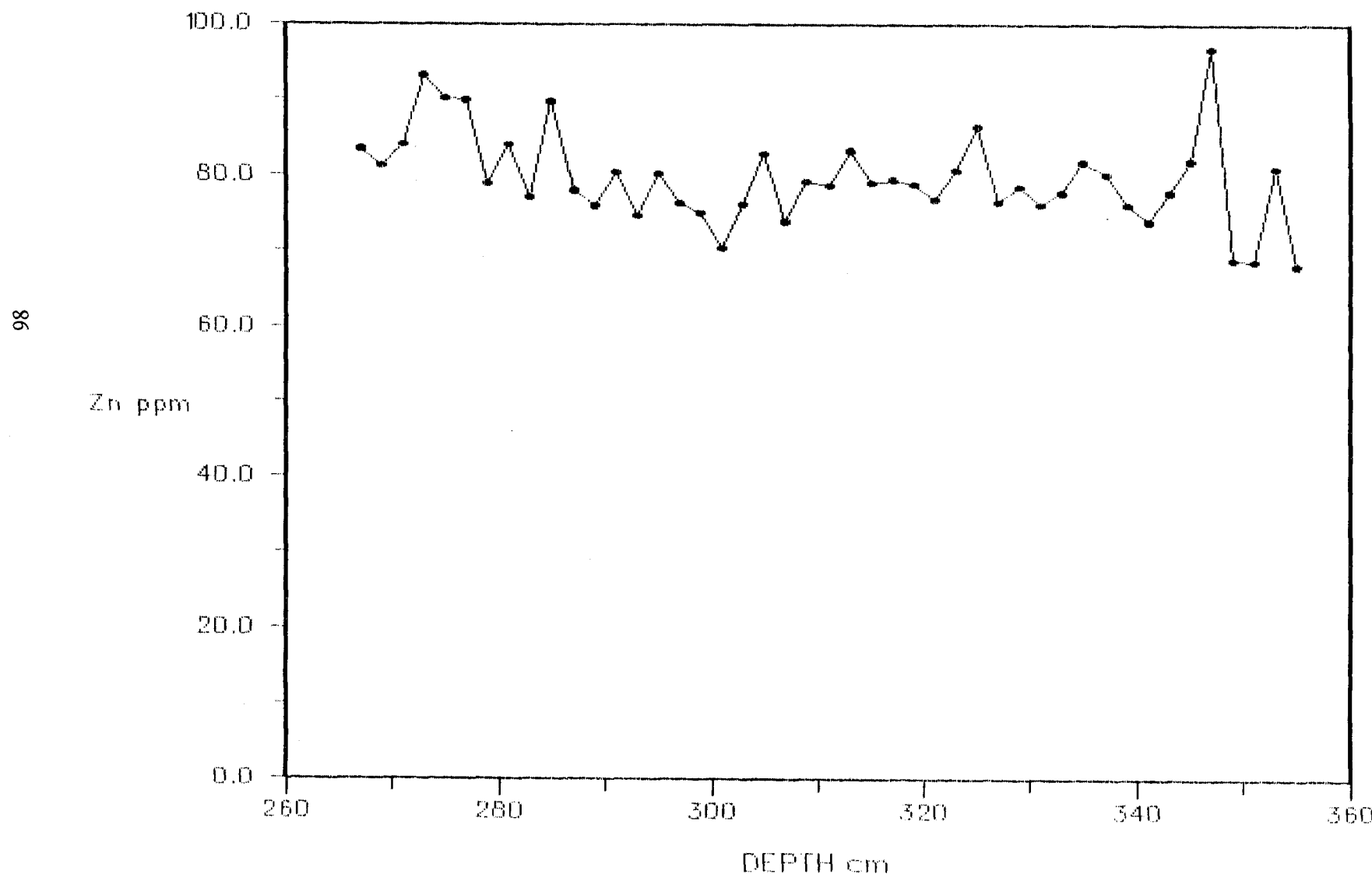


Fig 20.23

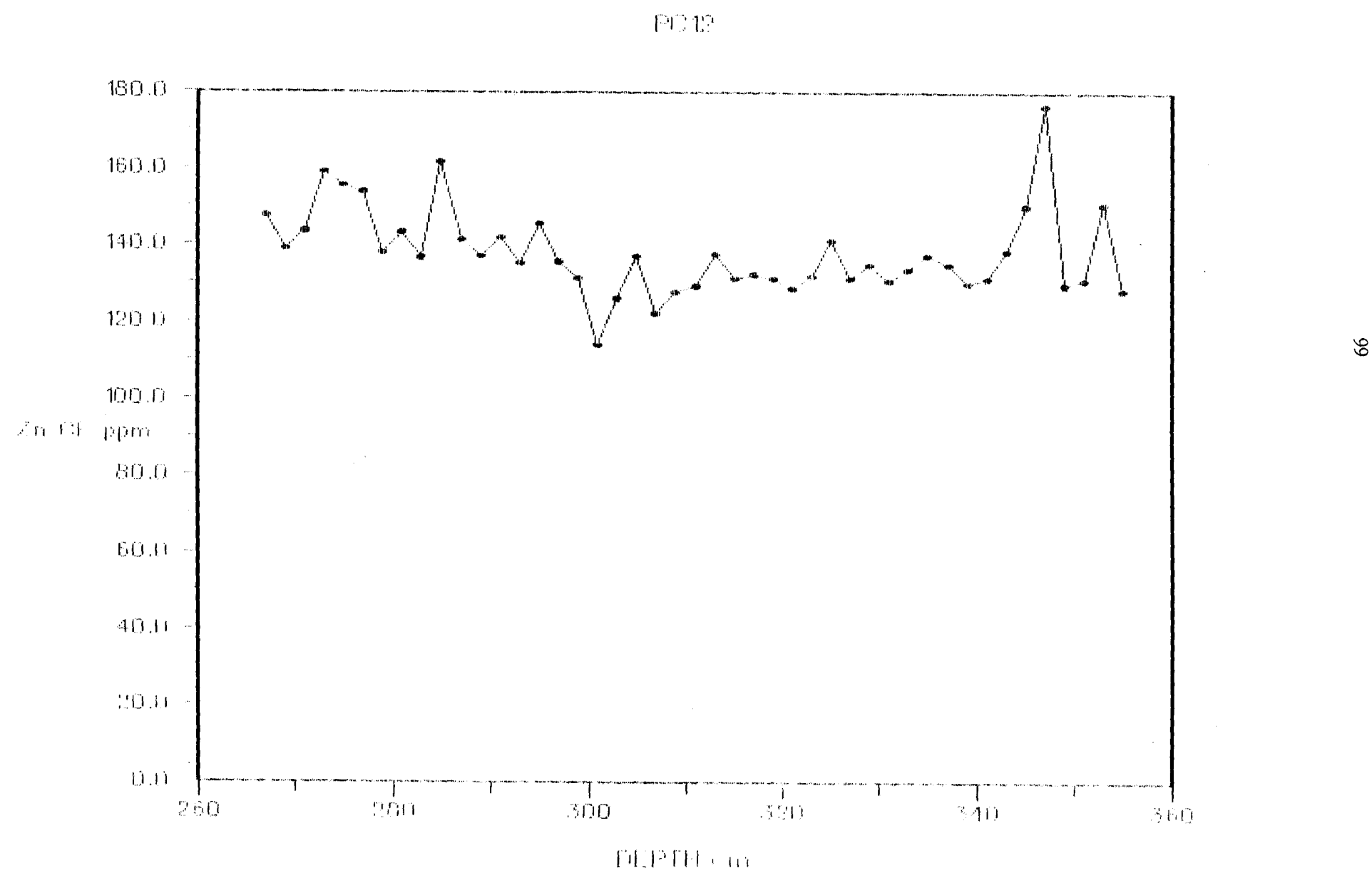


Fig 21.1

Fig 21. The calculated silica plots.

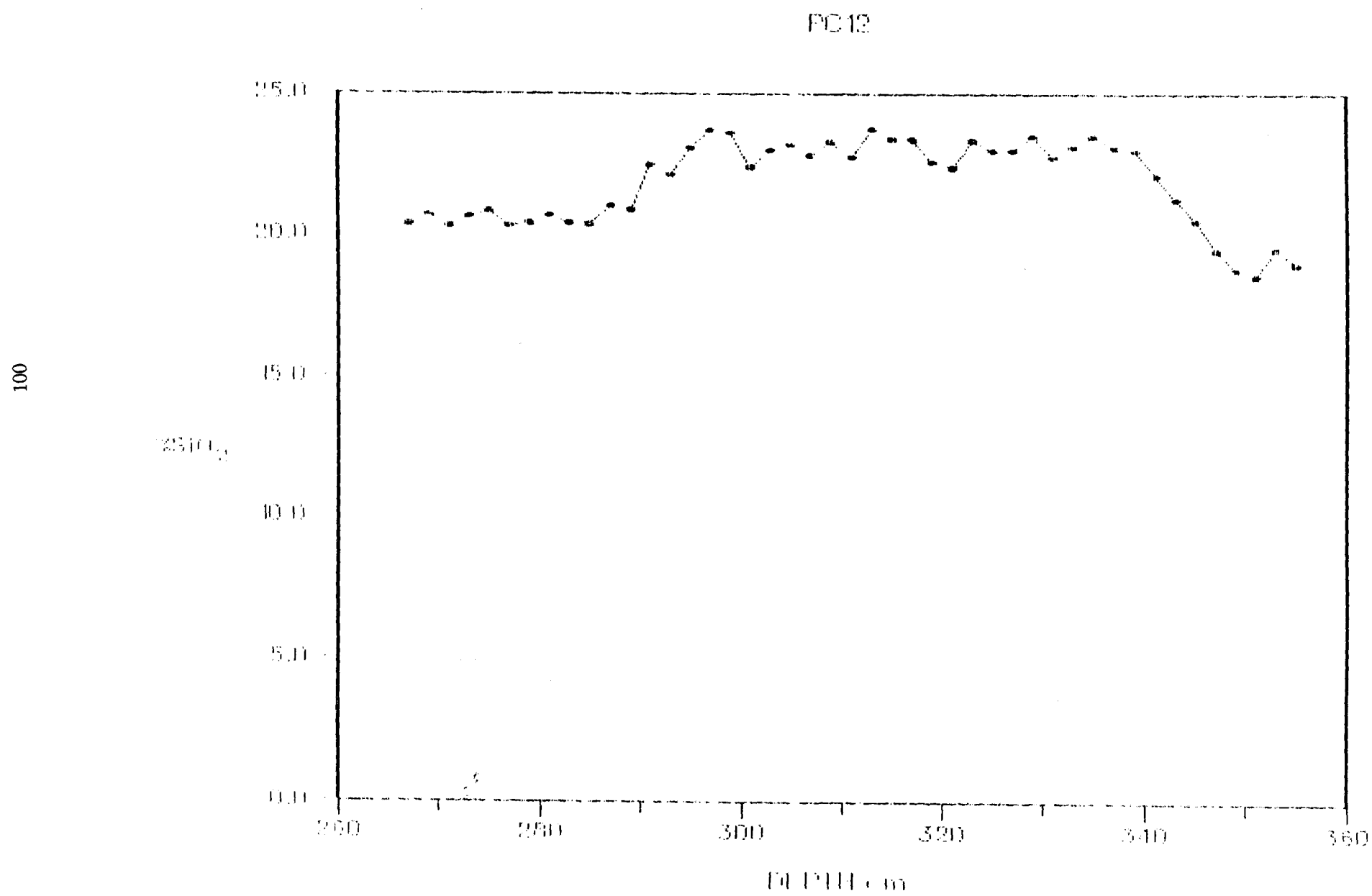


Fig 21.2

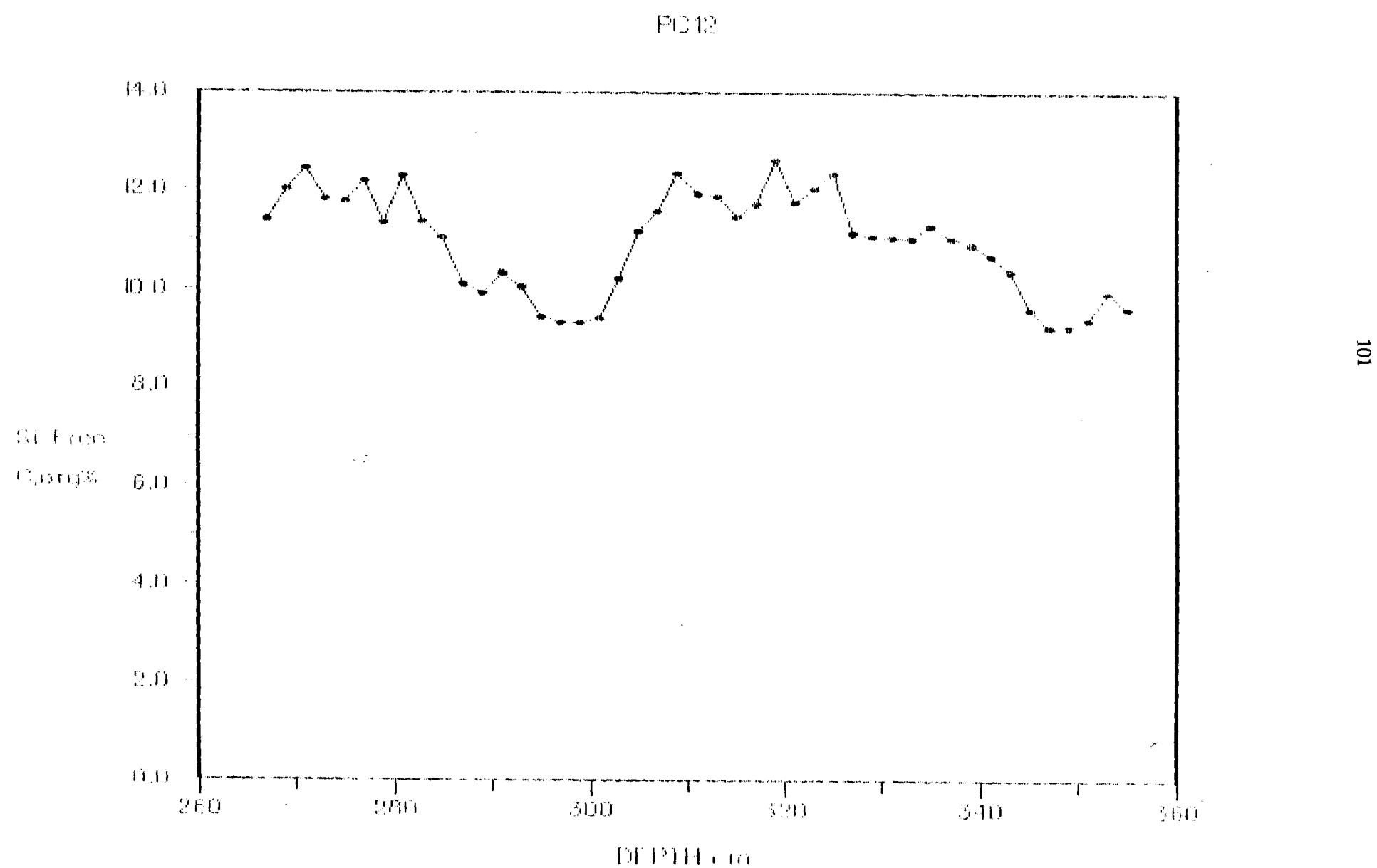


Fig 22.1

Fig 22. Limitations of the ICP-AES system.

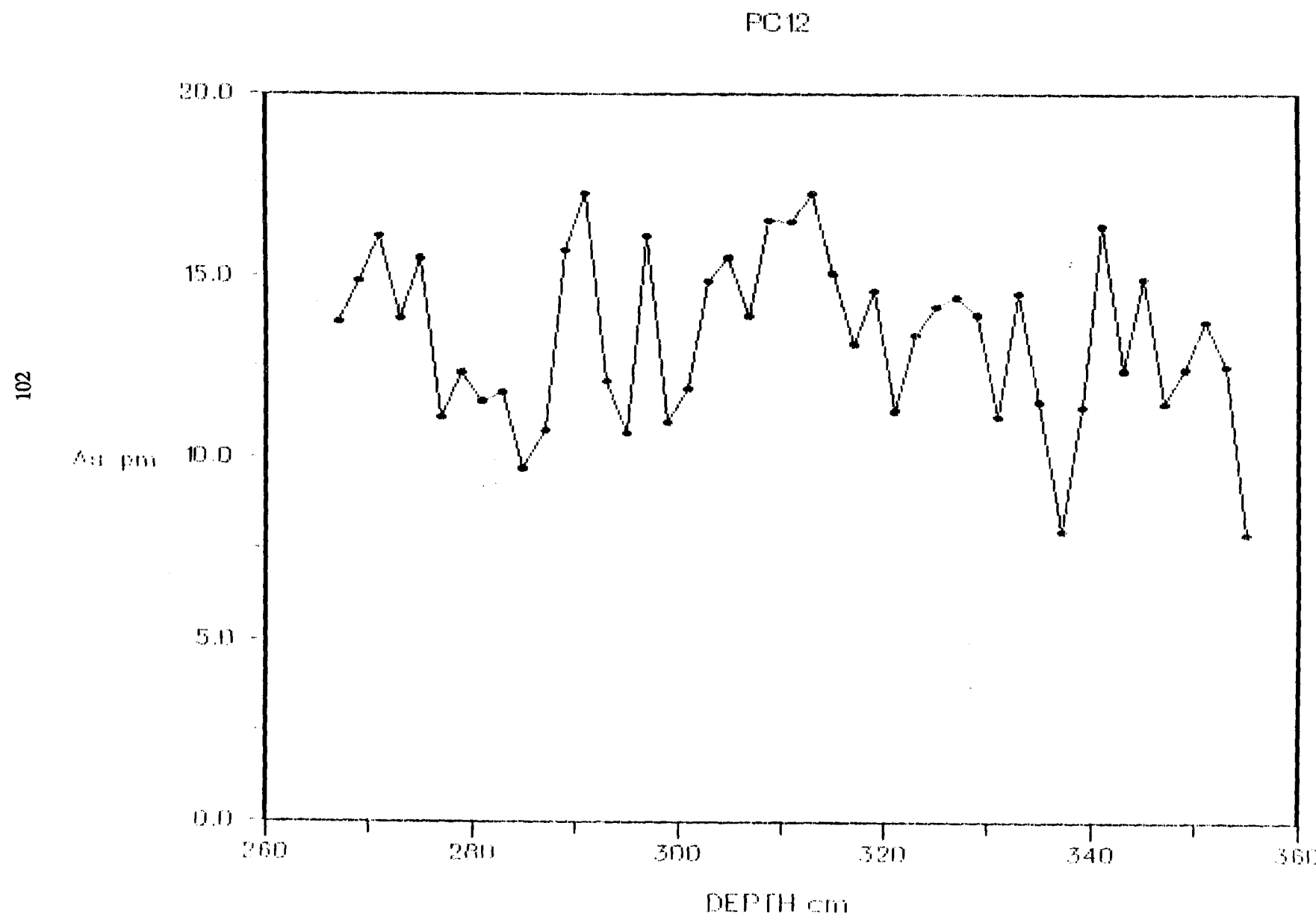


Fig 22.2

PC12

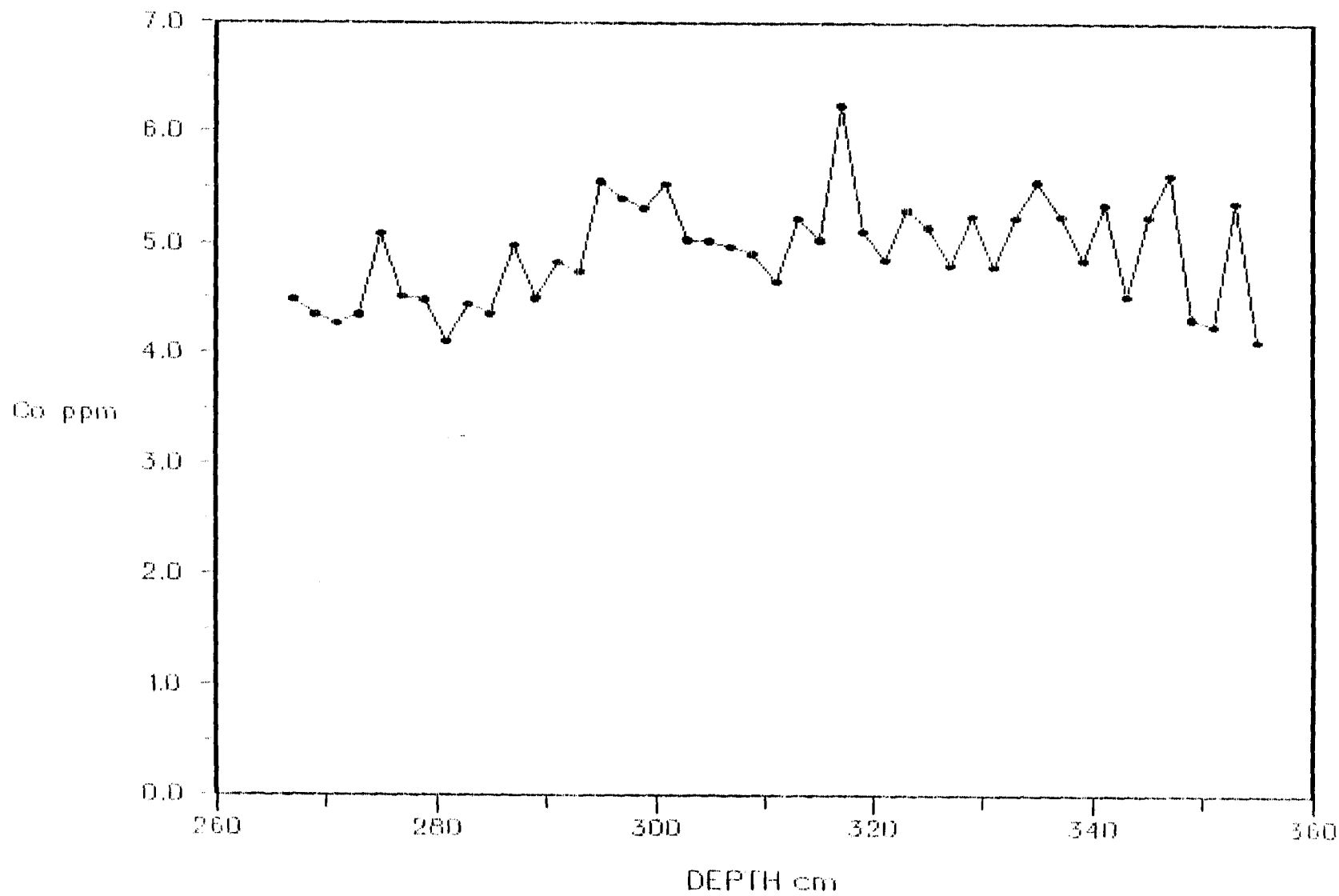


Fig 22.3

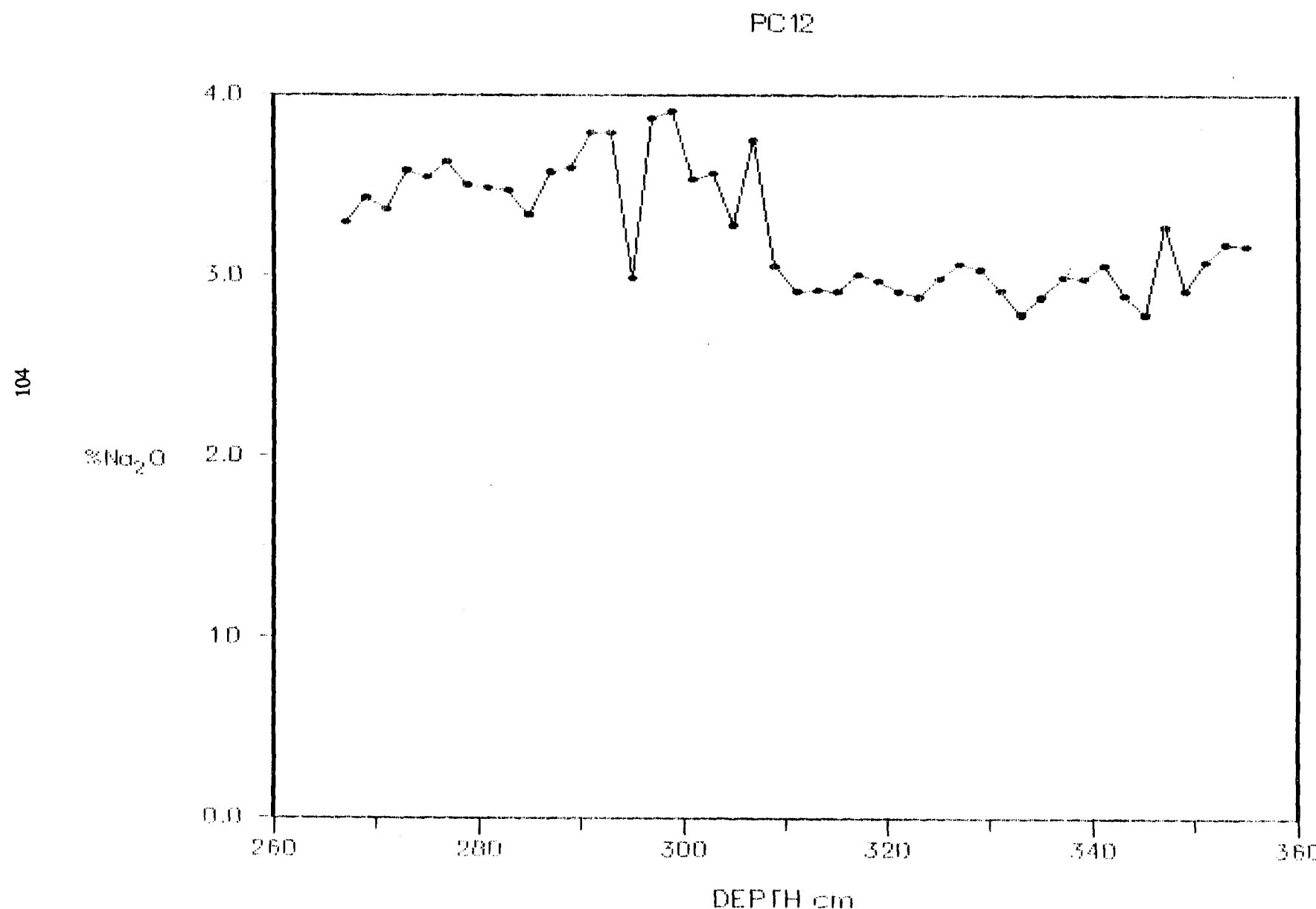


Fig 22.4

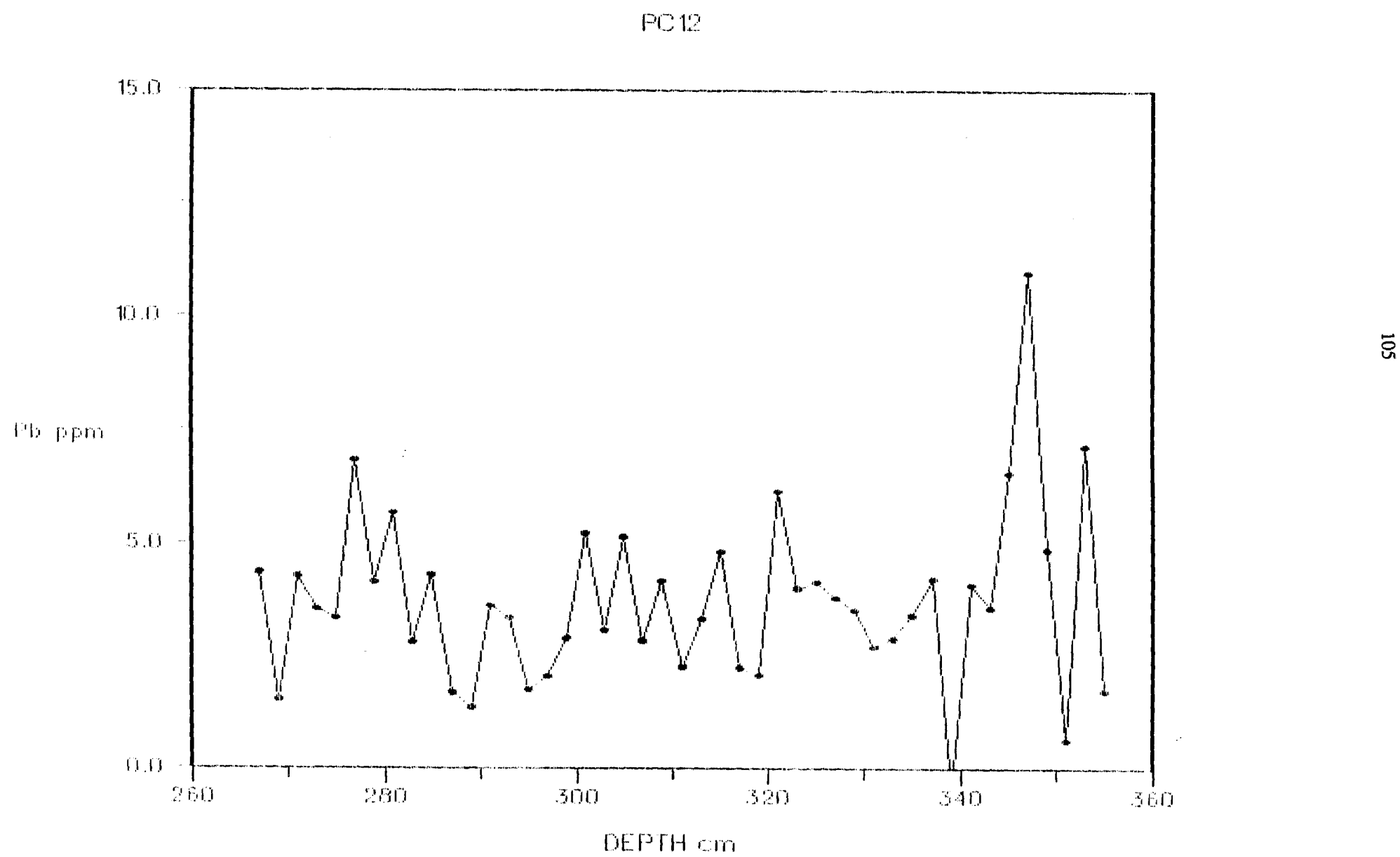


Fig 22.5

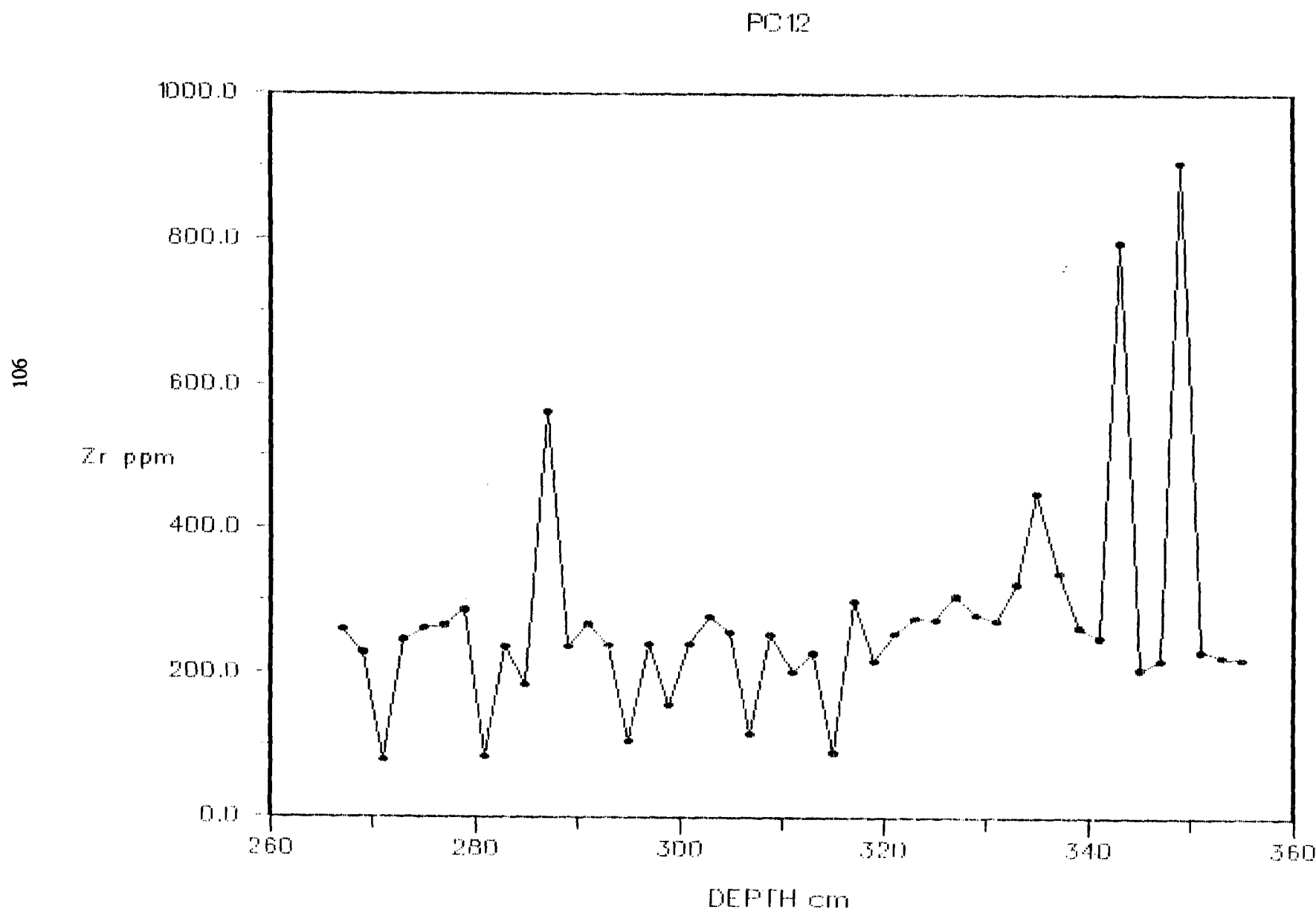


Fig 23. FFT of CaCO<sub>3</sub>%.

107

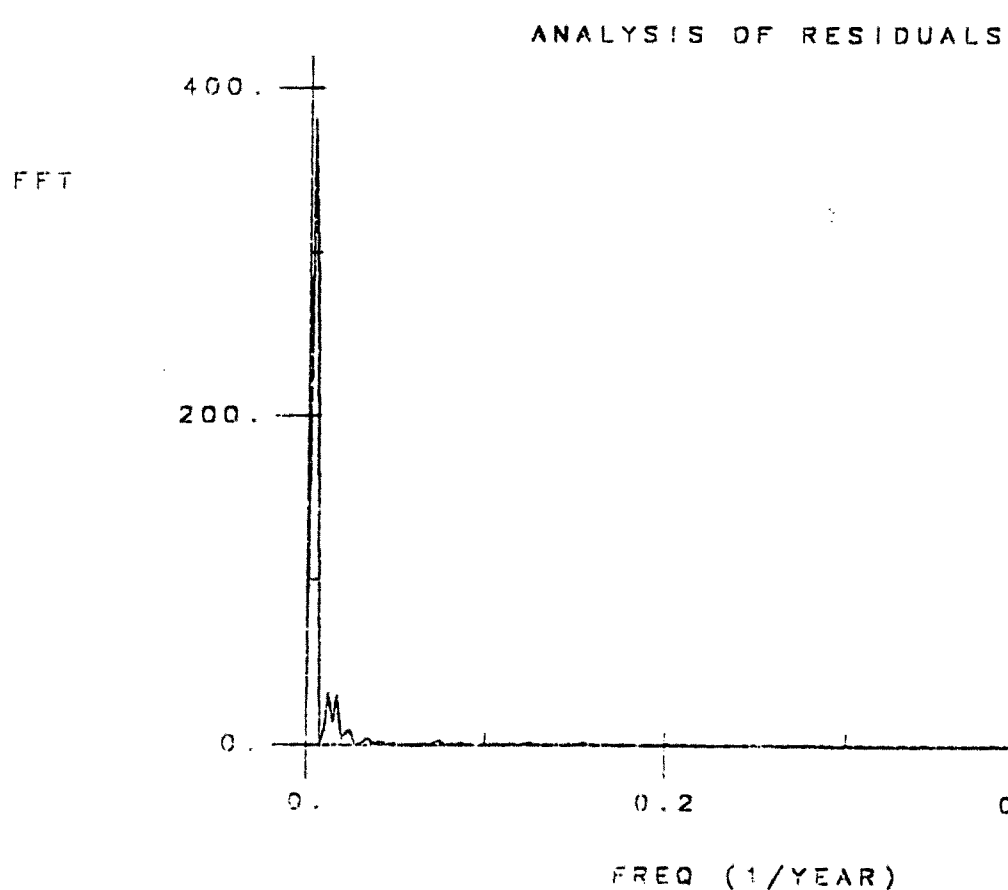
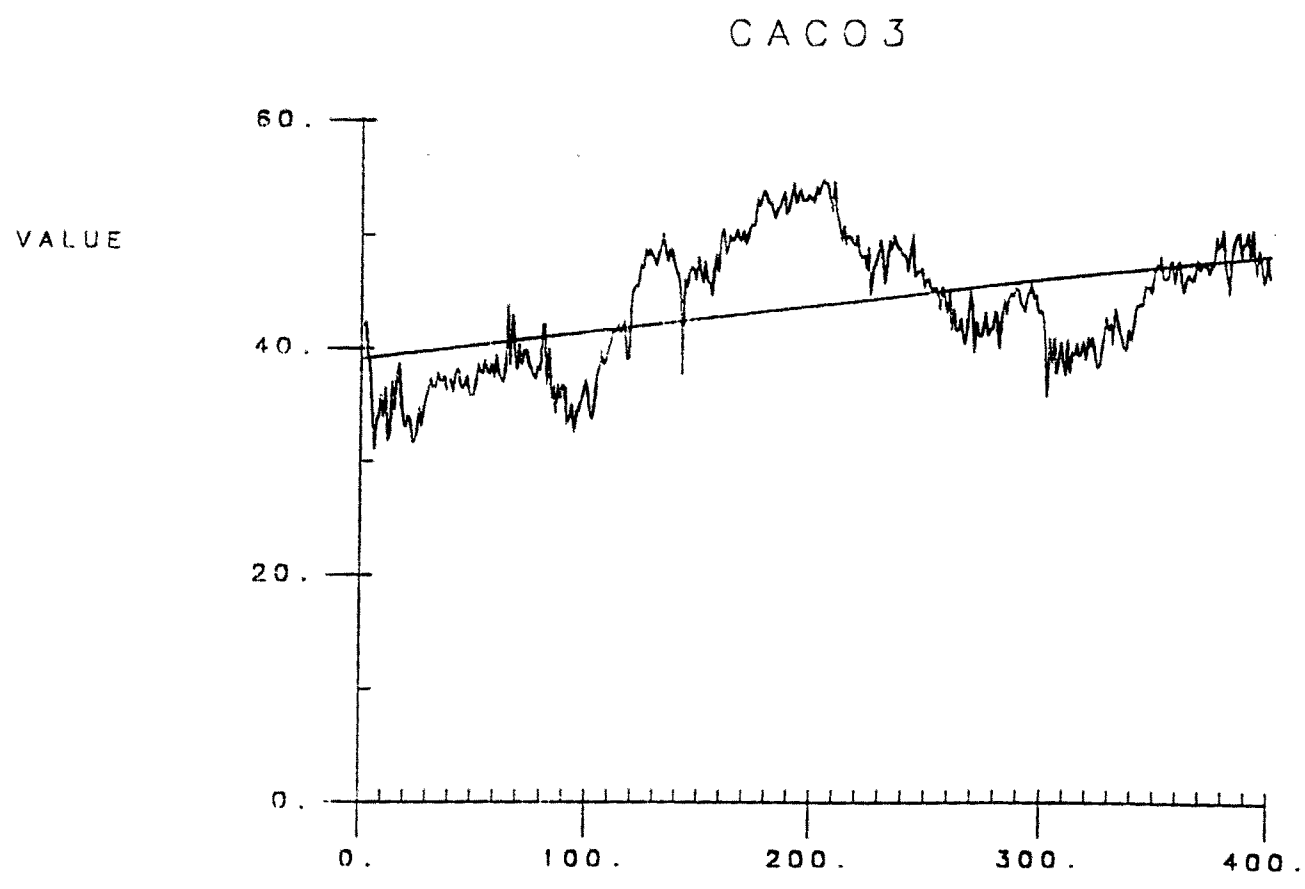


Fig 24. FFT of Corg%.

108

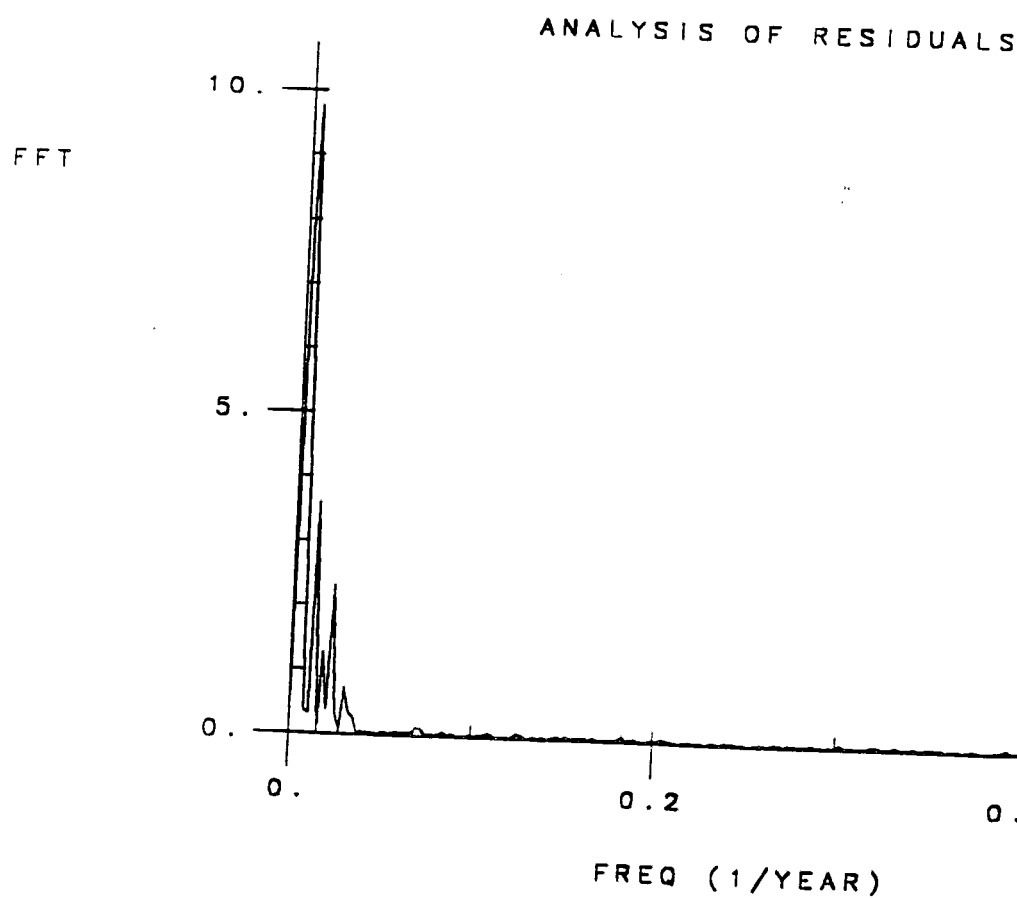
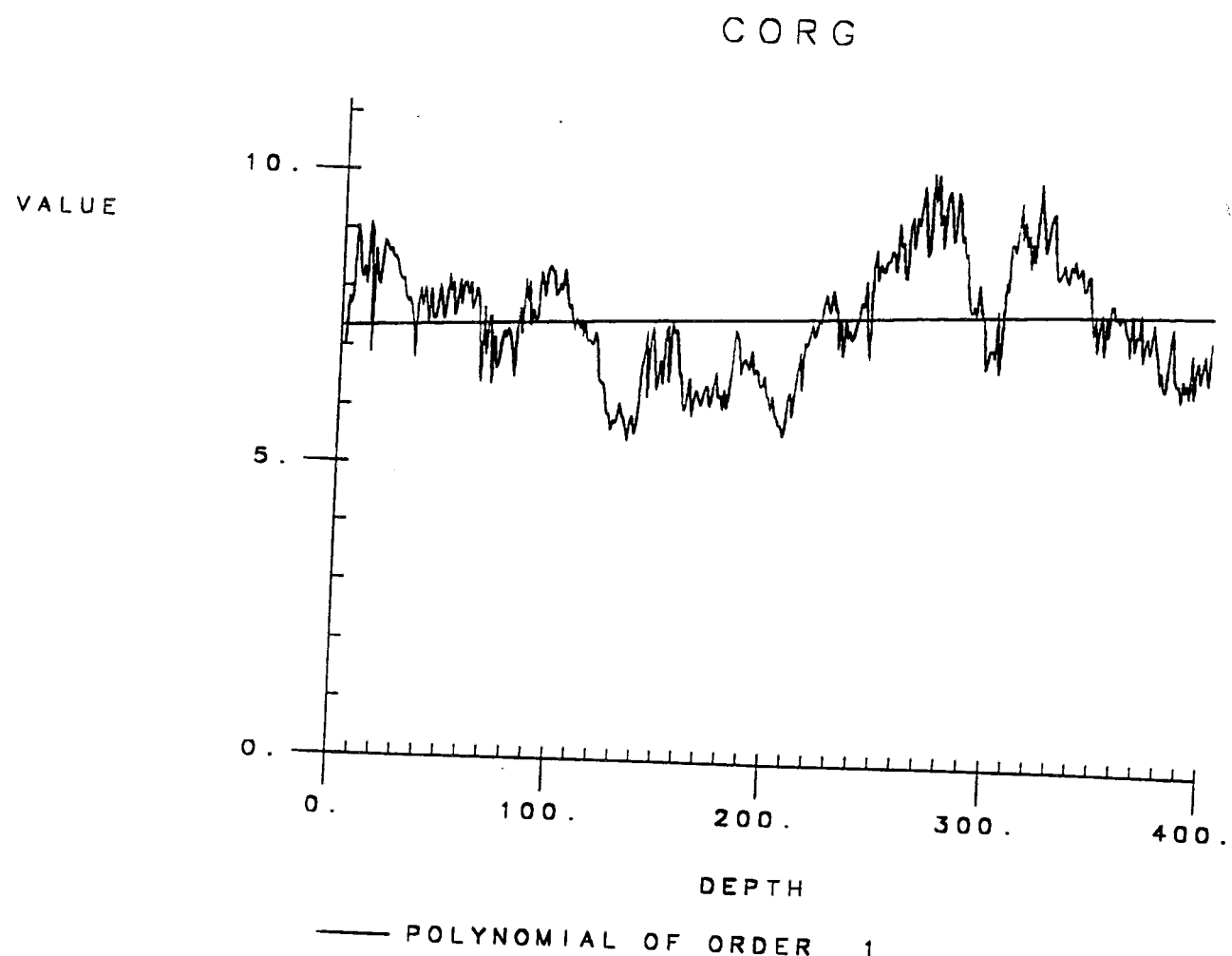
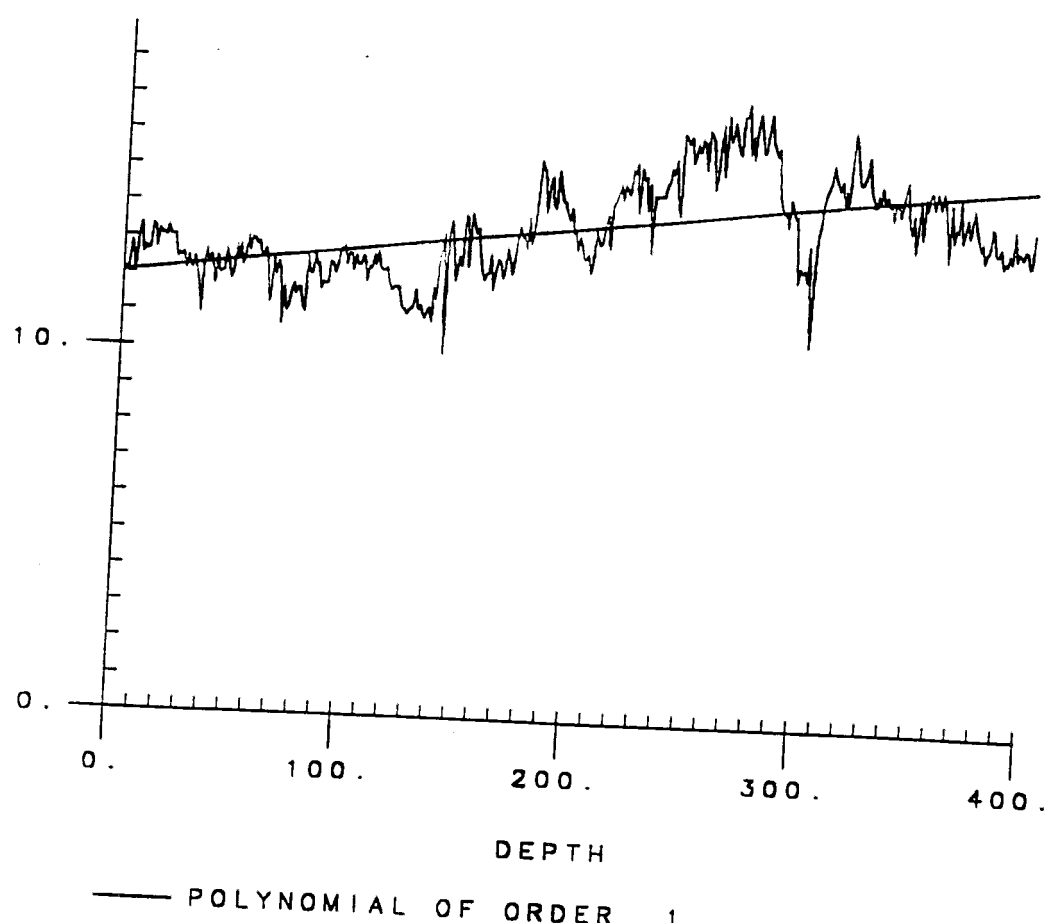


Fig 25. FFT of CF Corg%.

109

CF

VALUE



ANALYSIS OF RESIDUALS

FFT

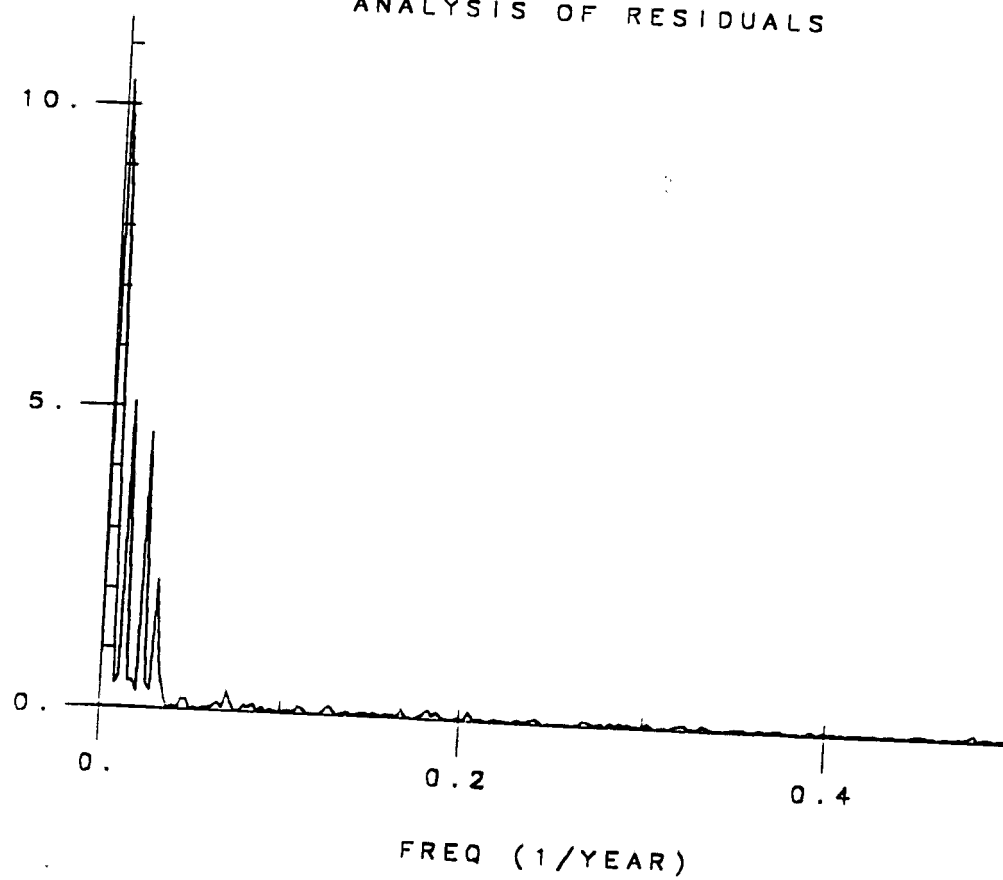
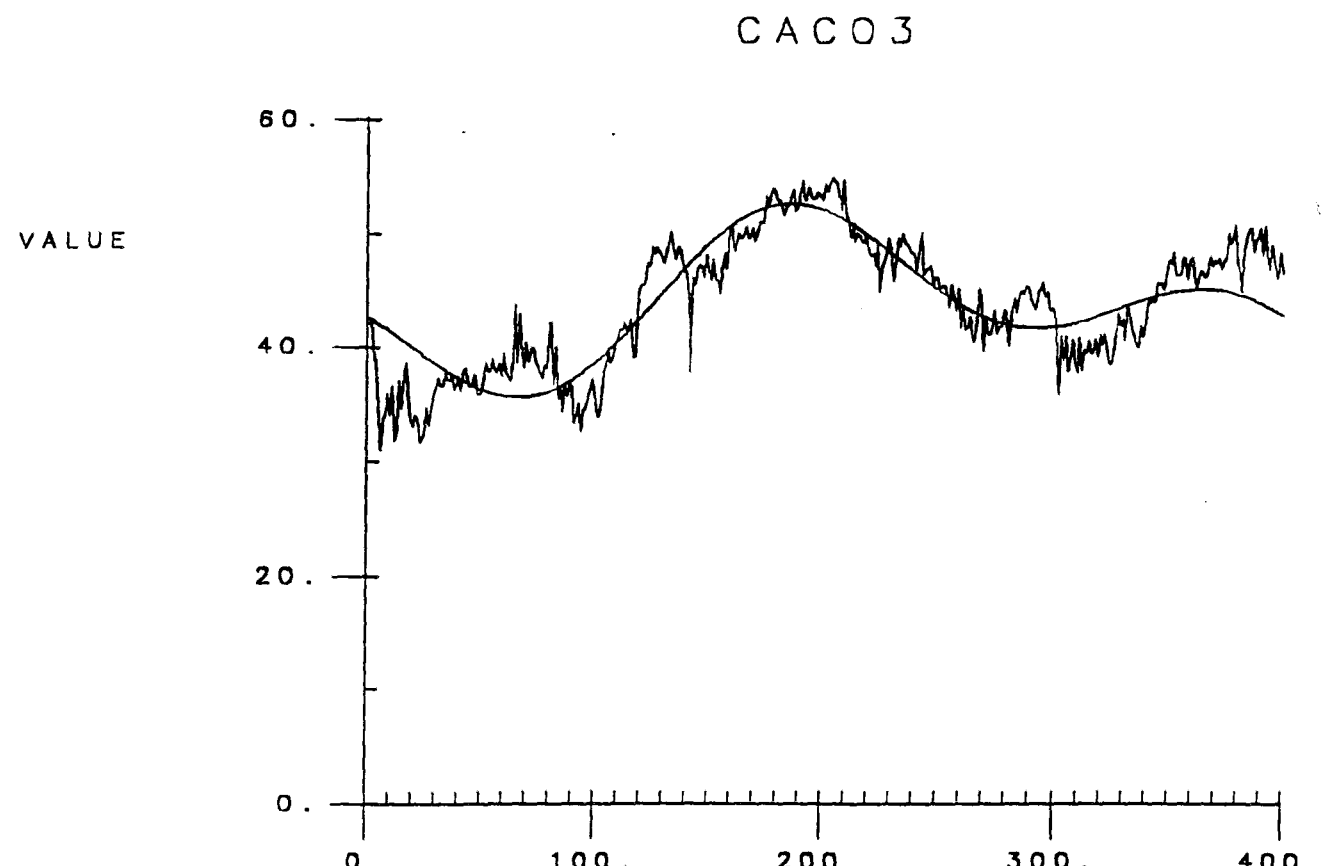


Fig 26. FFT of CaCO<sub>3</sub>% after removing the first 2 components.

— 2 COMP. S SUBTRACTED

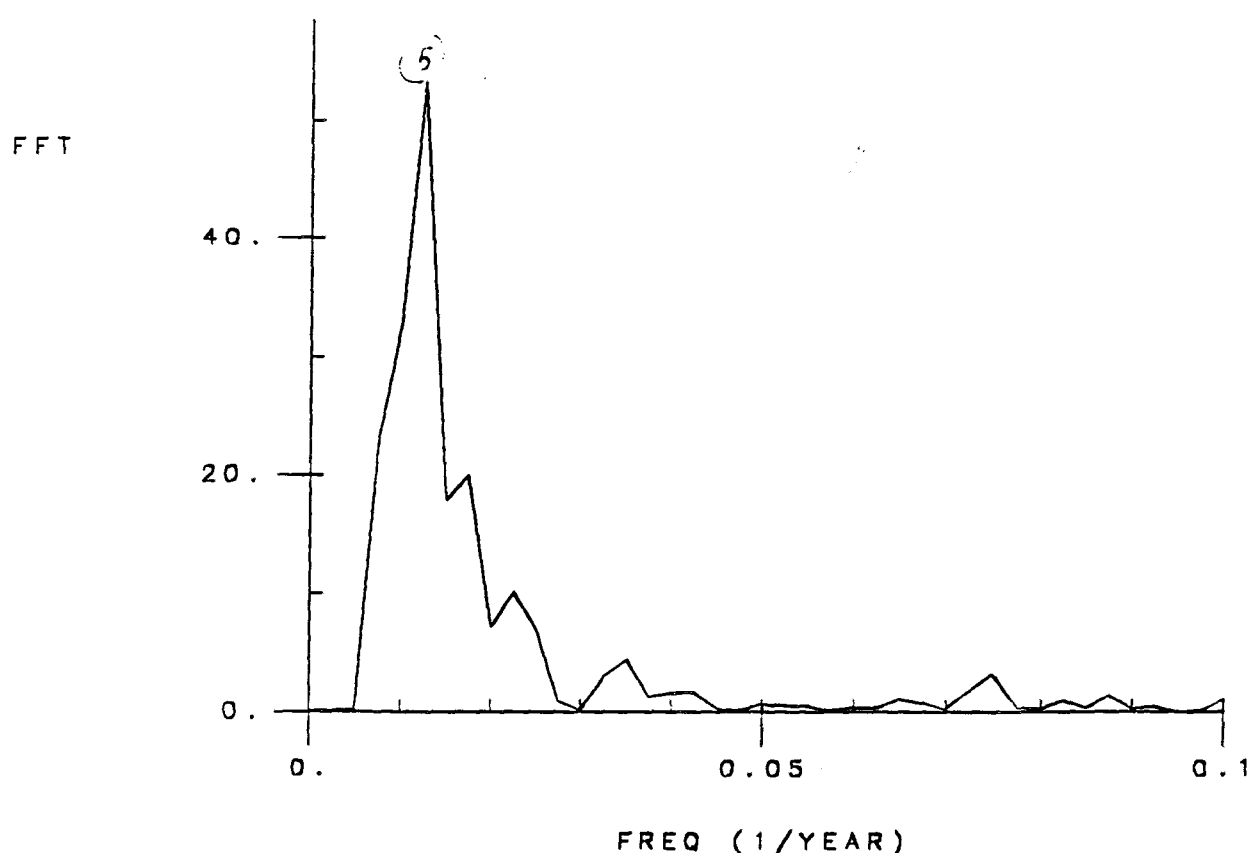


Fig 27. FFT of Corg% after removing the first 2 components.

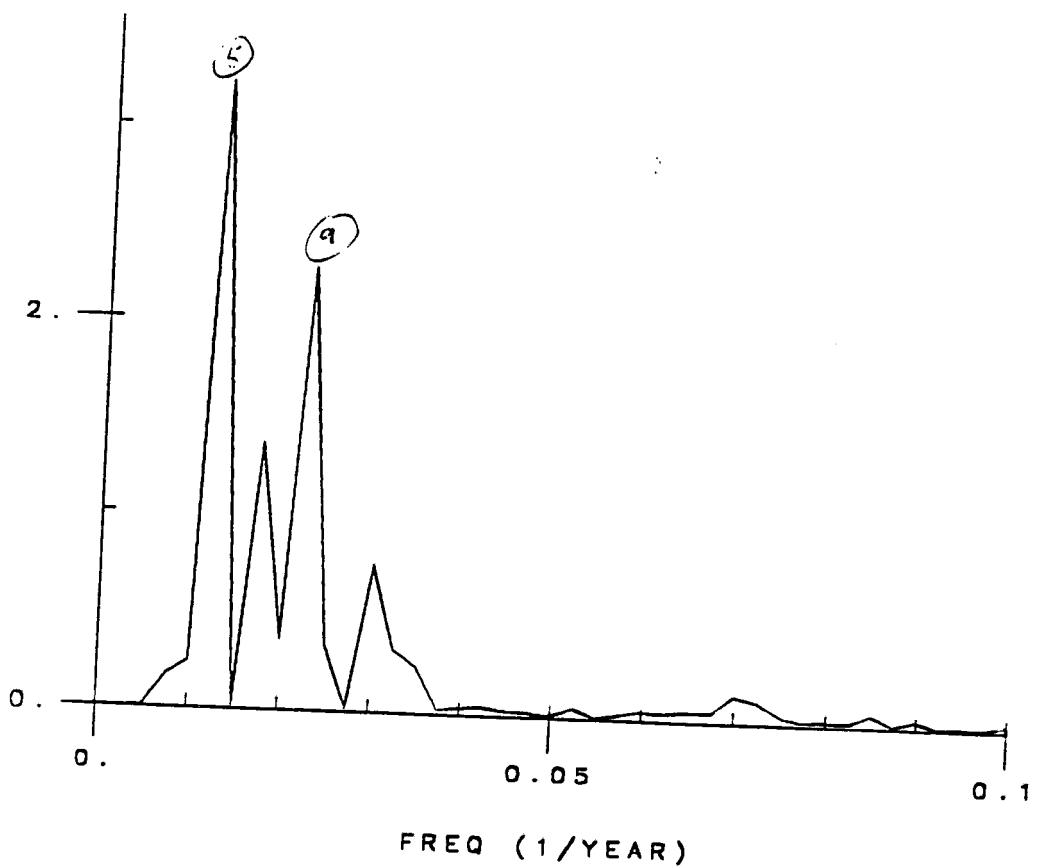
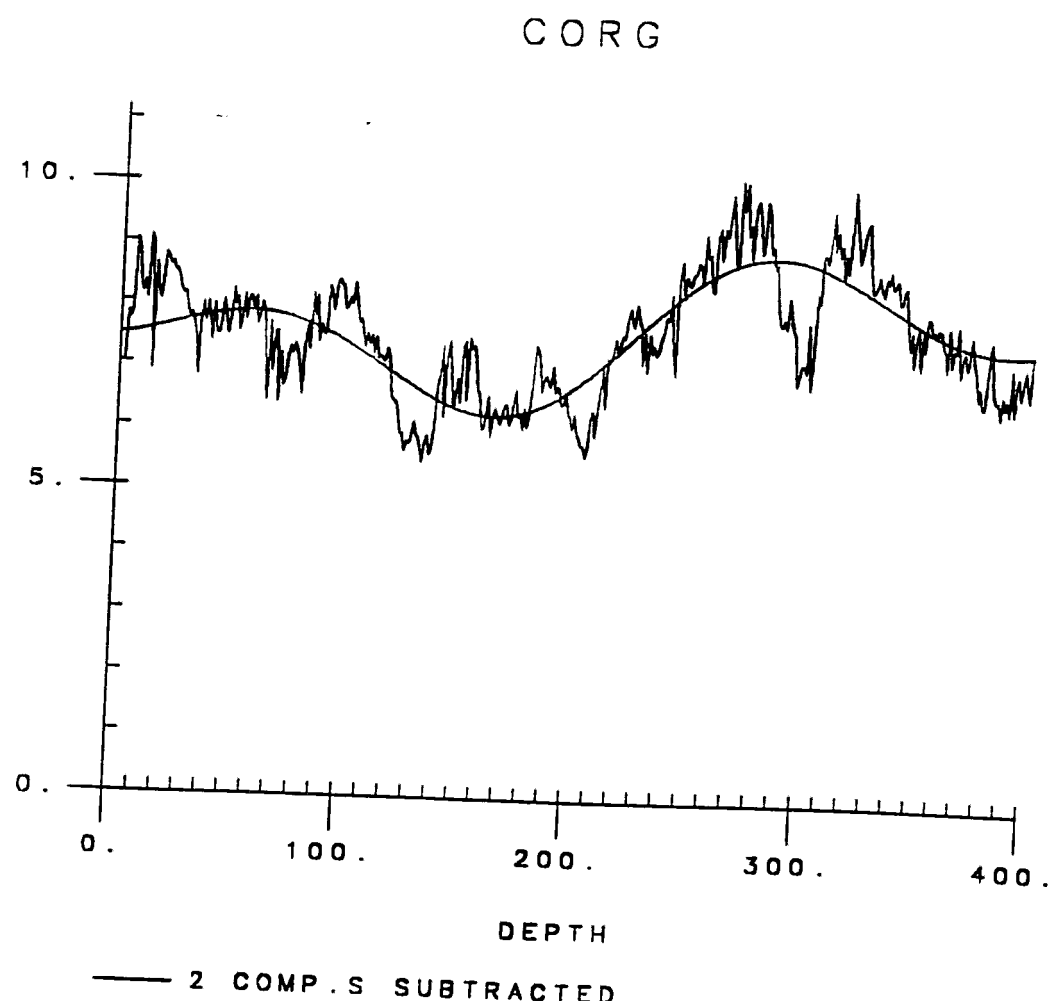
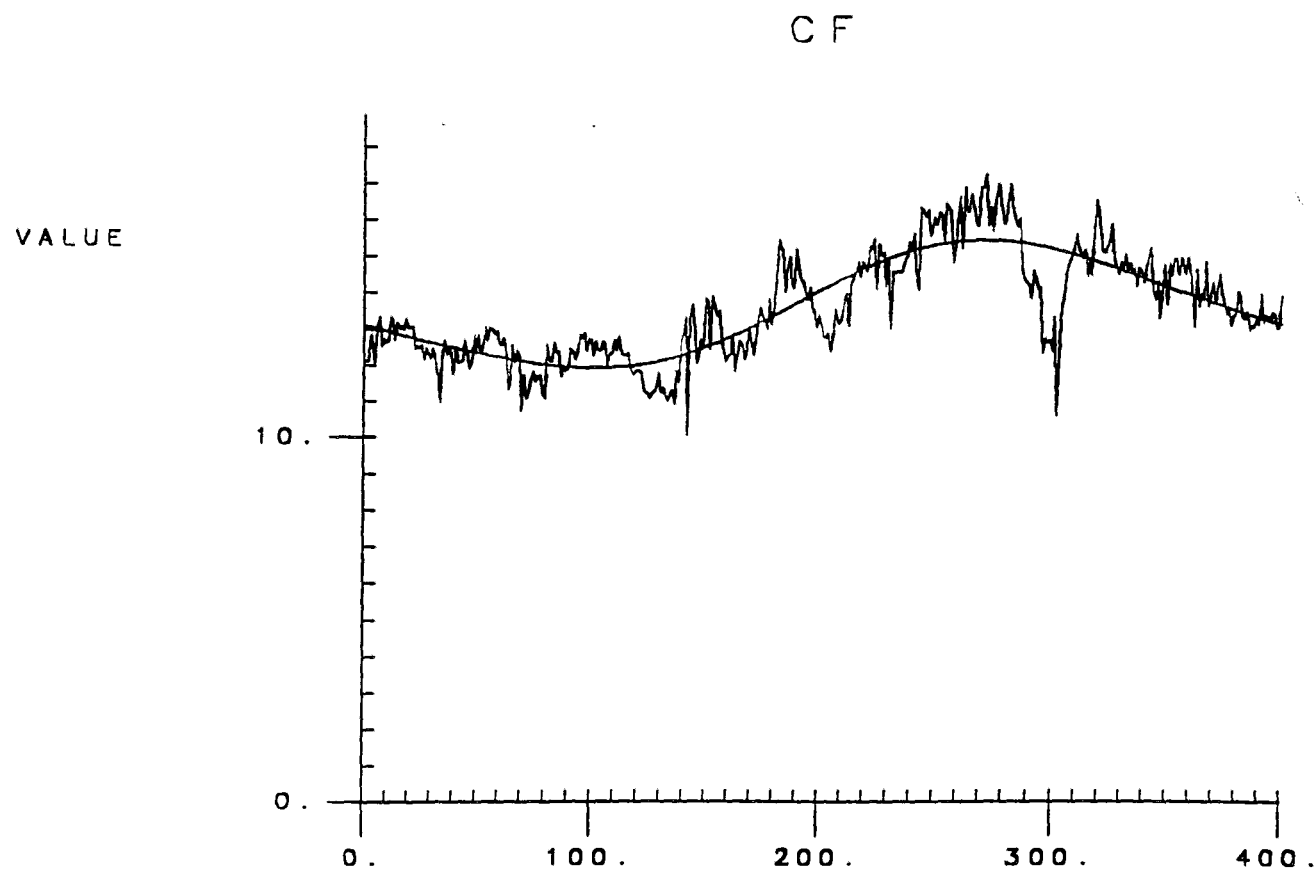


Fig 28. FFT of CF Corg% after removing the first 2 components.



— 2 COMP. S SUBTRACTED

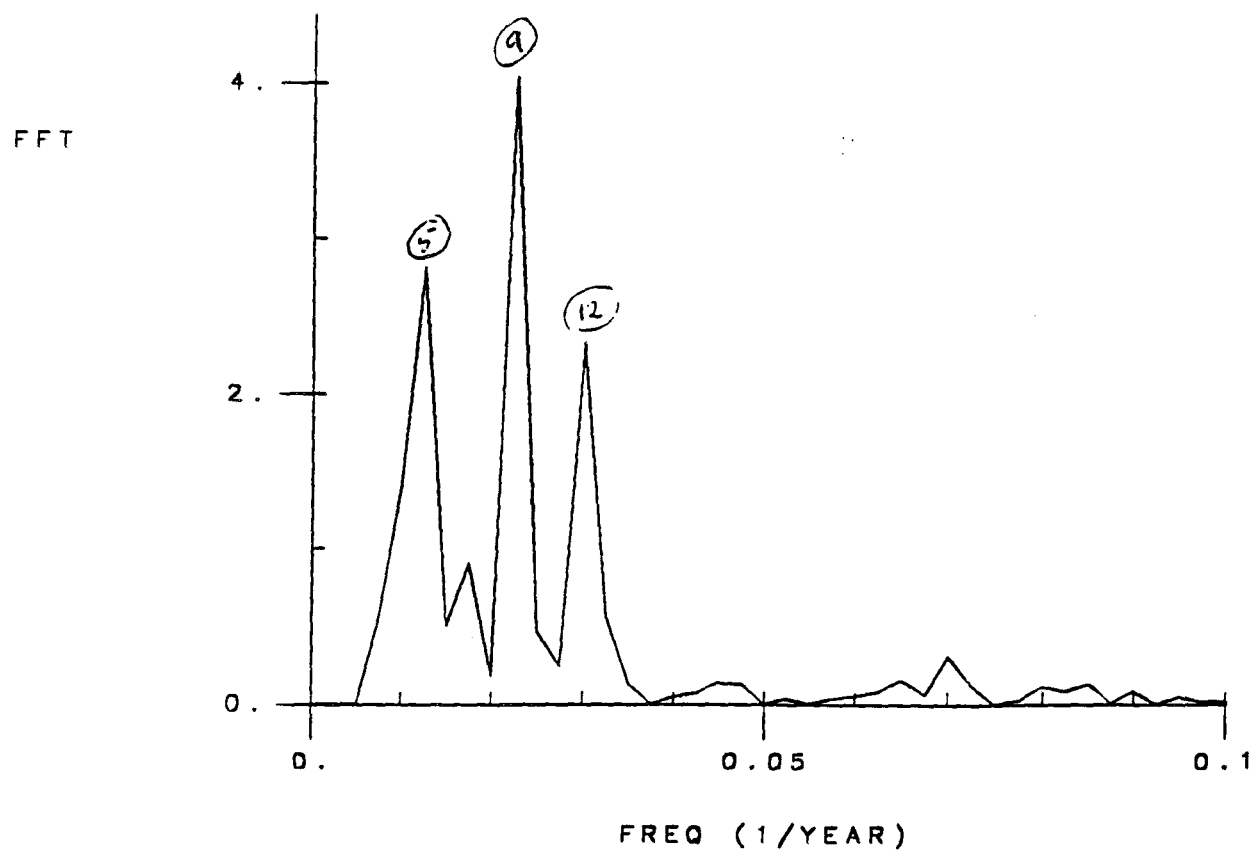
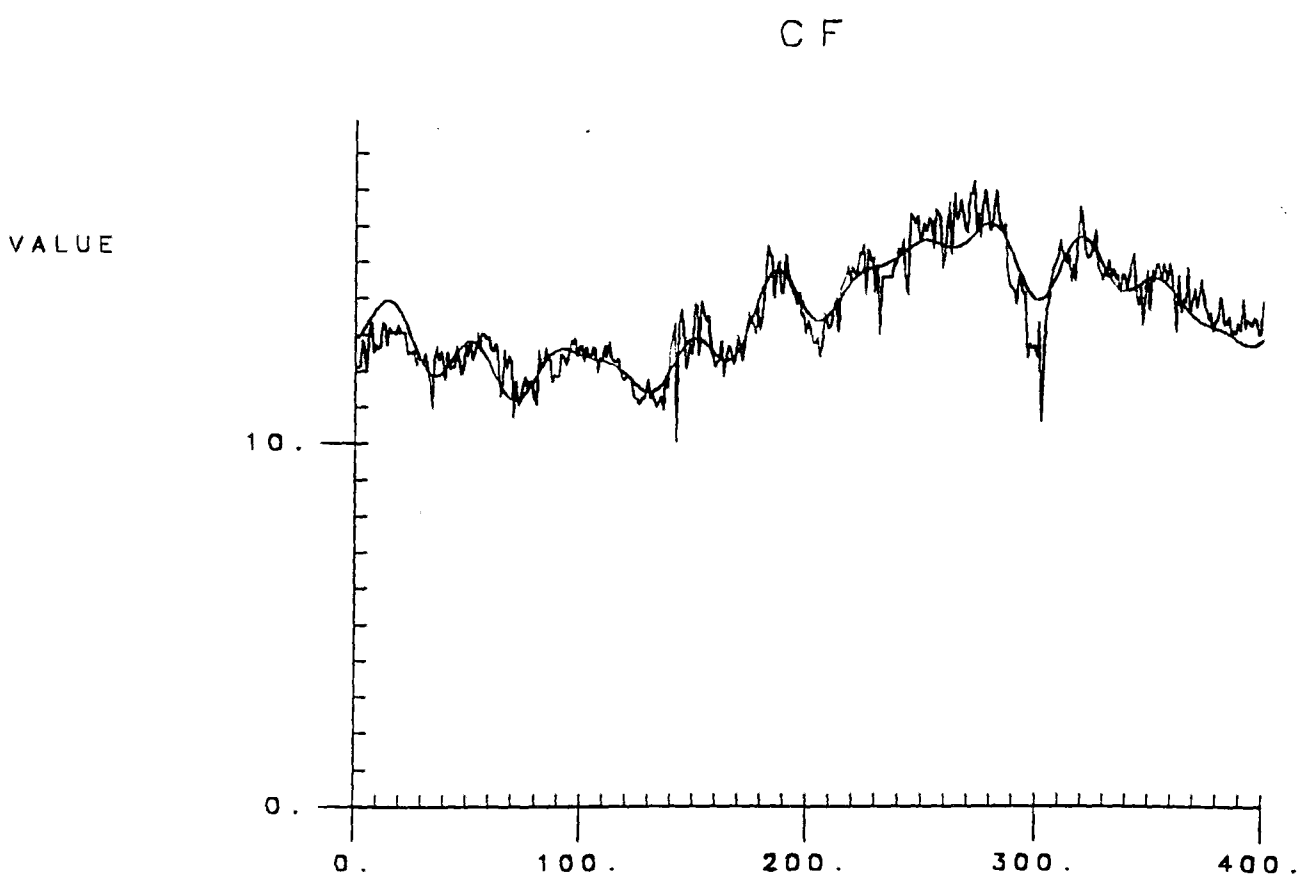
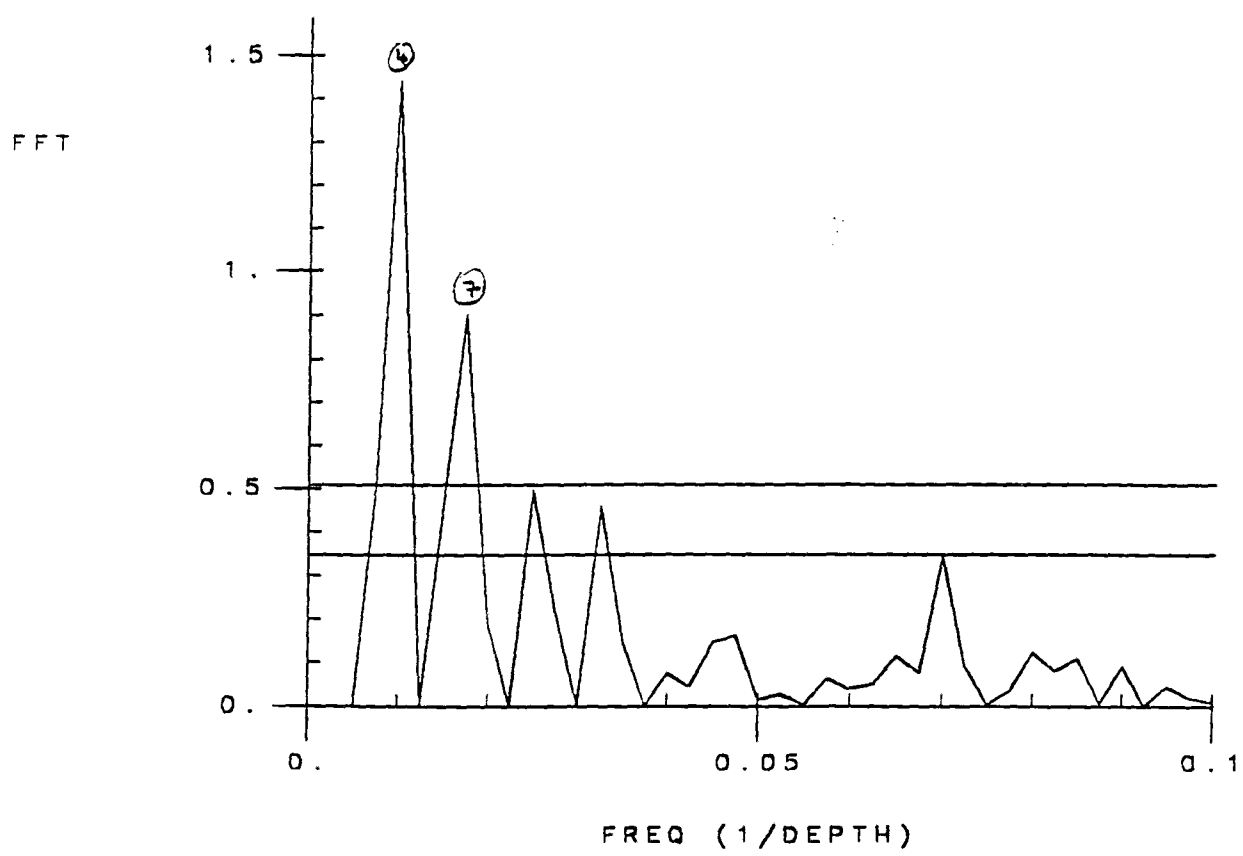


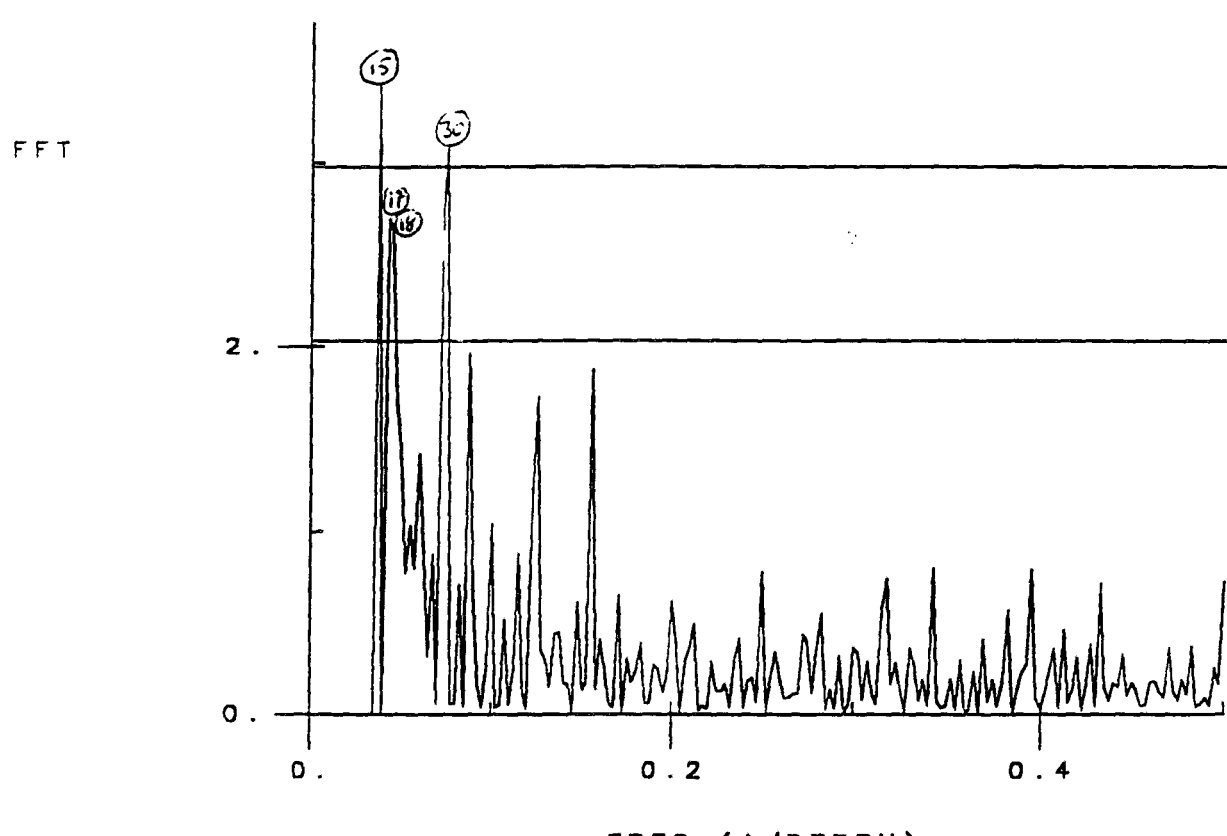
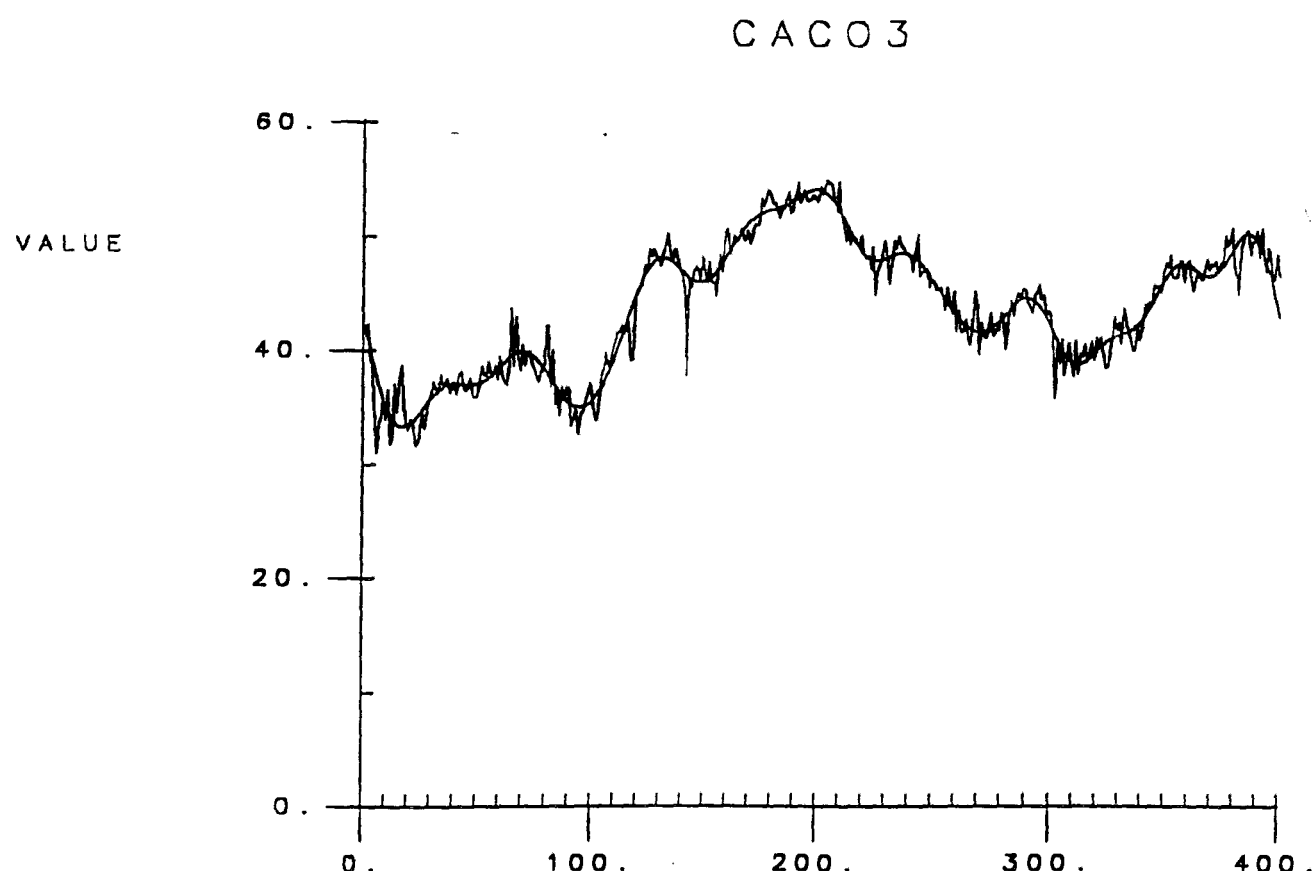
Fig 29. FFT of CF Corg% after removing the first 5 components.



— 5 COMP. S SUBTRACTED      1, 2, **5** 9, 12



— PROB (MAX > ) = 5% & 50%

Fig 30. FFT of CaCO<sub>3</sub>% after removal of the first 14 components.

— PROB(MAX> ) = 5% & 50%

Fig 31. FFT of Corg% after removal of the first 14 components.

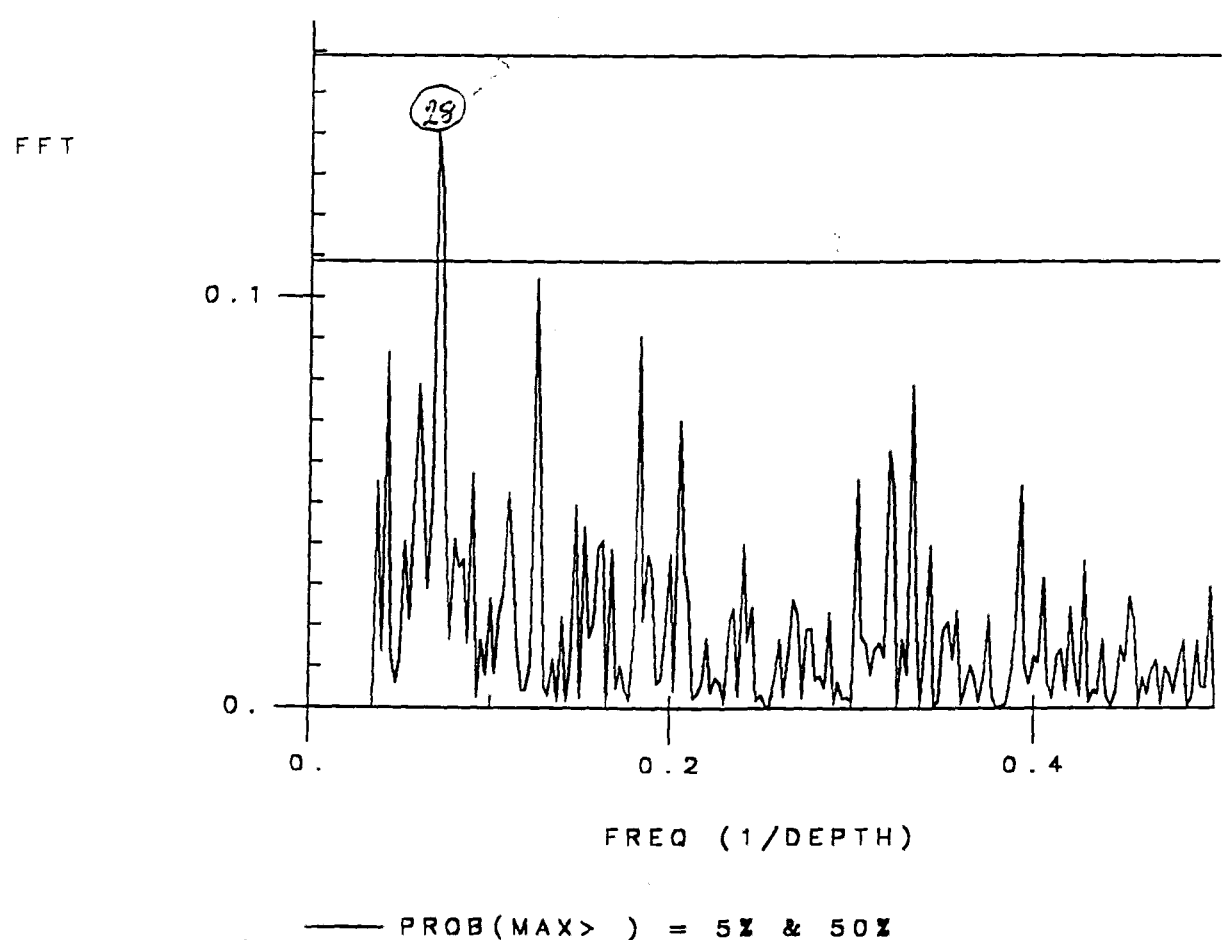
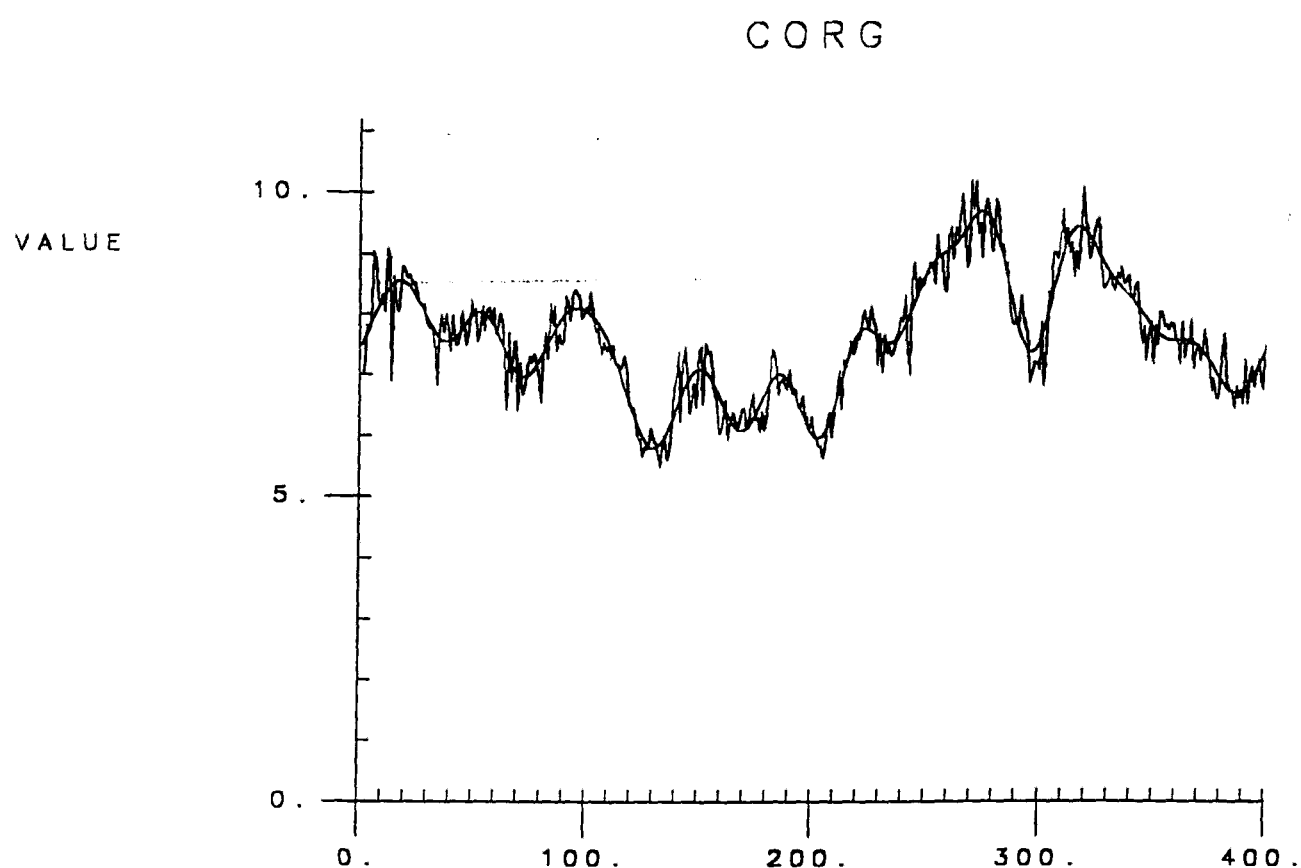


Fig 32. FFT of CF Corg% after removing the first 14 components.

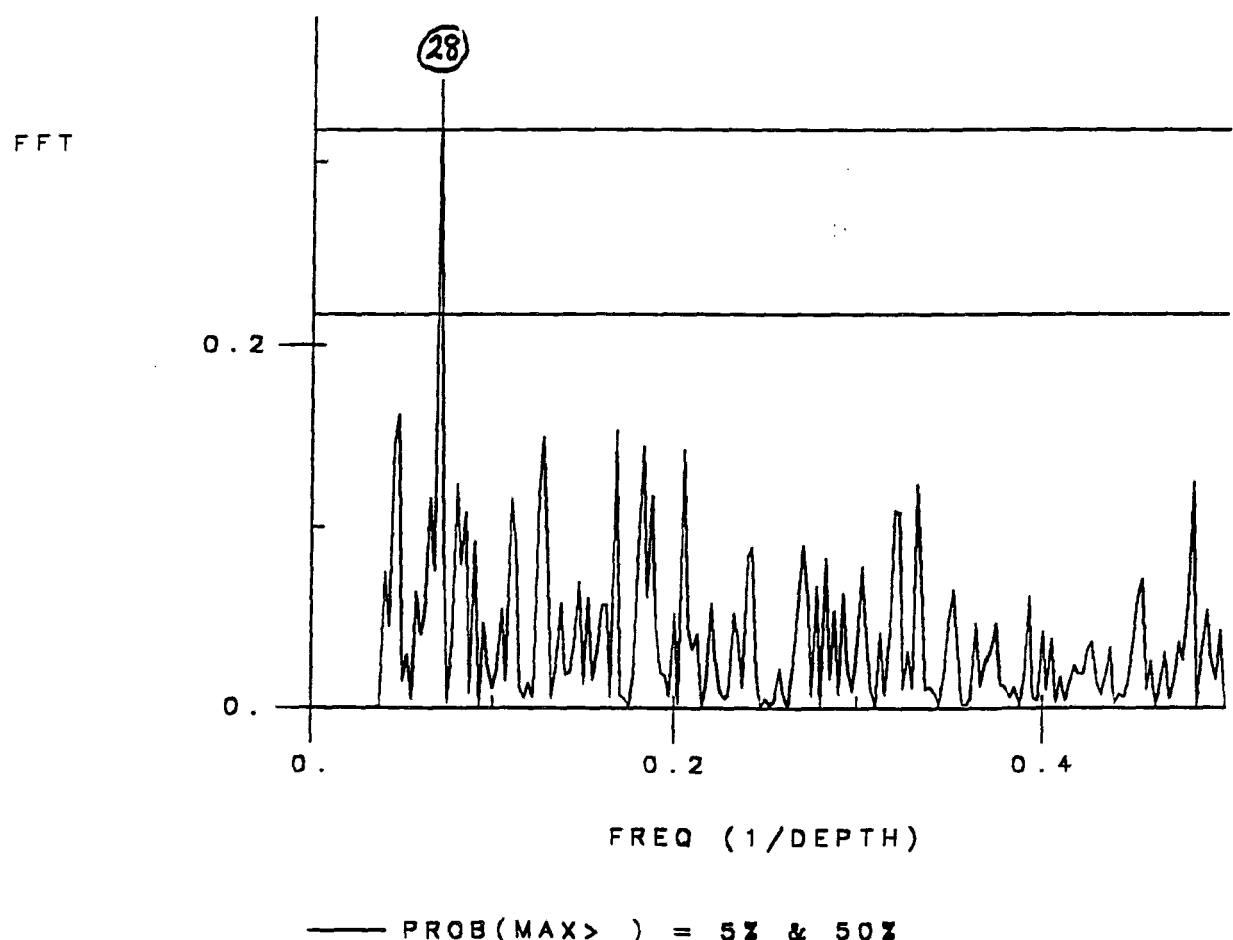
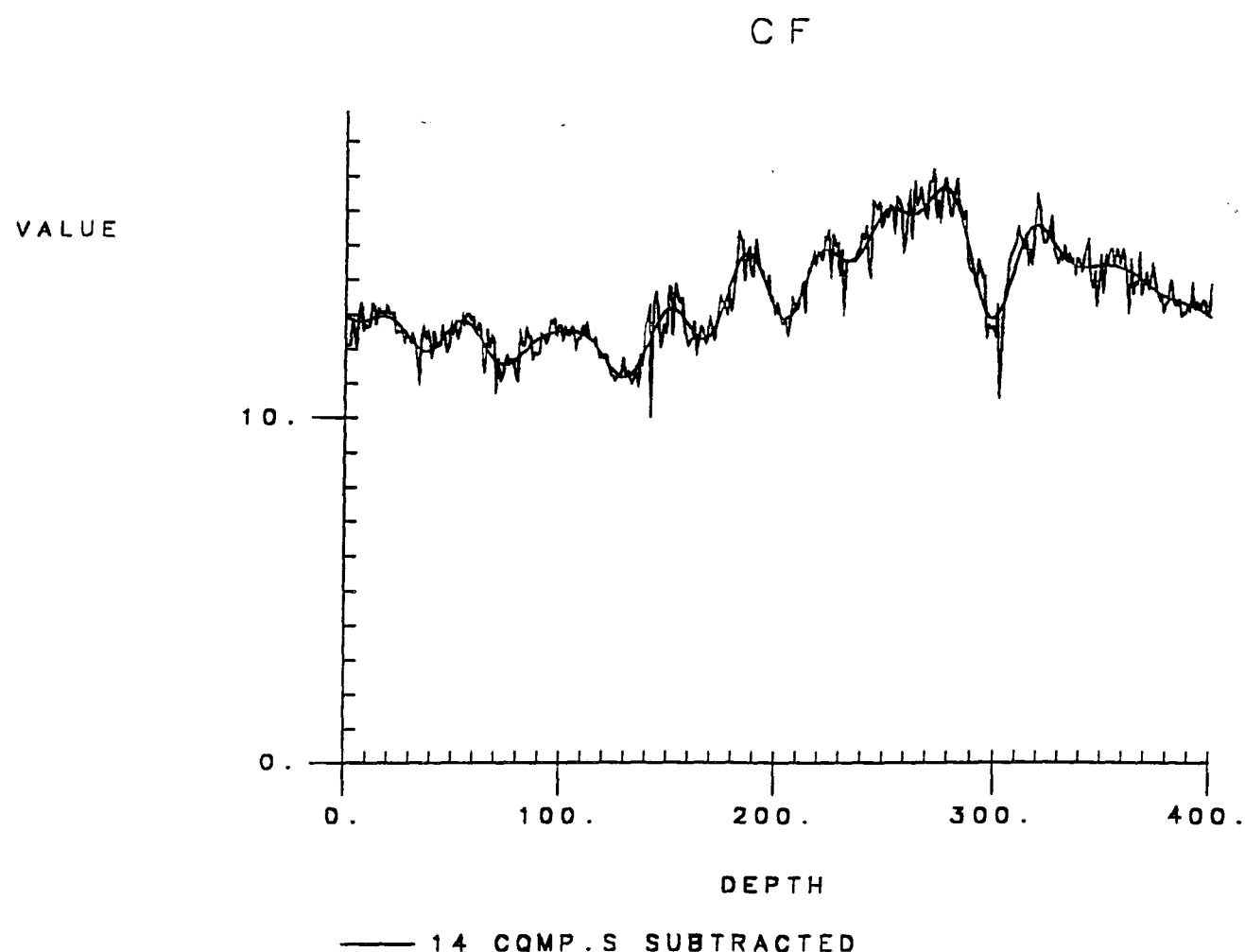
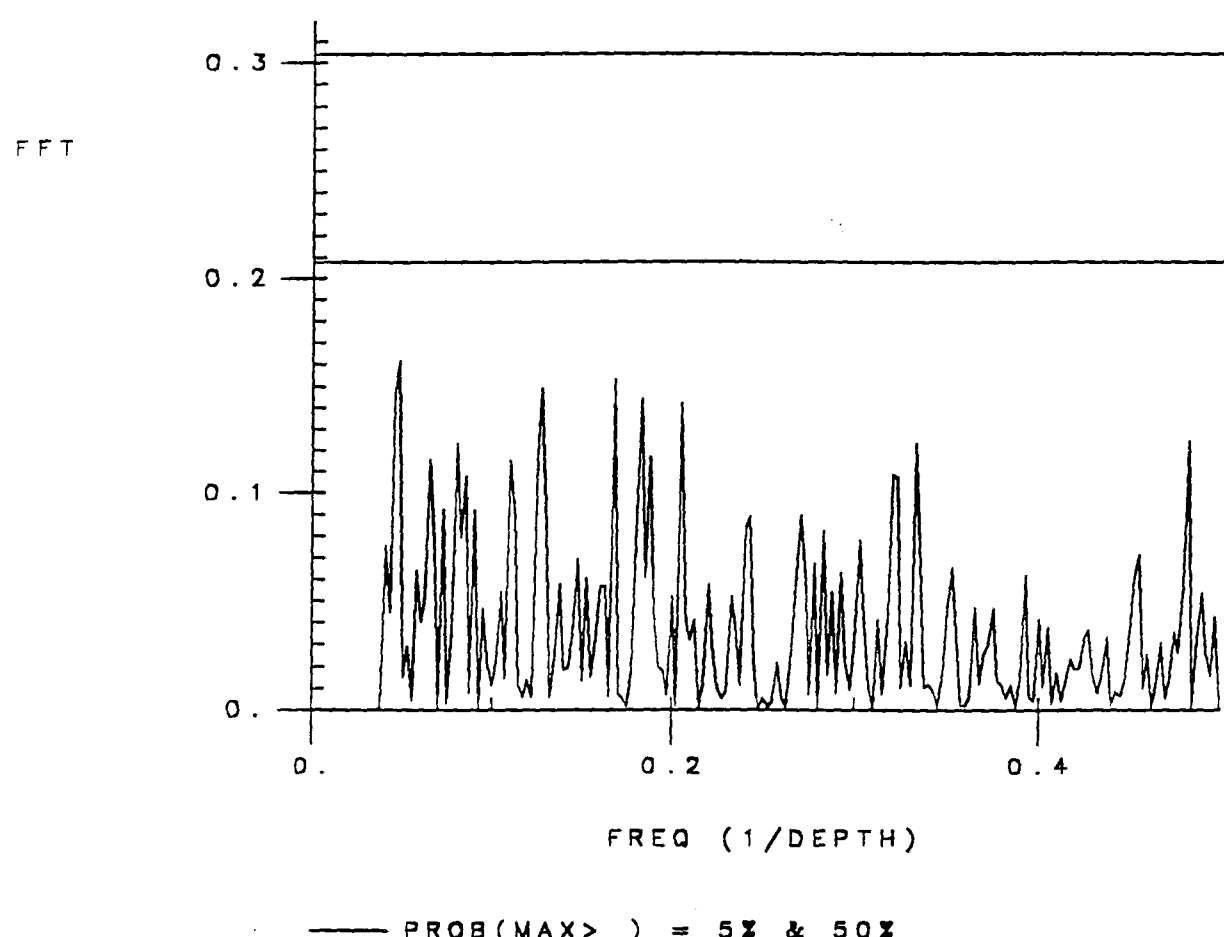
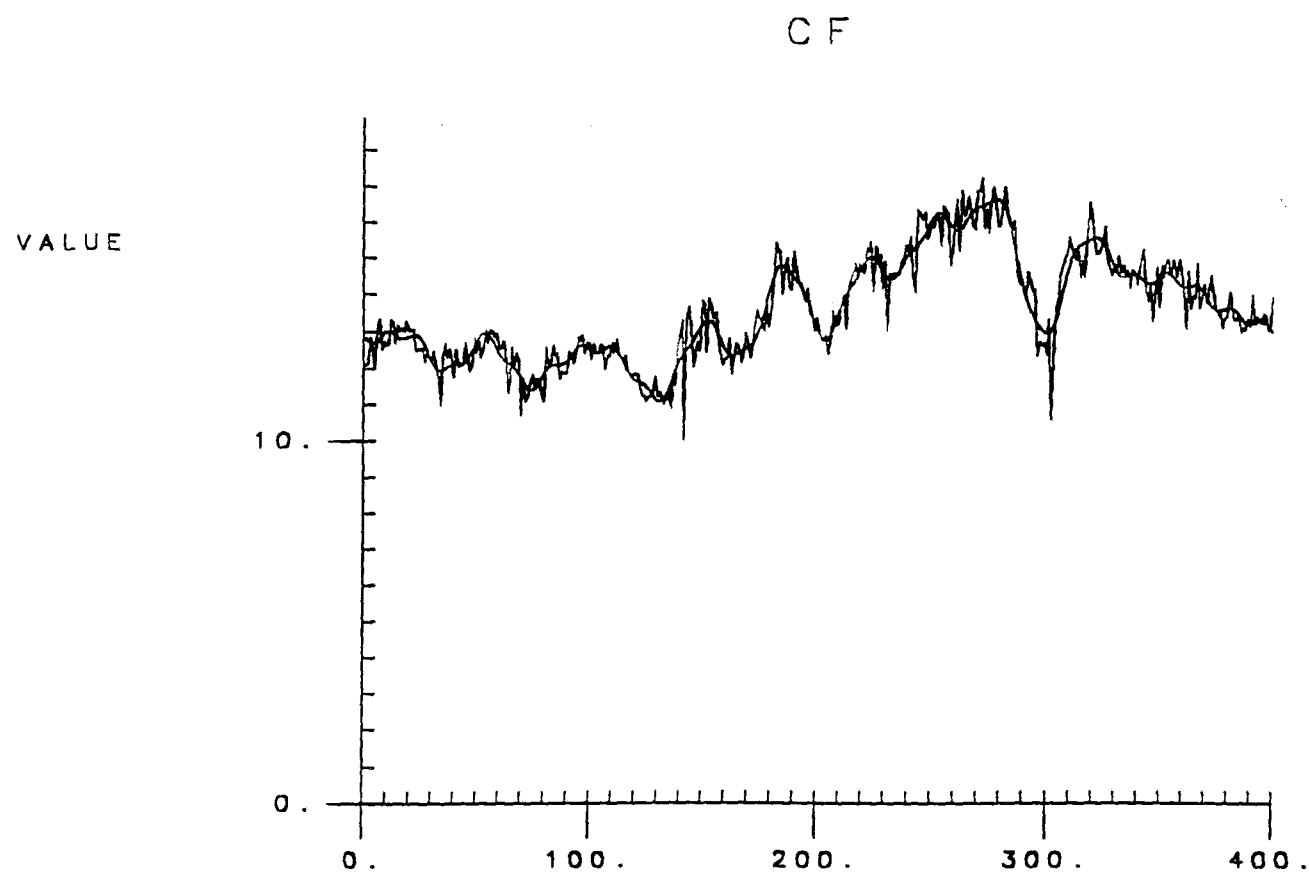


Fig 33. FFT of CF Corg% after removal of N=28.





## 4. RELATED ANALYTICAL WORK

### 4.1 Biostratigraphic data

#### 4.1.1 Introduction

The biostratigraphic data for PC12 was provided by Dr R Jordan at the Institute of Oceanographic Sciences Deacon Laboratory. This work involved studying the coccolithophorids in the sediment core. Coccolithophorids are unicellular, golden-brown algae that at some stage in their life cycle bear coccoliths, which are calcareous scales making up an outer shell. They can be of various shapes and sizes (Fig. 34).

Transport of these coccoliths from the water to the sediment occurs by two main processes:

- 1) in zooplankton fecal pellets;
- 2) in flocculent masses formed during seasonal coccolithophorid blooms.

The coccoliths are usually well preserved in the sediment and so can be studied by light microscopy. Coccolithophorid species are distinguishable by their coccoliths, and so the relative abundances of different coccolith species can be calculated down the core.

It is known from previous studies that certain species were dominant during particular times. Fig. 35 (Weaver and Hines, in press) shows this, and labels two of the acme zone (zone of dominance) boundaries with age (in ka). This data can be compared with the PC12 biostratigraphic data in order to estimate the age of various parts of the core. For example, if a *G.apesta* acme zone were observed in PC12, it would be apparent that the core was older than 150 ka.

Coccolith data may also give an insight into the character of the overlying water mass, as different coccolithophorid species prosper in different environmental conditions.

#### 4.1.2 The Method

Slides were prepared from the sediment samples for studying under the microscope. A small piece of raw sediment was mixed with a drop of distilled water to a paste on the slide. Ridges were made in the sediment paste so that there were alternate thick and thin patches. The slide was left to dry on a hot plate. A cover slip was attached with optical adhesive and allowed to set in the sun.

The sediment was then studied under a light microscope with polarised light at a magnification of x1250. The whole coccolith was not seen, but rather the interference pattern of the polarised light on the coccolith. This pattern was used to identify the species. A total of three hundred coccoliths of different species was counted on each side and the abundance of individual species was calculated as a percentage of the total (ie 300).

The sediment core was sampled at 20cm intervals.

#### 4.1.3 Results and discussion

Fig. 36 shows the profiles of the two most abundant coccolith species in the core - *E.huxleyi* and *G.muellerae*. Note that this profile includes the pilot core (0-80cm) and the piston core (90-610cm).

*E.huxleyi* should be dominant between present day and 75-83ka ago (Fig. 35). It dominates the pilot core, but not the top of the piston core. In an area of high sedimentation rate, such as this, it is unlikely that 80cm (the pilot core) is representative of 80,000 years. This evidence, therefore supports the theory made from the coulometric data that there is an amount of sediment missing from the top of the piston core.

*G.mullerae* is still dominant at the bottom of PC12, and there is no sign of the *G.aperta* acme zone. This means that the whole core is probably less than 150ka old.

Fig. 37 shows the abundance of the six most abundant coccoliths in the piston core. Whilst the age of the core is mostly deduced from *E.huxleyi* and *G.mullerae* data, valuable information about the prevailing environmental conditions can also be obtained from the other four species shown. For example, *C.pelagicus* is known to thrive in very cold conditions so its increased abundance at 20cm, 280cm, and 500cm may indicate the presence of cold water (ie increased upwelling). Also, *F.profundus* is notably increased at 100cm and 260cm. Since this species likes warm waters, these peaks may represent the intrusion of sub-tropical waters or the breakdown of upwelling.

Note that this data set cannot tell us the absolute abundance of coccolithophorids that were living in the water for two reasons:

- 1) variations in the number of coccoliths per cell occur between different species and between individuals of the same species;

2) the absolute numbers of coccoliths are not known ie. we do not know the number of coccoliths per gram of sediment.

## 4.2 Organic Geochemistry Data

### Introduction

In December 1991 I visited Tony Rosell and Prof. Geoff Eglinton at the School of Chemistry, Bristol University. I was able to help Tony Rosell in the preparation of our samples for organic geochemical analysis.

The main purpose of this analysis is to determine the abundance of specific organic compounds in the sediment, and to use one of these compounds to estimate what the sea-surface temperature was as each layer of the sediment core was deposited. Estimating sea-surface temperatures in this way is feasible because of the biochemical response of Prymnosiphite algae, which live near the surface of the ocean, to changes in water temperature. Species of these algae have existed for many 1000's of years and so their remains can be found even in very deep cores. The algae produce specific unsaturated alkenones with a chain length of 37 carbon atoms. These alkenones can be diunsaturated (ie. with 2 double bonds) or triunsaturated (ie. with 3 double bonds) and the ratio of one to the other is called the UK37 value.

$$\text{UK}_{37} = \frac{37:2}{37:2 + 37:3}$$

In live algae this value is proportional to the sea-surface temperature. It is thought that this is because the algae use the alkenones to regulate membrane fluidity by changing unsaturation levels with temperature, although this is not proven.

$$\text{UK}_{37} = 0.034T + 0.039$$

(T = temperature)

When the algae die, they fall to the bottom of the ocean and form part of the sediment. Although many organic remains are broken down in the sediment, these alkenones are resistant to breakdown probably because of the trans-configuration of the double bond on the side chain, which is uncommon in biosynthesised compounds.

Sometimes the alkenones can be found with 4 double bonds, but this is very rare and, with sea-surface temperatures above 40°C, may be ignored.

Salinity does not appear to affect UK<sub>37</sub> values, as sediment samples from the relatively fresh waters of the Black Sea give correct sea-surface temperatures. Also, the UK<sub>37</sub> values seemed not to be affected by how the cores are stored after collection (ie. whether they are stored at room temperature or frozen for up to 4 years).

The ratio of the alkenones to one another, and the abundance of other organics, were determined by gas chromatography but first the organic compounds in the raw sediment had to be extracted and converted into a volatile mixture.

#### 4.2.2 Sample preparation and analysis

It is important to remember that the gas chromatography system is sensitive to all organic compounds and great care must be taken against contamination during sample preparation. The sediment must not come in contact with the skin and must be kept in clean glass vials. The solvents used in sample preparation must not come in contact with any plastics, as organic compounds would be dissolved from them which may distort or conceal important peaks on the final chromatogram.

Since the samples were small, all available sediment was used and the mass was recorded. The mass of these samples was typically about 0.3g. The samples were freeze dried to remove all the water. Any large pieces of sediment were broken with a clean spatula. A blank sample was also prepared. That is an empty tube with no sediment which is treated as the other samples and run through the GC.

The first solvent used was a 2:1 mixture of dichloromethane (DCM) and methanol. This was found to be the best mixture to dissolve all the organics. 3.5mls of it was added to each of the samples. The mixture was then left to dissolve all the organics, a process which is speeded up by leaving the samples in an ultrasonic cleaning tank for 15 minutes.

The samples were placed in a centrifuge for 10 minutes at 4000 RPM. The organic rich solvent was then pipetted off from the remaining sediment (which had settled at the bottom) and transferred into clean labelled vials. These were put into a "speedvac concentrator" used to evaporate the solvent off. The vials are spun to prevent the solvent from boiling.

DCM (40 $\mu$ l) and N,O-Bis(trimethylsilyl)trifluoroacetamide, C<sub>8</sub>H<sub>18</sub>F<sub>3</sub>NOSi<sub>2</sub> (20 $\mu$ l) were added to the sample and left overnight to react. The acetamide is used to make the alcohol less volatile and more polar.

The solution was transferred into the GC vials and rediluted with DCM (about enough to fill two-thirds of the vials). The DCM was then evaporated off in the same way as before and then isoctane (100 $\mu$ l) was added. Isoctane is used at this point instead of DCM as it is less volatile so the concentration is more likely to stay constant. However, DCM was used before, as it has less impurities.

Lids were fastened onto the vials and the samples were then run through the GC.

#### 4.2.3 Results

A graph of the organic compound in the sample is produced (see Fig. 38). The abundances of total alkenones and alkenoates and pigments for each sample can be calculated from this. The C<sub>37</sub> alkenone is represented by peaks A and C, one representing the triunsaturated compound, the other representing the diunsaturated compound.

By comparing the areas of the two peaks, the ratio of the compounds is determined. This is the UK<sub>37</sub> value, which is converted to sea-surface temperature °C. Fig. 39 shows the plots of the three data sets - sea-surface temperature, abundance of total alkenones and alkenoates and total pigment abundance.

No data is available for the pilot core.

#### 4.2.4 Discussion and interpretation of results

The sea surface temperature appears to be at its lowest at 330cm, and there has been an overall warming of the sea surface from that point to the top of the core.

Pigment and alkenone/alkenoate abundances can represent productivity in the water column. Since upwelling links high productivity with low temperatures, we would expect to see peaks in the organic compounds at the same points as troughs in the sea surface temperature profile. In general, these data follow that rule. For example, at 420cm the temperature increases as the pigment abundance decreases. At the top of the core, the sea surface temperature is at its highest in the core whilst the alkenone and alkenoate abundance is at one of its lowest values.

The alkenone/alkenoate and pigment profiles both follow a very similar pattern in the bottom 200cm of the core. At the top of the core, however the values seem to digress.

### 4.3 Inorganic Geochemistry and Oxygen Isotope Stratigraphy

These analyses were carried out on PC12 samples at the University of Edinburgh.

#### Inorganic Geochemistry

Dr Brian Price analysed the core using X-ray fluorescence spectrometry (XRF). XRF can be used to determine the concentrations of a wide range of chemical elements using the intensity of their fluorescent X-rays. An X-ray beam is used to excite atoms in a sample; electrons near the nucleus emit secondary or fluorescent X-rays on their reversion to their ground states. The intensity of the radiation measured, relative to a standard, is proportional to the concentration of the element.

Unfortunately, the results of these analyses were not available before completion of this report.

#### Oxygen Isotope Stratigraphy

Dr Dick Kroon analysed the oxygen isotopes in the planktonic foraminifera species *Neoglobigerina pachyderma* in the core to provide an oxygen isotope stratigraphy.

Oxygen isotopes are used by geochemists for estimating past ocean temperatures. These estimates are based on the fact that the ratio of the stable isotopes,  $^{18}\text{O}$  and  $^{16}\text{O}$ , is temperature dependent in sea water. When it is warm, water containing the higher isotope evaporates preferentially, leaving the surface water enriched in  $^{18}\text{O}$ . Foraminifera growing in these surface waters incorporate the  $^{18}\text{O}$  rich oxygen in their growing carbonate skeletons. Interglacial periods are identifiable from the high  $^{18}\text{O}$  content of foraminiferal shells formed at these times. In contrast, when glacial periods prevail the world ocean is cooler and the foram shells produced at these times are rich in  $^{16}\text{O}$  relative to  $^{18}\text{O}$ . Acidification of the fossils of these organisms releases the oxygen. This can be analysed isotopically under carefully controlled conditions to give a record of past ocean temperatures.

In recent years oxygen isotope stratigraphy for the world ocean has been developed; it consists of stratigraphic stages, the ages of which are now known (Fig. 40). Stage 1, rich in  $^{18}\text{O}$ , is the present day interglacial that began twelve thousand years ago. An intermediate glaciation spike occurred about 10 thousand years ago. Stage 2 is a full glacial stage which began 29 ka ago, and so on.

The oxygen isotope curve for PG/PC12 is shown in Fig. 41. As with all the other data sets, it is obvious that some sediment is missing from the top of the piston core. The highest points in the profile represent the highest temperatures.

By comparison with the standard oxygen isotope curve (Fig. 40), it appears that the pilot core sediment represents oxygen isotope stage 1 - the present day interglacial. The top of the piston core has low  $^{16}\text{O}$  and represents stage 2 - the last glacial. The data show that the pilot core must be less than 9,000 years old because there is no sign in it of the glacial spike at 9-11 thousand years. This means that the average sediment rate for the pilot core was about 10cm/1000 years. This is quite a high value.

The stratigraphy of the rest of the core below stage 2 is unclear, and further isotope analysis is needed. From the data presently available, Dr Kroon is of the opinion that stage 4 begins at 490 cm in the pilot core. If this is correct it means the whole core (pilot and piston) is 60,000 years old. Again, this gives an average sedimentation rate of 10cm/1000 years. Stage 3 is an interglacial; stage 4 is an interstadial, a minor glaciation event. The isotope data of Dr Kroon and the coccolith data of Dr Jordan agree that the core does not reach stage 5, which contradicts the foraminiferal dating made by Bornhold (presented in Summerhayes et al, 1979) suggesting that the base of the core is about 150,000 years old. Further checking is needed before we can be sure of the precise age of the sediments.



Fig. 34. Two examples of coccolith types.

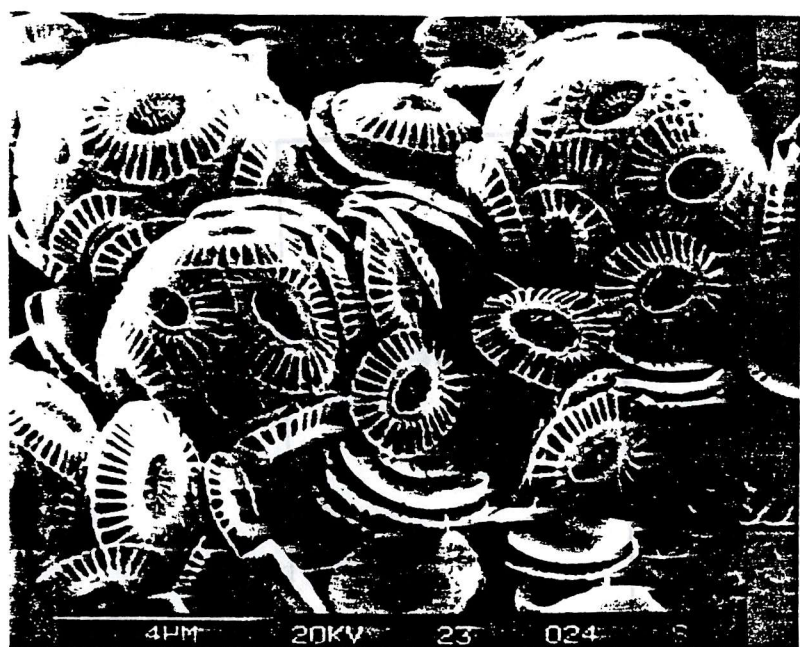


Fig 35. Generalised coccolith stratigraphy for temperate waters.

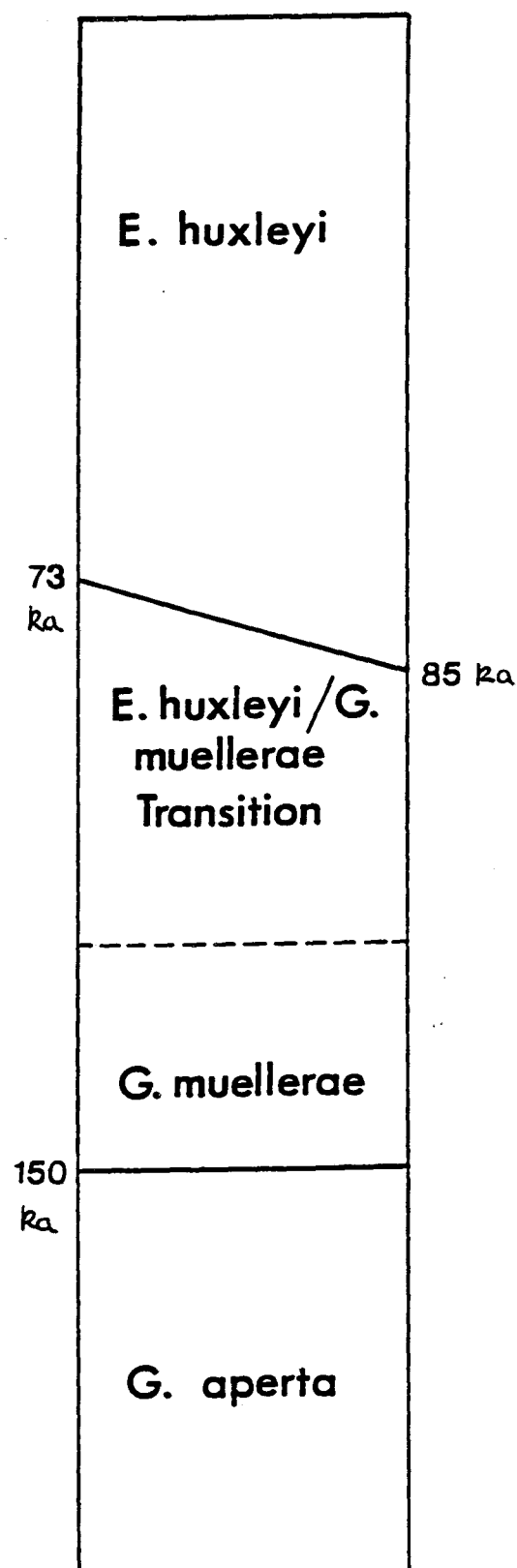
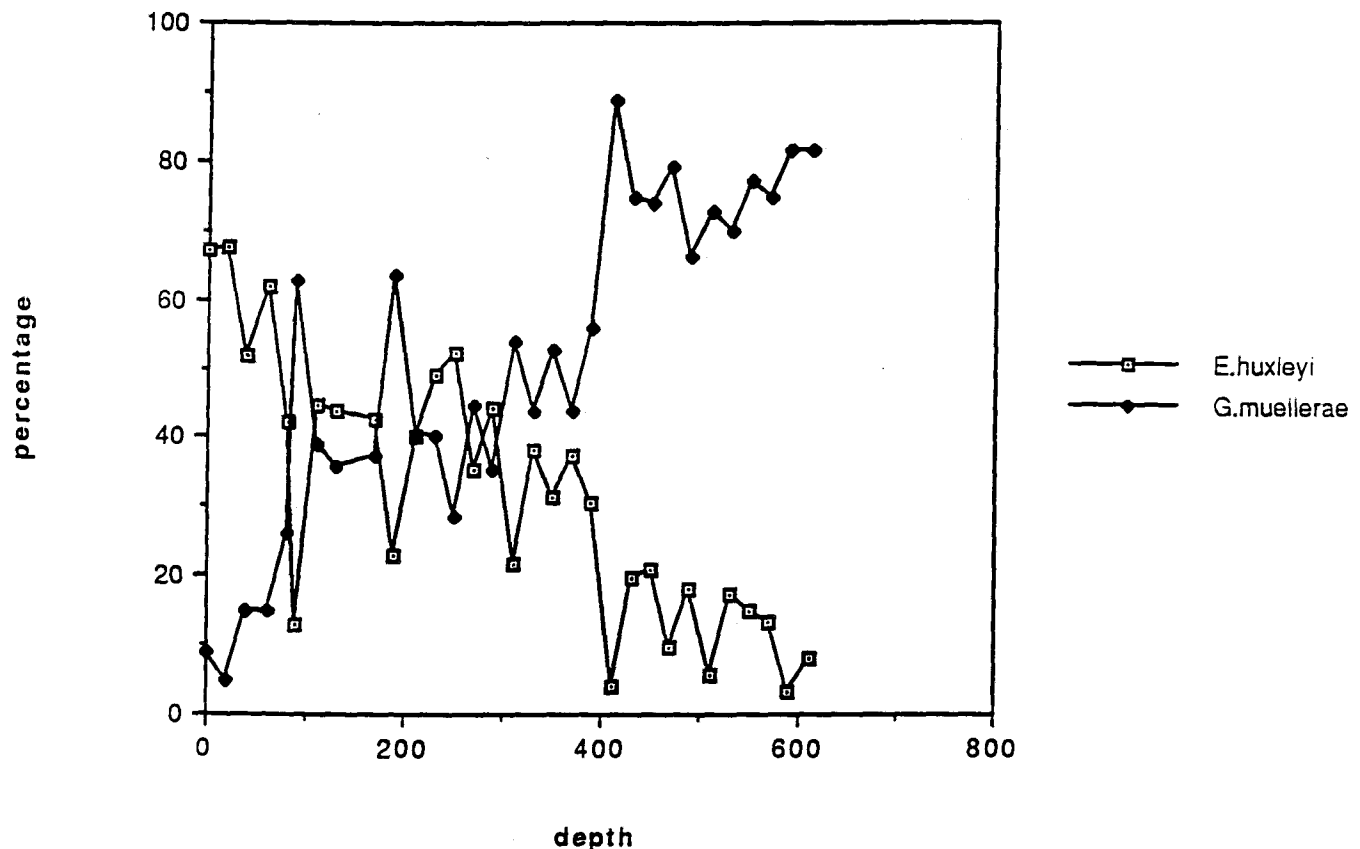
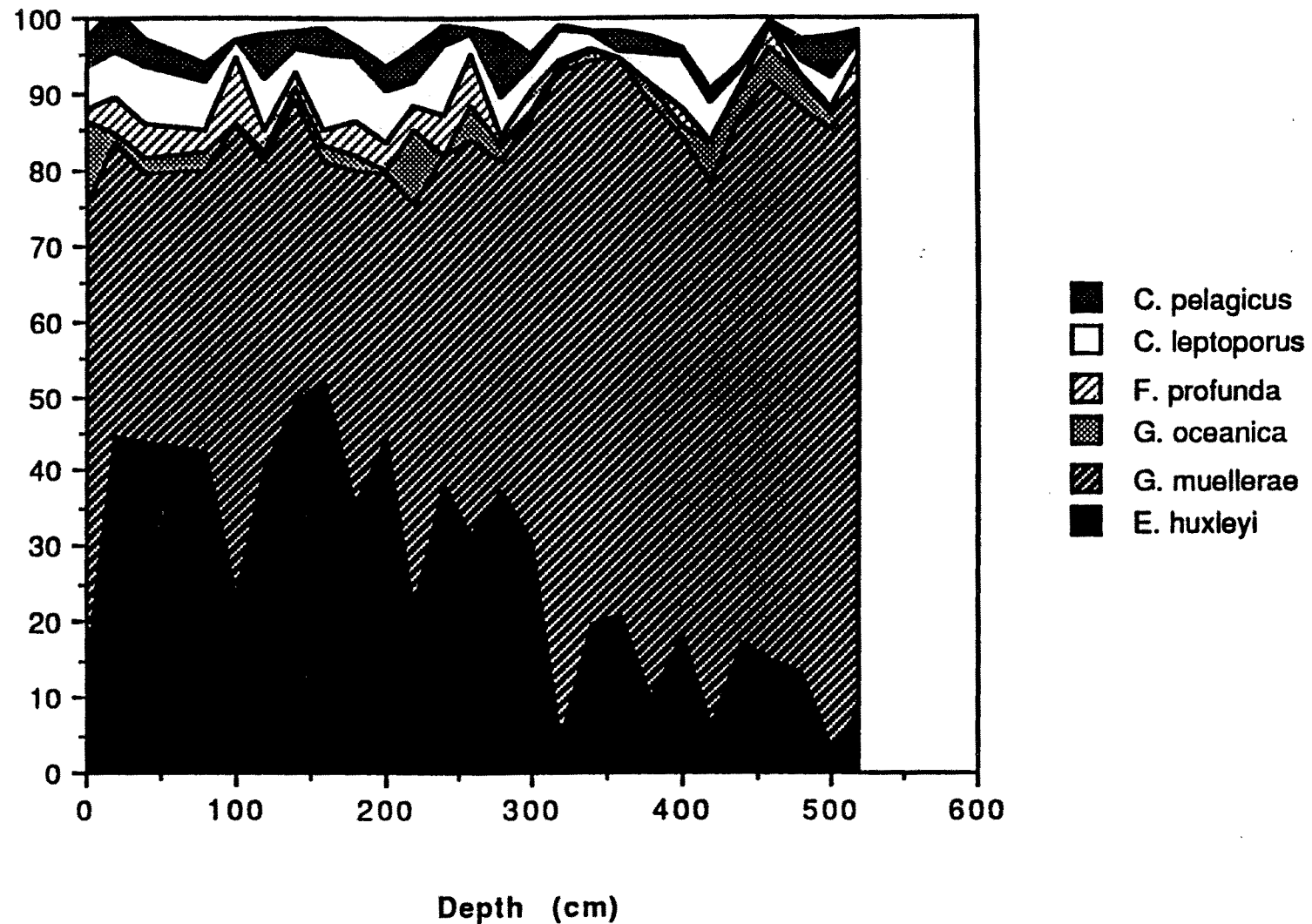


Fig 36. The relative abundances of two coccolith species in PG/PC12.



**Fig 37. The relative abundances of six coccolith species in PC12.**



**Fig 38. An example of a gas chromatogram from a PC12 sample.**

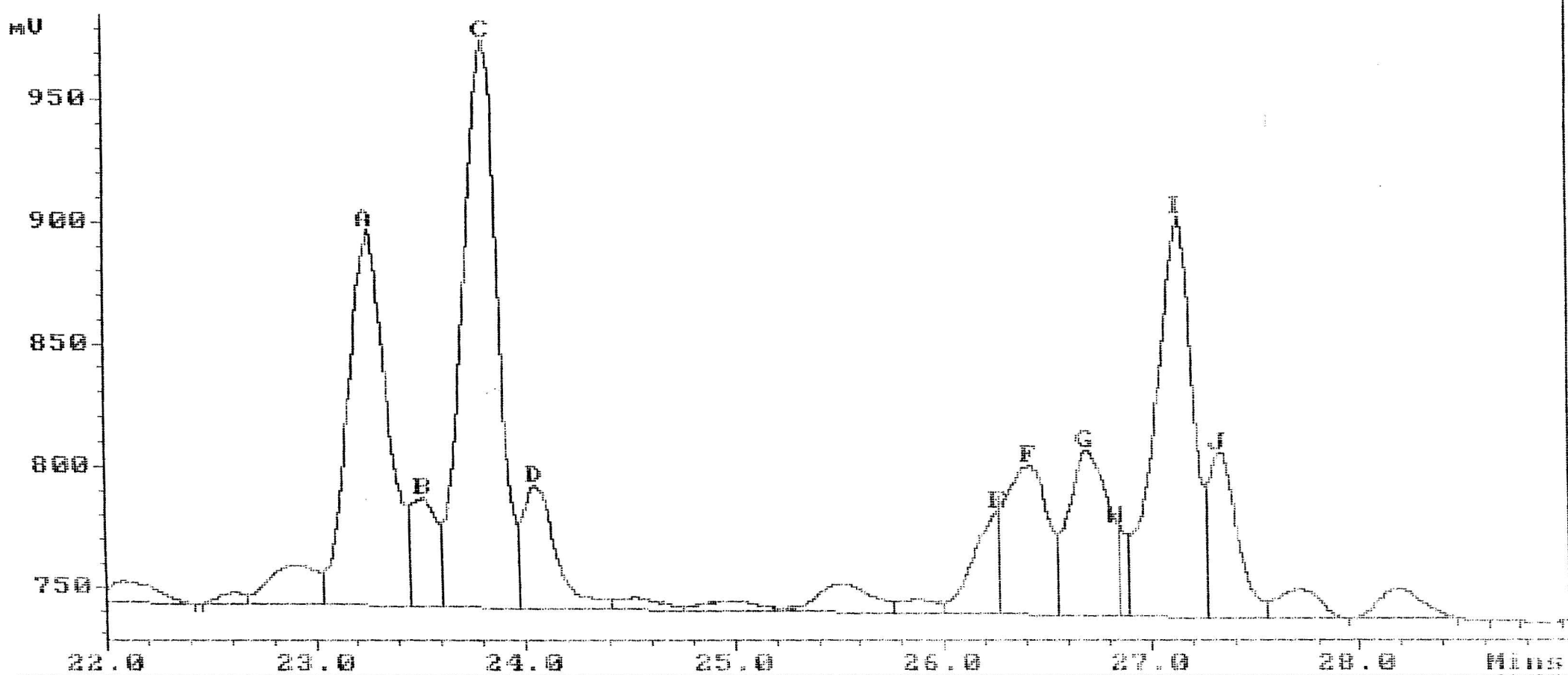


Fig 39. The organic geochemistry results.

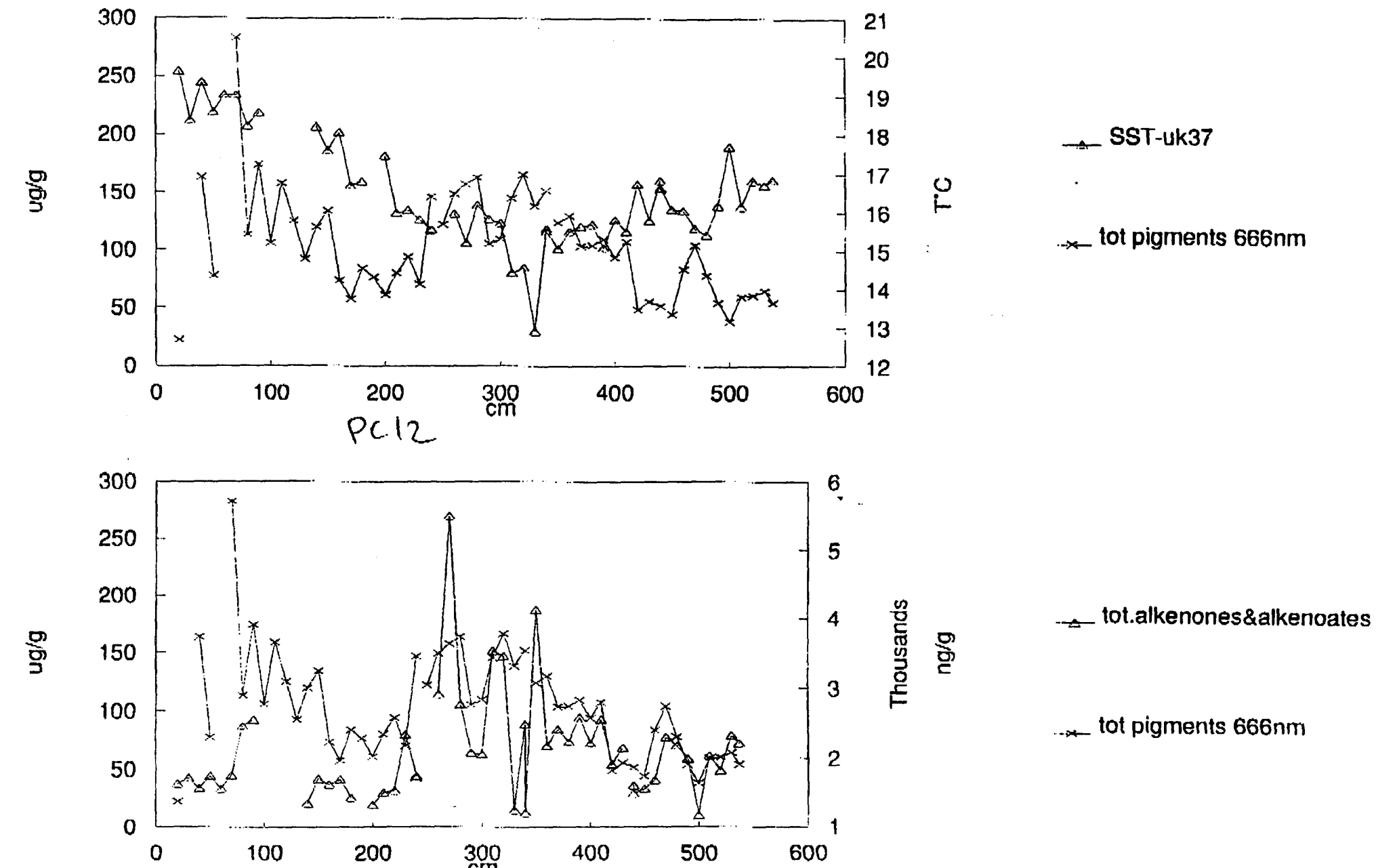


Fig 40. The oxygen isotope record.

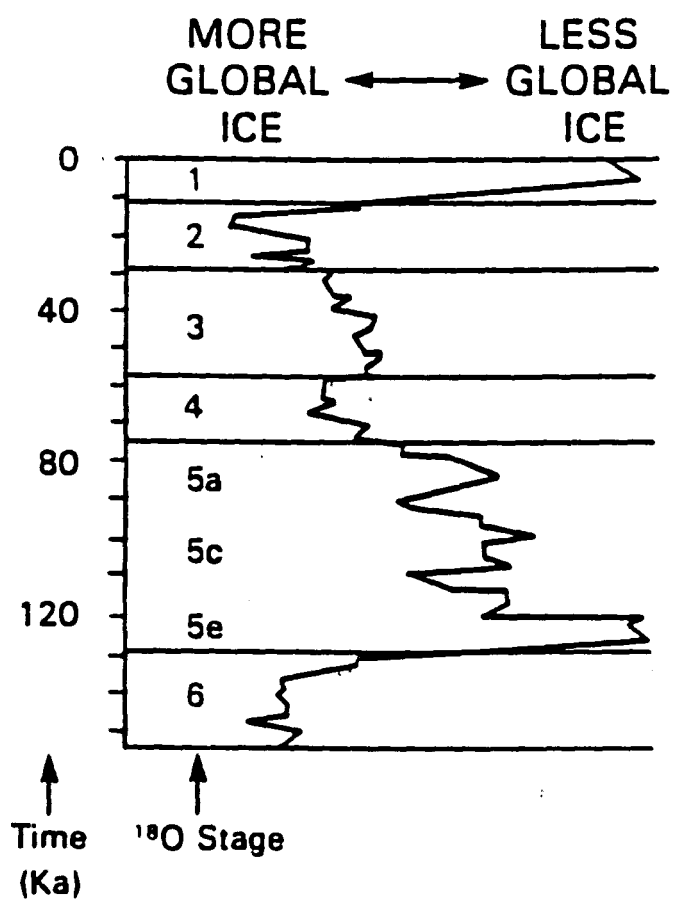
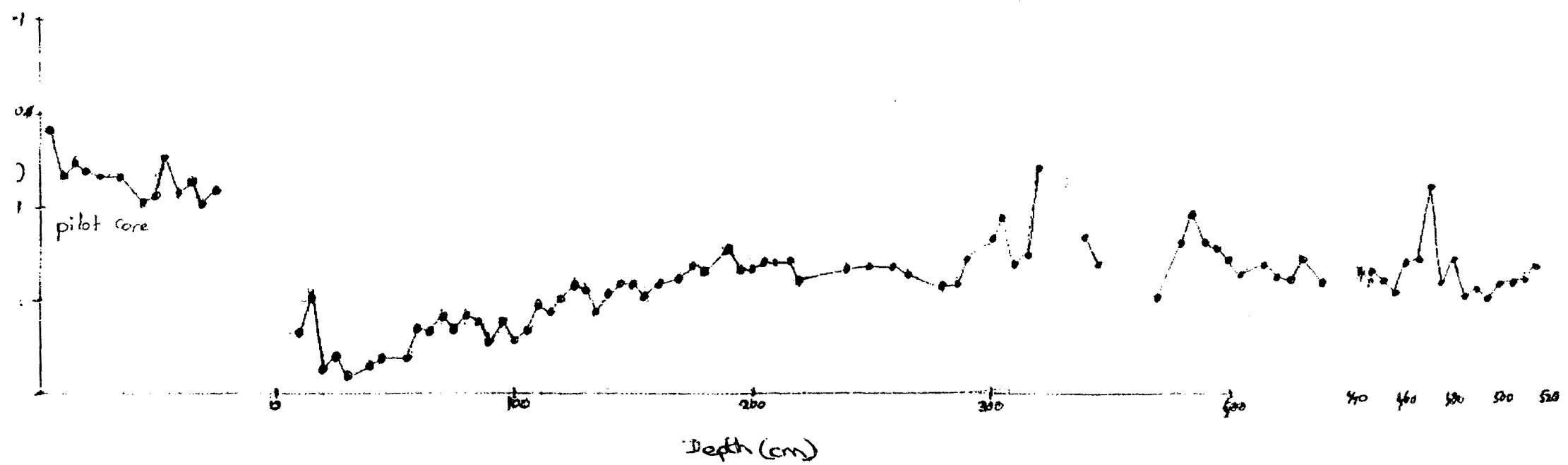


Fig 41. The oxygen isotope curve for PG/PC12.



## 5. INTERPRETATION AND CONCLUSIONS

### 5.1 Comparison and Interpretation of all available Data Sets

Fig. shows the organic geochemistry data sets and the carbonate and organic carbon profiles on the same scale. It illustrates the excellent correlation between the data sets. For example, at 500 cm, we see low organic carbon, low pigments and alkenones and high sea surface temperature. This indicates a period of low productivity because the waters were warm, i.e., no upwelling of cold, nutrient rich waters. Conversely, at 475 cm, there is a peak in organic carbon, pigments and alkenones with a drop in SST, i.e. increased productivity due to an increased upwelling of cold water. Most of the events in the organic carbon plot have corresponding peaks and troughs in the organic geochemistry data sets. This matching of data from independent analytical techniques gives us great confidence in the validity of the data.

There is much speculation about the age of the core and the sedimentation rate (S.R.). Bornhold's previous data suggests a S.R. of 2.3 cm/1000 yr; Jordan's biostratigraphy estimates 6 cm/1000 yrs and Kroon believes 10 cm/1000 yrs.

If Kroon's initial opinion was correct, then the results of the fast fourier transform would change such that climaatic cycles were occurring at the intervals listed below.

<u>N</u>	<u>Years</u>
1	40,000
5	8,000
9	4,400
12	3,300
15	2,700
18	2,200
28	1,400
30	1,300

Clearly, further dating investigation is needed before a firm conclusion can be reached.

There appear to be five periods of alternate low and high carbonate at each 100 cm in the piston core, which would support Jordan's estimation of 100 ka for the core (i.e. five alternate cold and warm periods). Within each there are several upwelling events indicated by organic carbon peaks.

The temperatures indicated by the oxygen isotope stratigraphy do not correspond with the sea surface temperatures. The fact that the isotope curve is obtained from analysis of organisms not living in the surface waters but further down in the water column might explain this

disagreement. Also the isotope curve is a measure of global change, while the UK37 data came from organisms growing at the sea surface. Kroon has observed that there is no simple relationship between the isotopes in foraminifera and the water temperature. We prefer to use the isotopes as a global signal affecting the water mass, and the UK37 as a measure of real local processes. The isotopes tell us more about the ice volume in Antarctica than about surface temperature off the African coast.

## **Summary**

The analysis of the core has indicated a number of oceanographic and climatic changes complicated still further by a complex upwelling system.

Whatever the age of the core, a cyclic pattern of climate change is apparent with local events occurring at least every 3.5ka and probably more frequently as well. With further investigation, this may lead to confident predictions about future climatic change.

### **5.2 Further Possible Studies**

Ideally, to continue this study of the upwelling system in the south east Atlantic, another core with a higher sedimentation rate should be analysed. This would enable us to decipher any local climatic cyclicity on a much finer time scale.

However, there are many other questions that could be answered without finding or collecting any new cores. For example, the organic geochemistry group at Bristol University could re-analyse the samples they already have for absolute amount of wax esters. These are indicators of land plants and would tell us a great deal about the input of terrestrial matter.

Carbon 13 isotopic data would be helpful, especially in the 250-350 cm section as this would clarify whether a dust or river input was causing a dilution effect on the other sediment components.

Inorganic geochemistry of the whole core is now in progress at Edinburgh University and will tell us about dust input and about opal (i.e. diatom and radiolaria) input.

The following abstract has been submitted and will be published in the abstract volume for the Fourth International Conference on Paleoceanography at Kiel, Germany. A poster will be presented at the conference during 21-25 September 1992.

In due course the data in this report will be merged with the completed data sets from Edinburgh and Bristol for publication in an appropriate scientific journal.

## Abstract

### MOLECULAR INDICATORS OF PALAEOPRODUCTIVITY: TOTAL PIGMENT AND ALKENONE-ALKENOATE ABUNDANCES AS PRIMARY BIOMASS INDICATORS COMPARED TO TOC AND COCCOLITH ABUNDANCES

J. Villanueva (CID-CSIC, Barcelona, Catalonia, Spain) & J. Grimalt.

A. Rosell (School of Chemistry, University of Bristol, Bristol, Great Britain) & G. Eglinton.

R. Hearn (Institute of Oceanographic Sciences Deacon Laboratory, Wormley, Godalming, Surrey, Great Britain), R. Jordan and C. Summerhayes

R. Kroon (Department of Geology and Geophysics, University of Edinburgh, Edinburgh, Great Britain).

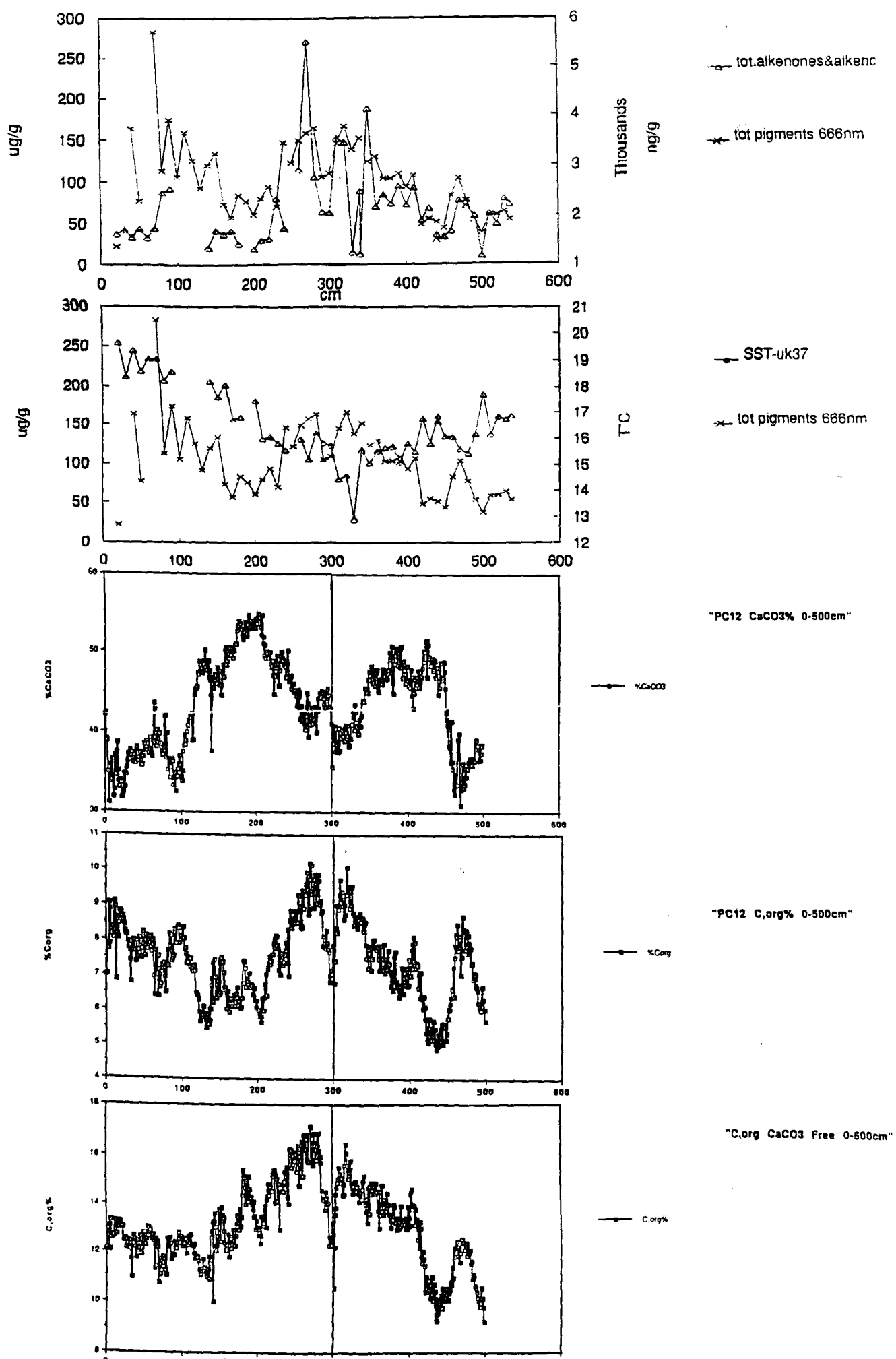
Organic compounds found in marine sediments can provide information about their source of input to the environment (e.g. marine or terrestrial; algae, bacteria, zooplankton) and about the water conditions at time of deposition (e.g. hypersalinity, toxicity/anoxicity) as well as about the prevailing climatic conditions (e.g. sea surface temperature,  $p\text{CO}_2$ , upwelling, wind stress).

We show how particular organic compounds measured down a piston core can be used to indicate fluctuations in total primary productivity (via total abundance of pigments) and the productivity of Prymnesiophyte algae (via alkenone-alkenoate abundances: AA). The core is PC12 from the continental slope off Walvis Bay in Southwestern Africa, a zone of intense upwelling in the Benguela Current. Our palaeoproductivity data are compared with total organic carbon, coccolith abundances, sea surface temperatures derived from the UK37 index and  $\delta^{18}\text{O}$  stratigraphy.

Diagenetic effects as well as degradation of the pigments and the AA in the water column have to be taken into account when relating the values found in the sediment with those from surface waters in order to derive absolute primary productivity. The pigment results correspond to marine inputs whereas the TOC data from areas close to coastal environments may have a strong terrestrial influence.



Fig 42. Comparison of the organic geochemistry and the coulometric data sets.





**Comparison of CaCO<sub>3</sub>% and total carbon % before and after re-drying****CaCO<sub>3</sub>%**

before drying	after drying	% change	mean % change	standard deviation
31.25	32.18	2.98	1.89	0.6676
41.45	41.93	1.16		
36.81	37.91	2.99		
33.05	34.03	2.97		
35.87	36.69	2.29		
36.36	36.80	1.21		
37.20	37.92	1.94		
37.82	38.16	0.90		
37.30	37.91	1.64		
36.53	37.23	1.92		
38.98	39.60	1.59		
36.91	37.50	1.60		
36.01	36.85	2.33		
33.23	33.74	1.53		
33.80	34.22	1.24		

**Total Carbon %**

before drying	after drying	% change	mean % change	standard deviation
11.75	12.14	3.32	3.44	1.0541
11.97	12.42	3.76		
12.00	12.68	5.67		
12.46	13.02	4.49		
12.22	12.53	2.54		
12.37	12.67	2.43		
11.77	12.30	4.50		
11.95	12.51	4.69		
11.68	12.33	5.57		
12.02	12.29	2.25		
11.63	12.10	4.04		
11.85	12.49	5.40		
12.21	12.53	2.62		
12.10	12.50	3.31		
12.05	12.26	1.74		
11.90	12.29	3.28		
11.82	12.15	2.79		
11.36	11.74	3.35		
11.90	12.16	2.18		
11.98	12.36	3.17		
11.49	11.85	3.13		
11.84	12.17	2.79		
11.83	12.17	2.87		
12.00	12.34	2.83		

**Total carbon analysis of PC12 104-105cm**

	Total Carbon %	
	1st analysis	2nd analysis
before drying	11.96%	11.98%
after drying	12.33%	12.43%

## Comparison of original PG12 samples with PG12 samples sent from Canada

Sample	CaCO <sub>3</sub> %		Total Carbon %		C <sub>org</sub> %	
	I.O.S.	Canada	I.O.S.	Canada	I.O.S.	Canada
0-2	63.12	60.85	11.89	11.97	4.31	4.67
10-12	62.01	60.79	12.06	12.22	4.62	4.92
20-22	63.08	63.95	11.79	12.66	4.22	4.99
40-42	63.88	63.62	11.42	11.38	3.76	3.75
60-62	63.88	63.56	11.12	11.35	3.48	3.72
70-72	60.56	60.28	11.40	11.33	4.13	4.10
80-82	59.60	63.92	11.04	11.56	3.89	3.89

## (i) Samples run on the LECO system

Sample 10554	LECO TC%	Coulometric TC%
34 - 36 cm	5.57	4.90 4.93
40 - 42 cm	5.19	5.09
45 - 47 cm	5.27	5.18

## (ii) Geostandard analysis

Geostandard	Literature TC%	Coulometric TC%
MESS-1	2.99	2.92
NBS88a	12.72	12.68
SGR-1	3.16	27.83

## (iii) TC% analysis of pure organic compounds

Organic Compound	Theoretical TC%	Coulometric TC%
Chitin <chem>C30H50O19N4</chem>	46.71	41.25, 40.25
Glycine <chem>NH2CH2CO2H</chem>	31.97	31.96, 31.71
EDTA <chem>C10H16O8N2</chem>	41.06	39.93, 39.95
Lysine mono HCl <chem>NH2(CH2)4CH(NH2)CO2H.HCl</chem>	39.42	38.33, 39.67
Cysteine HCl <chem>C3H9NSO2HCl.H2O</chem>	20.50	21.18, 19.28

## (iv) Organic Carbon Analysis at Bristol University

PC12 Samples	Bristol C <sub>org</sub> %	I.O.S. C <sub>org</sub> %
40 - 41 cm	7.61	7.97
210 - 211 cm	6.66	6.75
500 - 501 cm	5.78	5.90

## (v) Carbonate and organic carbon analysis at BP Research

Sample	CaCO <sub>3</sub> %		C <sub>org</sub> %	
	BP	IOS	BP	IOS
PG12 61-62 cm	73.93	64.40	2.99	3.34
PC12 75-76 cm	49.59	36.48	6.30	7.19
PC12 132-133 cm	61.34	50.04	4.92	5.47
PC12 265-266 cm	53.13	40.33	9.23	9.93
MESS-1	7.27	8.04	2.13	2.92

## Analysis of BP Standard Samples

Sample	CaCO <sub>3</sub> %		C <sub>org</sub> %	
	BP	IOS	BP	IOS
QA3	16.7	12.69	11.5	11.88
QA4	80.0	72.14	6.0	6.13
QA5	25.5	24.45	1.0	1.14
QA6	23.0	14.97	4.1	3.97
QA10	76.0	53.72	1.7	2.75

## APPENDIX 5

## Shale compositions from three literature sources

Mineral	% Composition			Average
	Ref (1)	Ref (2)	Ref (3)	
SiO <sub>2</sub>	58.38	51.0	58.5	55.9
Al <sub>2</sub> O <sub>3</sub>	15.40	51.11	15.11	15.21
Fe <sub>2</sub> O <sub>3</sub>	6.07	6.71	6.74	6.51
MgO	2.45	2.23	2.50	2.39
K <sub>2</sub> O	3.25	2.77	3.21	3.08

Ratio of SiO<sub>2</sub>: other 4 minerals = 55.96:27.19  
 = 2.06:1

## REFERENCES

Bornhold, B.D., 1973. Late Quaternary Sedimentation in the eastern Angola Basin. Tech. Rept. WHOI 73-80, Woods Hole. 212pp.

Chave, K.K., 1965. Carbonates association with organic matter in surface seawater. Science, N.Y. Vol. 148, p.1723.

Diester-Haass, L. 1985. Late Quaternary Sedimentation on the eastern Walvis Ridge, SE Atlantic (HPC 532 and four piston cores). Mar. Geol. 65, 145-189.

Diester-Haass, Heine, Rothe & Schrader, 1988. Late Quaternary History of Continental Climate and the Benguela Current off South West Africa. Palaeogeography, Palaeoclimatology, Palaeoecology, 65, 81-91.

Diester-Haass, Meyers & Rothe, 1986. Light-Dark cycles in opal-rich sediments near the Plio-Pleistocene boundary. DSDP Site 532, Walvis Ridge Continental Terrace. Mar. Geol. 73, 1-23.

Engleman, Jackson & Norton, 1985. Determination of Carbonate Ccarbon in Geological Materials by Coulometric Titration. Chem. Geol. 53, 125-128.

Froelich, P. 1980. Analysis of organic carbon in marine sediments. Limnol. Ocean. Vol. 225, 564-572.

Hedges & Stern 1984. Carbon and nitrogen determinations of carbonate containing solids. Limnol. Ocean. Vol. 29(3), 657-663.

Hsü & Weissert. South Atlantic Palaeoceanography.

Johnson, King & McN. Sieburth, 1985. Coulometric TCO<sub>2</sub> Analyses for Marine Studies; An Introduction. Mar. Chem. 16, 61-82.

Marlowe, Green, Neal, Brassell, Eglington & Course, 1984. Long chain (n-C<sub>37</sub>-C<sub>39</sub>) Alkenones in the Prymnosiophyceae. Distribution of Alkenones and other Lipids and their Taxonomic Significance. Br. Phycol. J. 19, 203-216.

Moore G.L. Introduction to Inductively Coupled Plasma Atomic Emission Spectrometry.

Morgans, J.F.C. 1956. Notes on the analysis of shallow water soft substrata. Jour. Anim. Ecol., Vol. 25, p.367.

Roberts, Palacas & Frost 1973. Determination of organic carbon in modern carbonate sediments. Jour. Sed. Petrol. Vol. 43, 1157-1159.

Ross, D.A. Introduction to Oceanography. Third Edition.

Suess, E., 1970. Interaction of organic compounds with calcium carbonate: I. Association phenomena and geochemical implications. Geochem. cosmochim. Acta. Vol. 34, 157-168.

Summerhayes, C.P. 1983. Sedimentation of organic matter in upwelling regimes. In Thiede, J. and Suess, E., eds, Coastal Upwelling, part B., Plenum, 29-72.

Summerhayes, C.P., 1987. Organic-rich Cretaceous sediments from the North Atlantic. Marine Petroleum Source Rocks No. 26, 301-316.

Summerhayes, Bornhold & Embley, 1979. Surficial slides and slumps on the continental slope and rise off South West Africa : A reconnaissance study. *Marine Geology* Vol. 31, 265-277.

Telek & Marshall 1974. Using a CHN Analyzer to reduce carbonate interference in particulate organic carbon analyses. *Marine Biol.* Vol. 24, 219-221.

